

FINAL REPORT
FOR
A DESIGN STUDY FOR AN OPTIMAL
NON-LINEAR RECEIVER/DEMODULATOR

31 August 1970

Contract No.: NAS5-10789

Prepared By
ELECTRAC, INC.
1614 Orangethorpe Way
Anaheim, California 92801

For
National Aeronautics and Space Admin.
Goddard Space Flight Center
Greenbelt, Maryland

FINAL PROJECT REPORT
FOR
A DESIGN STUDY FOR
AN OPTIMAL NON-LINEAR RECEIVER/DEMODULATOR

Contract No.: NAS5-10789

Goddard Space Flight Center
Contracting Officer: J. L. Turner
Technical Representative: V. R. Simas.

Prepared by:
Electrac, Inc.
1614 Orangethorpe Way
Anaheim, California 92801

By:
A. J. Mallinckrodt
R. S. Bucy
S. Y. Cheng

For
GODDARD SPACE FLIGHT CENTER
Greenbelt, Maryland
31 August 1970

ABSTRACT
FOR
FINAL REPORT
FOR A
DESIGN STUDY FOR
AN OPTIMAL NON-LINEAR RECEIVER/DEMODULATOR

This report presents the results of investigation on the optimal performance of the PM demodulator using Bucy's statistical non-linear filtering theory. A cyclic phase non-linear filtering technique has been developed for modular phase tracking system uses. A realizable implementation of the optimal cyclic phase non-linear filter based on the Fourier series representation of the cyclic density function has been derived.

The work described in this report is restricted to the first-order phase process, for faster computation in digital simulations and for extensive research results available in Weiner optimum phase-lock loop for comparison purposes. However, the technique developed in this program is equally applicable to higher-order systems as well.

The actual performance of the non-linear filter was investigated using Monte Carlo techniques. The classical phase-lock loop was also being simulated as a reference for the non-linear process. The cyclic phase non-linear filter appears

to be about 0.7 dB better than the phase lock with respect to noise alone where the maximum conceivable improvement is 2.2 dB, or the excess noise relative to the ideal is about $\frac{1}{3}$ less in dB than that of the phase-lock loop.

It was not possible due to computing limitations during the last part of the program to achieve simulation results on the question of signal suppression. However, an experimental or simulatable technique for measuring signal suppression has been devised. The total signal-to-noise ratio improvement relative to the phase-lock loop will consist of the noise improvement and signal suppression improvement.

The overall results of this study program is highly encouraging. Hardware implementation based on the cyclic phase scheme appears to be feasible. Significant improvement in performance in second-order loops is anticipated. More work on this line is strongly recommended.

TABLE OF CONTENTS

	<u>Page No.</u>
Terminology	ii
Superscripts and Subscripts	iv
1. Statement of Problem	1.1
2. Basic Orientation to the Optimal Non-Linear Phase Estimator	2.1
3. Basis of the Discrete Simulation	3.1
3.1. The Phase Signal in the Continuous Domain	3.1
3.2. Representation and Sampling of "White Noise"	3.4
3.3. Digital Representation of the Signal	3.10
4. Kalman-Bucy Filter-Linearized Problem	4.1
5. Phase-Locked Loop	5.1
5.1. Non-Linear Analysis of Phase-Locked Loop	5.2
5.2. Discrete Phase-Locked Loop	5.6
6. The Non-Linear Theory	6.1
6.1. Relation to the Phase-Locked Loop	6.4
7. Cyclic Solutions to the Non-Linear Phase Estimator	7.1
7.1. Recursion Relation for the Cyclic Density	7.5
8. Fourier Series Expansion of the Cyclic Density	8.1
8.1. Difference Equation Form	8.4
9. Computing Details	9.1
9.1. Determining M and F	9.1
9.2. Monte Carlo Analysis	9.2
10. Simulation Results	10.1
10.1. Details of a Typical Run	10.1
10.2. Monte Carlo Results	10.3
10.3. Significance of the Phase Noise Results	10.4
11. Implementation	11.1
12. Conclusions	12.1
Appendix 1. Sequential Bayes Estimation	A1.1
Appendix 2. Bayes Theorem and Digital Realizations for Non-Linear Filters	A2.1
Appendix 3. Program Description	A3.1
References	R.1

TERMINOLOGY

<u>Ref. Page</u>	<u>Symbol</u>
3.1	$s(t)$ = signal, $A \cos(\omega_0 t + x(t)) + w(t)$
3.1	$w(t)$ = "white" additive measurement noise
3.1	ξ_0 = spectral density, two-sided, of $w(t)$ (Watt-sec)
3.3	r = noise density/signal power ratio = $2\xi_0/A^2$ (sec)
3.1	$x(t)$ = phase process
3.1	$u(t)$ = white noise derivative of $x(t)$ $\dot{x}(t) = Ku(t)$
3.2	q = spectral density (two-sided) of Ku , $\left(\left(\frac{\text{rad}}{\text{sec}}\right)^2\right)\text{sec}$
3.13	$d\tilde{u}(t) = u(t) dt$ (formally)
3.5	$d\tilde{w}(t) = w(t) dt$ (formally)
3.6	z_1, z_2 = low-pass normalized equivalents of s $z_1 = \cos x(t) + v_1(t)$ $z_2 = \sin x(t) + v_2(t)$
3.10	$z_{i_n} = (z_i)_n = n^{\text{th}}$ discrete time sample of z_i , $i = 1, 2$ Z = vector observation (z_1, z_2)
3.10	$C = \frac{2r}{\Delta} =$ discrete measurement noise variance on z_{1_i} = RF (dimensionless)
3.10	$B = q\Delta =$ discrete driving noise variance on u_i = R/F (rad^2)
3.3	$R = \sqrt{2rq} =$ phase error variance for the optimal estimator = \sqrt{BC} in the associated linear problem (dimensionless)
3.3	$F^* = \sqrt{\frac{2r}{q}} =$ time constant for the optimal estimator in the associated linear problem (seconds)
3.10	Δ = sample interval (seconds)

TERMINOLOGY, Cont'd.

<u>Ref. Page</u>	<u>Symbol</u>	
3.7	$O[y(t)]$	= observation operator on y $= \frac{1}{\Delta} \int_t^{t+\Delta} y(t_1) dt$
3.8	y_n	= $O[y(n\Delta)]$
3.11	F	= F^*/Δ = time constant for the optimal estimator in $= \sqrt{\frac{C}{B}}$ the discrete associated linear problem (dimensionless)
6.1	$J(x, t)$	= conditional probability of x (phase) based on all observation through time t
	ϵ	= $x - x^*$ = estimate error
	$f_x(x)$	= $\frac{\partial}{\partial x} f(x)$
7.4	$L(\epsilon)$	= cyclic loss function $2(1 - \cos \epsilon)$
	$M(\epsilon)$	= $\epsilon \pm n 2\pi$ such that $-\pi < M(\epsilon) < \pi$ = modulo 2π operator

SUPERSCRIPTS AND SUBSCRIPTS

- denotes any variable
- $\hat{\bullet}$ = conditional or a posteriori expectation of • based on all measurements to date, a random variable, function of the measurements
- * = an estimate of •
- $\int_0^t \bullet dt$ (formally)
- so that
- $d\bullet = \bullet dt$ (formally)
- _i = ith discrete sample of •
- $\bar{\bullet}$ = time average
- _p = pertaining to phase-locked loop estimate
- _c = pertaining to cyclic estimate $x_c^* = ATN \frac{\widehat{\sin x}}{\widehat{\cos x}}$
- _s = pertaining to static phase estimate (Sec.6)
- _m = pertaining to conditional mean estimate
- $\langle \bullet \rangle$ = a priori expectation of •

LIST OF ILLUSTRATIONS

<u>FIG. NO.</u>		<u>PAGE</u>
1-1	Overall Diagram for Comparative Study of Phase Estimation Filters	1.3
5-1	Comparison of Variance for First-Order-Phase-Locked-Loop with Results of Approximate Analyses	5.5
7-1	Conditional Probability Density Plot - 350th Time Point	7.8
7-2	Cyclic Density on the Unit Circle	7.9
7-3	Cyclic Loss Function $L(e) = 2(1 - \cos e)$	7.9
10-1a	Simulation Run Comparing Phase-Lock and Cyclic Non-Linear Estimates	10.1a
10-1b	Simulation Run Comparing Phase-Lock and Cyclic Non-Linear Estimates	10.1b
10-1c	Simulation Run Comparing Phase-Lock and Cyclic Non-Linear Estimates	10.1c
10-2	Conditional Probability Density Plot - the 70th Time Point	10.2a
10-3	Conditional Probability Density Plot - the 75th Time Point	10.2b
10-4	Conditional Probability Density Plot - the 80th Time Point	10.2c
10-5	Conditional Probability Density Plot - the 85th Time Point	10.2d
10-6	Conditional Probability Density Plot - the 90th Time Point	10.2e
10-7	Conditional Probability Density Plot - the 95th Time Point	10.2f
10-8	Conditional Probability Density Plot - the 100th Time Point	10.2g
10-9	Conditional Probability Density Plot - the 105th Time Point	10.2h

List of Illustrations (Continued)

LIST OF ILLUSTRATIONS

<u>FIG. NO.</u>		<u>PAGE</u>
10-10	Conditional Probability Density Plot - the 200th Time Point	10.2i
10-11	Conditional Probability Density Plot - the 350th Time Point	10.2j
10-12	Monte Carlo Simulation Results	10.3e
10-13	Signal Suppression Measurement	10.4a
11-1	Implementation #1	11.1a
11-2b	Further Simplification	11.1b
11-3	Implementation	11.2a

<u>TABLE NO.</u>	<u>LIST OF TABLES</u>	<u>PAGE</u>
10-1	Results of Individual Runs M=56 R=1.0 F=10.	10.3a
10-2	Results of Individual Runs M=56 R=.75 F=10.	10.3b
10-3	Results of Individual Runs M=56 R=.50 F=10.	10.3c
10-4	Results of Individual Runs M=56 R=.25 F=10.	10.3d

1. STATEMENT OF PROBLEM

Phase-locked loops in a number of variations constitute one of the very important basic circuit building blocks available to the communication system designer. Commonly PLL's are used in preference to passive band-pass filters in cases where some special narrow banding or sensitivity requirement precludes the latter.

The sensitivity limit of the ordinary phase-locked loop is reached where the signal drops to a level such that the output phase jitter is somewhere in the order of $1/2$ radian. Beyond this point the phase-locked loop is quite likely to lose lock and the phase jitter increases very rapidly.

Since even a very few db extension of this threshold may be of considerable economic value in applications where sensitivity is critical, the subject of threshold and threshold extension has received considerable theoretical and developmental emphasis, Van Trees (7), Develet (8,9), Cahn (10), Spilker (12), among others have given first-order approximate analysis of the threshold phenomenon. Viterbi (5) has introduced the Fokker-Plank analysis which provides an exact threshold solution in certain cases. Charles and Lindsey (Ref.12) have published experimental data generally confirming Viterbi's Fokker-Plank analysis. Various modifications of the basic phase-locked circuit including FM feedback (16), Tanlock (13,15), bank division (14), and sub-harmonic operation (17) have been studied as means of extending the threshold of the basic PLL prototype to some extent in special cases.

The present study was motivated by recent developments (1,2) in the theory and practical realization of optimum non-linear filters or estimators, capable in principle of achieving the Bayesian optimal estimate of a variable (here phase, θ) given some noisy observations of a non-linear functional (here $\sin \theta$, $\cos \theta$ of the variable plus a dynamical model of the statistics of the variable (i.e., a state model of the phase). This theory is the natural extension of the linear Kalman-Bucy theory into the domain of non-linear

functional observations and as such includes the latter as well as the Wiener theory as special cases.

This approach leads at the outset to the abandonment of the basic PLL prototype. Rather, the form of the optimum phase estimator is developed as an outcome of the theory and the prototype is seen to be quite different in general. In the special case where the signal-to-noise ratio is very high, i.e., well above the threshold of the corresponding PLL, the optimal non-linear filter is shown to approach the phase-locked filter asymptotically in form as well as performance, an intuitively satisfying result. In general, however, for low signal/noise ratio the form of the optimal filter differs from the PLL in a form that would have been quite difficult to derive intuitively; this is probably the major contribution of the present development.

The overall framework of the present study may be illustrated as a block diagram as in Figure 1-1. The signal is modelled as an integrated white noise or Brownian motion phase modulating a carrier frequency signal $\cos \omega_0 t$. This type of signal could arise, for example, from frequency modulation by a signal having an essentially white or flat spectrum, or alternatively, by doppler effect due to transmitter motion with the target velocity (doppler frequency) having an essentially flat spectrum.

The choice to restrict the present exploratory study to the first-order phase process (Brownian motion phase) was dictated by several factors including the fact

- 1) the Wiener optimum phase-lock loop which is to be used as a point of performance reference is of first-order and much more extensive analyses are available than for higher order loops
- 2) the optimum non-linear filter is one-dimensional and this makes it much easier to simulate digitally (i.e., faster computation).

However, the basic technique is equally applicable to higher-order problems and loops and with the expectation that any improvement differential will be even more apparent in the higher-order loops where the consequences of loss of lock are more serious.

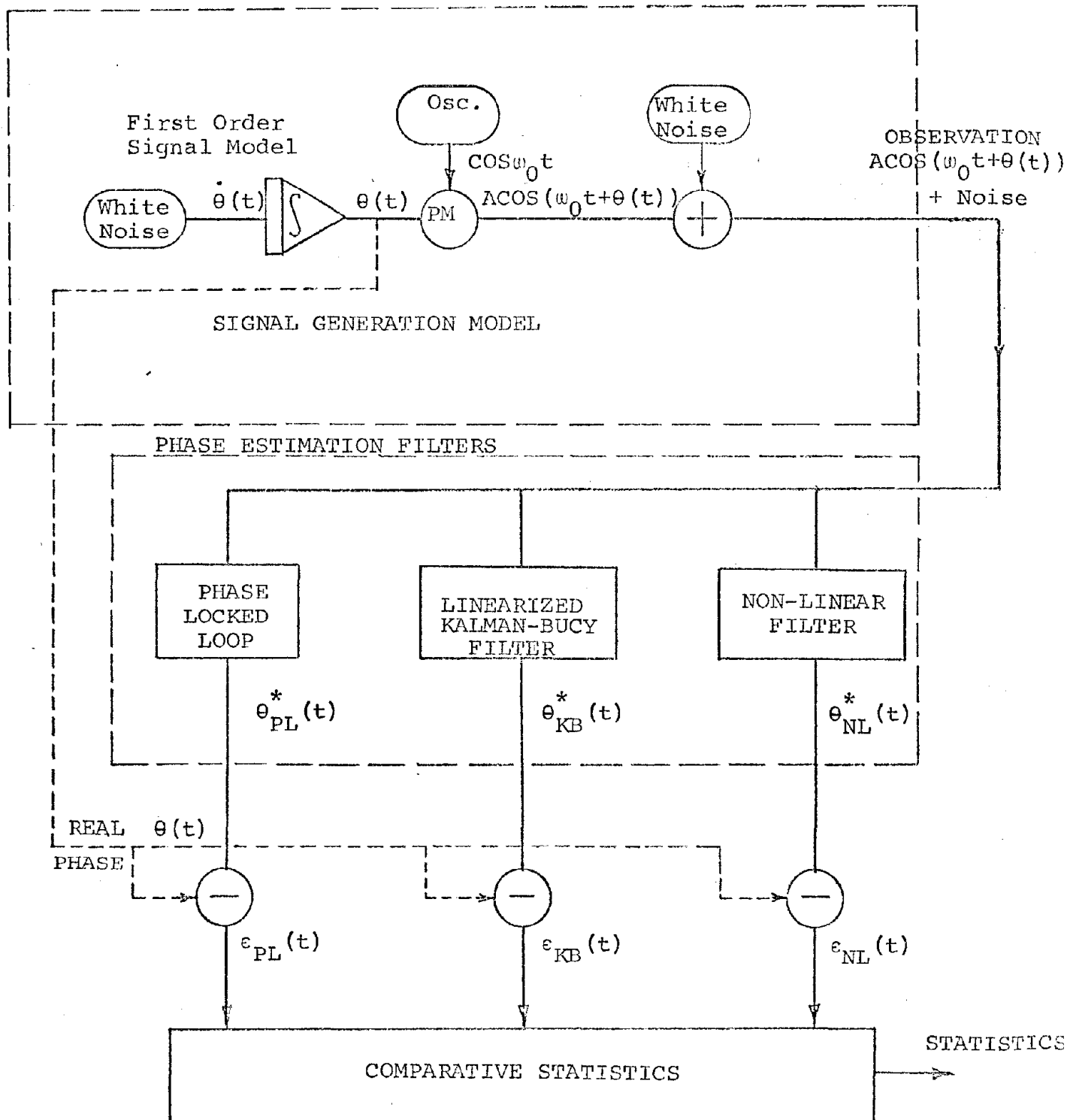


Figure 1-1
OVERALL DIAGRAM FOR COMPARATIVE STUDY OF
PHASE ESTIMATION FILTERS

Continuing with reference to Figure 1-1. The true signal $A \cos(\omega_0 t + \theta(t))$ is corrupted by additive white noise. This noisy phase modulated signal then constitutes the available observation and the problem is to compare various means of extracting an estimate, $\theta^*(t)$, of the phase or information. As a reference for this process we take the classical phase-locked loop. The second estimator is the Linearized Kalman-Bucy Filter, and finally the optimum Non-Linear filter. Since in the simulation we have available the true phase $\theta(t)$ we can find the error of each estimate and finally extract the various error statistics.

For the phase-locked loop and linearized KB filter good approximate expressions are available against which to compare the experimental statistics. For the non-linear filter this is not the case, in general, and experimental or Monte Carlo techniques of this type are the only presently known way of studying its actual performance.

It should be recognized at the outset that there are two basically different types of utilization of the phase-locked loop and correspondingly two different types of criteria against which they may be optimized and evaluated. To distinguish these two types we define the terminology

Continuous Phase Tracking to denote problems such as Doppler tracking where an accurate cumulative count of elapsed cycles is significant and cycle slips induce a lasting error

Modular Phase Tracking to denote problems such as phase demodulation where only the phase error modulo 2π is of significance and cycle slips are of importance only in their transient effect on this modular error.

In the present study we have addressed particularly the latter problem, i.e., Modular Phase Tracking and our approach has been optimized and evaluated relative to such a criterion. Some incidental results on cycle slippage fall out but it should be emphasized that more efficient approaches may well exist where continuous phase tracking is a prime objective.

The next few chapters will expand the details of the discrete (sampled) time representation of the signal processes and optimization of the various estimators for the problem at hand.

2. BASIC ORIENTATION TO THE OPTIMAL NON-LINEAR PHASE ESTIMATOR

Our purpose in this section is to describe the theoretic results in a general way to try and paint the "big picture" and in general we leave the details to the references or the later chapters in the text.

First of all, we should discuss the notion of an optimal estimate, for example, of phase, based on some observations. In general, noise effects will mean that we can seldom if ever hope to estimate the phase perfectly. The most we can ask is that the average error of estimate be minimized in some sense; and this sense needs careful definition. The mean-square error criterion, i.e., $\langle \epsilon^2 \rangle$, is but one of any number of possible "loss functions", $L(\epsilon)$. We shall find in the present context of a phase estimator that the error criterion $L(\epsilon) = (1 - \cos \epsilon)$ has attractive properties in that it is equivalent to ϵ^2 when ϵ is small but has the appropriate periodicity when ϵ is large.

Having defined a loss function the estimation problem reduces to choosing that estimate of the variable which minimizes the expected value of the loss function, given the observations. This may be derived directly from the conditional probability density function of the variable given the measurements, i.e.,

$$p(x \mid z_1, z_2, \dots)$$

which summarizes the spread of uncertainty as to the true value of x given all the measurements z_1, \dots to date. If this conditional density is available the problem of choosing an "optimal" estimate relative to the loss function $L(\epsilon)$ reduces simply to choosing an estimate x^* such as to minimize the expected loss in the light of the observations

$$\hat{L}(x^*) = \int L(x^* - x) p(x \mid z_1, z_2, \dots) dx \quad 2.1)$$

or x^* is the solution of

$$0 = \int L'(x^* - x) p(x \mid z_1, z_2, \dots) dx \quad 2.2)$$

provided that

$$\hat{L}_{xx} \geq 0$$

The estimation is thus straightforward once we are given the conditional density function $p(x|z_1, \dots)$. Finding this conditional density function thus constitutes the heart of the estimation problem. Our approach is based on sequential application of Bayes Lemma and results in a recursive scheme whereby the old density

$$p(x_i | z_{i-1}, z_{i-2}, \dots, z_1)$$

and a new measurement

$$z_i$$

are combined to give the updated density

$$p(x_{i+1} | z_i, z_{i-1}, \dots, z_1)$$

This sequential Bayes rule is developed in simple form in Appendix 1 and the consequences of its application to the present problem are briefly previewed in the following paragraphs.

We will be concerned with the problem of a phase process given by

$$\text{Model} \quad x_{n+1} = x_n + u_n : \text{ or } dx = d\tilde{u} \quad \dagger \quad 2.3)$$

where u_n and $d\tilde{u}$ are discrete and continuous Gaussian band-limited white noise processes with variance $B = q\Delta$ and two-sided spectral density q respectively. Of course, Δ is the discrete time step, and we will assume that Δ is small enough so that

\dagger We use the nomenclature

$$\tilde{u}(t) = \int_0^t u(t_1) dt_1, \quad d\tilde{u} = \int_t^{t+dt} u(t_1) dt_1$$

where $u(t)$ is band-limited white noise.

$\tilde{u}(t)$ is then similar, at least in its important low-frequency characteristics, to Brownian motion, for which equations of this type (2.3) have a complete theory. In the sequel we will approximate the \tilde{u} process as Brownian motion in order to bring this theory to bear and equations of the form of 2.3) may be interpreted as stochastic differential equations. See section 3.2.

either equation describes essentially the same phenomenon. Our interest will be centered on finding estimators x_n^* or $x^*(t)$ which are functions of the observations.

We take our observation to be of the form, in the continuous domain

$$z(t) = A \cos(\omega_0 t + x(t)) + w(t)$$

where $w(t)$ is white noise of two-sided spectral density $\bar{\Phi}_0$.

A and ω_0 are assumed known so that by normalizing to unit amplitude and heterodyning down to baseband via in-phase and quadrature detectors we have, without any loss in generality, the effective standardized observations with which we will deal henceforth.

	Discrete Time Form	Continuous Time Form	
<u>Observations</u>	$z_{1n} = \cos x_n + v_{1n} \quad \dagger$ $z_{2n} = \sin x_n + v_{2n}$	$d\tilde{z}_1 = \cos x dt + d\tilde{v}_1$ $d\tilde{z}_2 = \sin x dt + d\tilde{v}_2$	2.4)

where

$$v = w/A$$

$dv_i \quad i = 1, 2$ are independent white noises of two-sided spectral density:

$$2r = \frac{\bar{\Phi}_0}{A^2/2} = \frac{\text{noise density (two-sided)}}{\text{signal power}}$$

$v_{in} \quad i = 1, 2$ are independent Gaussian sequences of variance:

$$C = \frac{2r}{\Delta}$$

The phase estimation problem consists in finding an estimator x_{n+1} , or $x^*(t)$ for the phase process as a function $z_{i_n} \dots z_{i_0}$ or sample functions $z_i(t)$.

The phase-locked loop is of such form, namely:

$\dagger z_{1n}$ denotes $(z_1)_n$, i.e., the n^{th} discrete time point of z_1

$$dx^* = \frac{1}{F^*} (\cos x^* d\tilde{z}_2 - \sin x^* d\tilde{z}_1) \quad 2.5)$$

$$= \frac{1}{F^*} (\sin(x-x^*) dt + \cos x^* d\tilde{v}_2 - \sin x^* d\tilde{v}_1)$$

or in discrete form

$$x_{n+1}^* = x_n^* + \frac{\Delta}{F^*} (\cos x_n^* z_{2n} - \sin x_n^* z_{1n}) \quad 2.6)$$

$$= x_n^* + \frac{\Delta}{F^*} (\sin x_n - x_n^*) + \cos x_n^* v_{2n} - \sin x_n^* v_{1n}$$

($\frac{\Delta}{F^*}$ is small, see Section 3)

where $F^* = \sqrt{\frac{2r}{q}}$. The gain F^* in this case is determined by approximating $\sin(x-x^*)$ by $x-x^*$ and choosing F^* to minimize the mean-square error in the Wiener sense which can be seen to be $R = \sqrt{2qr} = \sqrt{BC}$ (see Section 4).

The actual error performance of the phase-lock loop can be determined as Viterbi has done by finding the distribution of $\epsilon = x-x^*$ using the Fokker-Plank equation. The result is that the error probability density function, $p(\epsilon, t)$ is given as the solution to

$$\frac{\partial p(\epsilon, t)}{\partial t} = \frac{\partial}{\partial \epsilon} \left(\frac{1}{F^*} \sin(\epsilon) p \right) + q \frac{\partial^2}{\partial \epsilon^2} p \quad (1)$$

which has the steady state solution, for the error modulo 2π ;

$$p(\epsilon) = \frac{e^{\alpha \cos \epsilon}}{2\pi I_0(\alpha)} \quad \text{with } \alpha = \frac{1}{R} \quad 2.7)$$

(=linearized loop S/N)

where I_0 is the 0th order Bessel function of imaginary argument. As one might expect when R is small the classical phase-lock loop performs in an optimal fashion, and for all values R the variance of $p(\epsilon)$ predicts well the error performance of the phase-lock loop.

(1) Viterbi analyzes a plant noise free case, but the same analysis is valid for our more general situation, see Section 5.

The purpose of the present study is to design a phase estimator with optimal performance for all values of R . Using the theory of non-linear filtering the optimal filter relative to the Loss Function $L(\epsilon) = 1 - \cos \epsilon$ for the case $B = 0$, i.e., a constant phase, can be determined analytically as

$$\begin{aligned} dC_1 &= \frac{d\tilde{Z}_1}{2r} \\ dS_1 &= \frac{d\tilde{Z}_2}{2r} \\ dx^* &= \frac{1}{2rD} (\sin(x-x^*) dt + \cos x^* d\tilde{V}_2 - \sin x^* d\tilde{V}_1) \end{aligned} \quad (2) \quad 2.8)$$

$$\text{where } D = (C_1^2 + S_1^2)^{1/2}$$

The reader should note the similarity between this filter which we call the static phase filter and the phase-lock loop; they differ only in a non-linear, i.e., data dependent gain factor, D .

In the general case with state noise ($B, q \neq 0$) one must first solve for the conditional density function, $J(x)$, as developed in Section 3; then the optimal estimate relative to the loss function $L(\epsilon) = 1 - \cos \epsilon$ is

$$x^* = \arctan \frac{\hat{S}}{\hat{C}}$$

where \hat{S} , \hat{C} are the conditional expectations of $\sin x$ and $\cos x$, namely

$$\begin{aligned} \hat{S} &= \int \sin(x) J(x) dx \\ \hat{C} &= \int \cos(x) J(x) dx \end{aligned}$$

Now although not yielding a fully closed solution it is of interest to see what differential equation x^* satisfies in order to relate the optimal non-linear filter to the PLL. This is shown to be

$$dx^* = - \frac{w \cdot d\tilde{I}}{D^2 2r} \quad 2.9)$$

(2) C_1 and S_1 are related to $\widehat{\cos x}$ and $\widehat{\sin x}$ for $B = 0$.

$$d\hat{C} = -\frac{q}{2}\hat{C}dt + \frac{k_2}{2r}d\tilde{I}$$

$$d\hat{S} = -\frac{q}{2}\hat{S}dt + \frac{k_1}{2r}d\tilde{I}$$

$$dD = \left[-\frac{q}{2}D + \frac{1}{4rD^3} \|\underline{w}\|^2 \right] dt + \frac{\underline{\ell} \cdot d\tilde{I}}{2rD}$$

$$\text{with } d\tilde{I} = \begin{vmatrix} d\tilde{z}_1 - \hat{C}dt \\ d\tilde{z}_2 - \hat{S}dt \end{vmatrix}$$

$$\underline{w} = \hat{S}k_2 - \hat{C}k_1; \quad \underline{\ell} = \hat{C}k_2 + \hat{S}k_1; \quad \underline{w} \cdot \underline{\ell} = 0$$

$$k_1 = (\hat{S}\hat{C} - \hat{S}\hat{C}, \hat{S}^2 - \hat{S}\hat{S})$$

$$k_2 = (\hat{C}^2 - \hat{C}\hat{C}, \hat{S}\hat{C} - \hat{S}\hat{C})$$

where the $\hat{\cdot}$'s denote conditional expectation and $D = (\hat{S}^2 + \hat{C}^2)^{1/2}$

Now when R is small we show later that $\underline{w} = RD(-\sin x^*, \cos x^*)$ and $D \approx 1$ for small R so that the x^* equation agrees with the phase-lock loop as it should.

Unfortunately in order to build the optimal filter as \underline{w} and D are in general unknown the above equation is not a closed solution and it is necessary to find the conditional density J_n of x_{n+1} given $z_{i_0} \dots z_{i_n}$. This conditional density summarizes all the information contained in z_{i_0} sequence about the phase, so that knowledge of this density allows the determination of the estimate which minimizes any loss function. From our analysis for small R the phase-lock estimate effectively minimizes the expected value of $1 - \cos(x - x^*)$ as x^* ranges over all possible estimators, as we have seen in this summary and will see in detail later on the estimate which minimizes the above loss for all R , x^* differs by a non-linear gain factor from the phase-lock loop, and, in fact, the minimum loss is $1 - D^2 \doteq 1 - e^{-R} \approx R$ for R small.

We use a sequential convolution equation which updates $J_n(x)$ to $J_{n+1}(x)$ and evaluate the performance of x_{n+1}^* computed from knowledge of $J_{n+1}(x)$ by Monte Carlo trials. The non-linear filter has been used as an effective design tool for other problems with spectacular success, see Ref.2. The thesis of Lo (Ref.3) describes examples where non-linear processing is mandatory for good performance. Finally we report some preliminary results on practical synthesis using Fourier methods. The practically oriented reader may comment that it is too bad that only a first-order phase model was used, as in practise a phase-lock loop is pertinent only for detecting randomly accelerating phases. Our approach was dictated by exigencies of time and the fact that until the research of (Ref.2) appeared it seemed that two-state dimensional problem required inordinate computing for Monte Carlo evaluation. We plan to investigate the general problem in the next year and feel that the non-linear approach offers even more spectacular performance betterment for this more realistic problem.

3. BASIS OF THE DISCRETE SIMULATION

The ultimate objective of the present development is a phase estimator working in real time. This may be either a continuous (analog) or discrete time (sampled) system.

The present simulation effort, however, is based on discrete time, digital representation of the signal, measurement, and filter.

This section treats certain subtle points concerning the sampled representation of the continuous noise-like signal and measurement, establishes the basis of the discrete time model, and the optimum phase-locked loop and Kalman-Bucy filter to serve as points of reference for the non-linear filter.

3.1. The Phase Signal in the Continuous Domain

The continuous signal serving as common input to all three estimators corresponds to phase modulation by integrated white noise as might correspond, for example, to either frequency modulation by a random white noise-like signal or doppler resulting from a target moving with velocity modeled as a white-noise-like process. The observed signal with additive noise is then

$$s(t) = A \cos [\omega_0 t + x(t)] + w(t) \quad 3.1)$$

where

$$x(t) = K \int_0^t u(t) dt \quad 3.2)$$

$$\text{or } \dot{x}(t) = Ku$$

$w(t)$ is narrowband white noise of spectral density δ_0 (two-sided)

$u(t)$ is low-pass white noise of spectral density G_u (two-sided).

It follows that the spectrum of $x(t)$ is

$$G_x(f) = \frac{K^2 G_u}{(2\pi f)^2}$$

or defining

$$q \equiv K^2 G_u, \quad \omega = 2\pi f \quad 3.3)$$

$$G_x(f) = \frac{q}{\omega^2}$$

It is convenient to represent the additive noise w in terms of its quadrature components

$$w(t) = w_1(t) \cos(\omega_0 t) - w_2(t) \sin(\omega_0 t)$$

where w_1 and w_2 are low-pass, independent white noise processes of two-sided spectral density

$$G_{w_1} = G_{w_2} = 2\Phi_0 \quad 3.4)$$

The negative sign on w_2 here is chosen for later convenience.

The factor 2 in 3.4) may be viewed as arising because of folding of the full IF bandwidth B into the low-pass bandwidth $B/2$ and may be confirmed by noting that the total noise power is the same in either representation. With this convention

$$s(t) = A \cos[\omega_0 t + x(t)] + w_1(t) \cos \omega_0 t - w_2(t) \sin \omega_0 t \quad 3.5)$$

Now, since none of the estimators being considered depends on the carrier frequency directly, the discrete simulation of this process is simplified by considering it heterodyned down to essentially zero or D.C. Intermediate-Frequency. As is well known, in order to preclude a loss of information due to the folding inherent in this process it is necessary to provide separate in-phase and quadrature channels for the D.C., I.F.. At the same time it will be convenient to normalize the amplitude A to unity. Accordingly, multiplying by again $\frac{1}{A}$, heterodyning by the local oscillator signals $(2 \cos \omega_0 t)$ and $(-2 \sin \omega_0 t)$ and discarding the double carrier frequency terms yields the zero frequency IF terms z_1 and z_2 :

$$z_1(t) = \frac{1}{A} (2 \cos \omega_0 t) \cdot s(t)$$

$$\boxed{z_1(t) = \cos x(t) + v_1(t)} \quad 3.6)$$

$$z_2(t) = \frac{1}{A} (-2 \sin \omega_0 t) \cdot s(t)$$

$$\boxed{z_2(t) = \sin x(t) + v_2(t)} \quad 3.7)$$

where v_1 and v_2 are independent white noises of spectral density (two-sided)

$$2r = \frac{2\bar{\sigma}}{A^2}$$

and x is integrated white noise of spectral density (two-sided)
 q/ω^2

The two signals z_1 z_2 are biuniquely equivalent to s in the sense that they are derivable from s by a simple gain and heterodyne operation and conversely s is derivable from z_1 and z_2 similarly. There is no loss or addition of essential information by representing the narrowband process s by the two quadrature low-pass processes z_1 and z_2 (or the complex process $z_1 + iz_2$).

It is convenient at this point to define the basic parameters

$$\begin{aligned} R &= \sqrt{2rq} \\ &= \text{phase error variance} \\ F^* &= \sqrt{\frac{2r}{q}} \\ &= \text{time constant} \end{aligned}$$

for the optimal estimator in the associated linear problem.

3.2. Representation and Sampling of "White Noise"

The continuous signal described above, includes "white noise" sources and as such cannot be represented with any fidelity whatsoever by discrete samples at a finite spacing Δ . Nevertheless, we know intuitively that in some sense the loop filter operation on such signals can be accurately simulated with such discrete samples provided that they are spaced much closer than any significant loop time constants. To resolve these apparently conflicting ideas it is necessary to observe that while we may in principle refer to a particular signal as "white noise", physically it must have some cutoff at high frequencies. Furthermore, any observing instrument we use to look at the noise has its own high frequency cutoff so that we can never see "white noise" even if it were present (for one thing, since it would have infinite variance, it would immediately burn out our instrument). Thus, whenever we speak of "white noise" what we really mean physically is noise whose spectrum is flat at least up to frequencies high enough that they are no longer of significance in the problem at hand, or "low-pass white noise".

One way of dealing with such noise rigorously would be to assign a cutoff frequency f_c to each "white noise" generator, and very carefully keep track of the effect of such cutoffs all the way through the circuit analysis until the very end where (hopefully) it could be shown that they could be made high enough that they had no effect, i.e., that the circuit performance was asymptotically independent of f_c for f_c greater than some critical value.

There is, however, a simpler and more tractable approach in terms of the Ito calculus of stochastic differential equations. This results from representing a "white noise" process, say " $w(t)$ ", wherever it occurs as the rate of the associated "Brownian noise" " $\tilde{w}(t)$ " defined as the integrated "white noise":

$$\tilde{w}(t) = \int_0^t w(t_1) dt_1 \quad 3.8)$$

For purely white noise the above integral has no meaning and must be replaced by a stochastic integral, however, for physical "white noise" the operation is perfectly legitimate and leads to the relationship

$$"d\tilde{w}" = "w(t)" dt \quad 3.9)$$

where the quotation marks denote always that we are referring to band-limited or physical quantities. Now physical white noise is not at all well represented by pure white noise - there is infinite variance in the error of the best such representation.

$$"w(t)" \neq w(t)$$

however, physical (bandlimited) Brownian noise is well represented by its pure Brownian noise counterpart

$$"\tilde{w}(t)" \approx \tilde{w}(t)$$

so that at this point we can legitimately, if somewhat heuristically, forget the physical bandwidth limitation (and the quotation marks). By this artifice we make available to the problem at hand the full facilities of the very powerful theory of stochastic differential equations.

A peculiarity of Brownian motion is that the variance of $\tilde{w}(t)$ is given by

$$E[\tilde{w}(t)^2] = \int_0^t \int_0^t E[w(t_1) w(t_2)] dt_1 dt_2 \quad 3.10)$$

but if w has two-sided spectral density r then the covariance function in the integral is just $r\delta(t_1 - t_2)$ so

$$\boxed{E[\tilde{w}(t)^2] = rt} \quad 3.11)$$

i.e., linear in t .

In a formally similar way, since the successive increments of \tilde{w} are independent

$$\begin{aligned} E[d\tilde{w}^2] &= E[(w(t) dt)^2] \\ &= r dt \end{aligned} \quad 3.12)$$

Thus we can write eqtn. 3.1) and 3.2) in the form of stochastic differential equations (Ref.22, sec.2.6)

$$d\tilde{z} = A \cos [\omega_0 t + x(t)] dt + d\tilde{v} \quad 3.13)$$

$$dx = K d\tilde{u} \quad 3.14)$$

$$\text{where } E[d\tilde{u}^2] = q dt \quad 3.15)$$

$$E[d\tilde{v}^2] = r dt \quad 3.16)$$

from which it follows also that

$$E[dx^2] = K^2 q dt \quad 3.17)$$

$$E[d\tilde{z}^2] = E[d\tilde{v}^2] = r dt \quad 3.18)$$

Note that $x(t)$ as given above is inherently a Brownian motion, in other words, it inherently has a high frequency cutoff so that we can deal with x directly.

The reasons for this transformation are

- 1) We have obviated the necessity for dealing with intractable "white noise"
- 2) In place of white noise we now have increments of Brownian motion for which a full and powerful theory is available (see Ref.1).

Our estimates, as it will turn out, will involve differential equations driven by z , i.e., equations of the form

$$\dot{y} = f(y) + g(y) \cdot z \quad 3.19)$$

or in the present nomenclature, since z is a "white noise" process

$$dy = f(y) dt + g(y) d\tilde{z} \quad 3.20)$$

$$\text{where } d\tilde{z} = A \cos (\omega_0 t + x) dt + d\tilde{v}$$

and we note that by the former rules

$$E[(dy)^2] = f^2 dt^2 + g^2 E[(dz)^2] \quad 3.21)$$

$$= g^2 r dt \quad 3.22)$$

We will also be concerned with smooth functionals, say $g(y)$, of smooth functions such as $y(t)$ and the differential equations they implicitly satisfy. That is, for any such functional:

$$dh(y) = h'(y) dy + \frac{1}{2} h''(y) (dy)^2 + \dots \quad 3.23)$$

Now in ordinary calculus we would ignore the second term on the right as being of second-order infinitesimal; in the present case of stochastic differential equations, however, we see that it has a component, namely its expectation, which is of first-order as given above. This leads to the very important Ito lemma

$$dh(y) = h'(y) dy + \frac{1}{2} h''(y) E[(dy)^2] \quad 3.24)$$

$$dh(y) = h'(y) [f(y) dt + g(y) dz] + \frac{1}{2} h''(y) g^2 dt \quad 3.25)$$

The extension to successive functionals and to vector valued independent or independent variables is obvious.

We now show how the same concept of replacing white noise by increments of its associated Brownian motion leads also to a precise and physically satisfying definition of its discrete samples. We have already noted that while any physically realizable observing instrument has a finite bandwidth, the exact form of its bandwidth restriction does not matter provided the bandwidth is in some sense "sufficient". Consequently we are free to choose the form of the bandwidth restriction for convenience. One form of pre-sampling bandwidth restriction that is particularly relevant is

$$O[v(t)] = \frac{1}{\Delta} \int_{t-\Delta}^t v(t_1) dt \quad 3.26)$$

i.e., the normalized definite integral of the function over one sample interval. This is just the integrate and dump transfer function incorporated in so-called "integrating" digital voltmeters. Note, that by the normalization, that for a constant or slowly varying (smooth) voltage v

$$O[v(t)] = v(t - \epsilon) \quad 0 < \epsilon < \Delta \quad 3.27)$$

that is, a valid sample of v at some intermediate point by the mean value theorem.

The transfer function equivalent of this observation operator is a low-pass-type having zeroes at all multiples of the sampling frequency so that on sampling at intervals Δ there is no aliasing of high frequency parts into very low frequencies. Our sample then for any function $v(t)$ defined in the continuous domain and which may include "white noise" or smooth variables is:

$$v_n = O[v(n\Delta)] \quad 3.28)$$

$$= \frac{1}{\Delta} \int_{(n-1)\Delta}^{n\Delta} v(t_1) dt_1 \quad 3.29)$$

$$\boxed{v_n \equiv \frac{1}{\Delta} [\tilde{v}(n\Delta) - \tilde{v}((n-1)\Delta)]} \quad 3.30)$$

i.e., our samples are just the increments of the Brownian motion \tilde{v} associated with v . This somewhat drawn out definition of what we mean by a sample is essential if our sample is to have any meaning for "white noise" as well as for better behaved functions.

It will be important for the following parts to note that if v is white noise of spectral density r such that

$$E[(d\tilde{v})^2] = r dt \quad 3.31)$$

then

$$E[v_n^2] = \frac{r\Delta}{\Delta^2} = \frac{r}{\Delta} \quad 3.32)$$

This is fully equivalent to stating that the sample process has an effective two-sided noise bandwidth

$$\boxed{B_{\text{eff}} = \frac{1}{\Delta}} \quad 3.33)$$

since then

$$E[v_n^2] = rB_{\text{eff}} = \frac{r}{\Delta} \quad 3.34)$$

The important thing about this operational definition of the samples is that if the continuous functions are related by a given stochastic differential equation then their samples so defined should be related by the corresponding difference equation.

That is, if

$$dy = f(y) dt + g(y) d\tilde{v} \quad 3.35)$$

then for sufficiently small Δ we should expect that:

$$y_n - y_{n-1} = \Delta[f(y_{n-1}) + g(y_{n-1}) \cdot v_n] \quad 3.36)$$

Eqtn. 3.36) is indeed seen to follow from 3.35) and the above definitions if we integrate over one sample period

$$\int_{(n-1)\Delta}^{n\Delta} dy = \int_{(n-1)\Delta}^{n\Delta} f(y) dt + \int_{(n-1)\Delta}^{n\Delta} g(y) d\tilde{v}$$

but for $\Delta \rightarrow 0$, since y , f , and g are smooth this approaches

$$\begin{aligned} y_n - y_{n-1} &= f(y_{n-1})\Delta + g(y_{n-1}) \cdot \Delta \cdot \left[\frac{1}{\Delta} (\tilde{v}(n\Delta) - \tilde{v}((n-1)\Delta)) \right] \\ &= \Delta[f(y_{n-1}) + g(y_{n-1}) \cdot v_n] \end{aligned}$$

from the definition, eqtn. 3.28), q.e.d..

Also, as a special case, for our measurement equations which appear in the form

$$d\tilde{z} = h(x) dt + d\tilde{v}$$

it follows that

$$z_n = h(x_n) + v_n$$

3.3. Digital Representation of the Signal

Based on the foregoing theory, the digital, i.e., sampled, simulation of the signal process may be represented by the following equations.

$$x_i = x_{i-1} + u_{i-1} \quad 3.37)$$

$$z_{1_i} = \cos(x_i) + v_{1_i} \quad 3.38)$$

$$z_{2_i} = \sin(x_i) + v_{2_i} \quad 3.39)$$

v_1, v_2 , and u are independent random normal variates with variance defined by

$$\overline{v_{1_i}^2} = v_{2_i}^2 = C \quad 3.40)$$

$$u_i^2 \equiv B \quad 3.41)$$

To relate to the continuous case let one simulation step represent a real-time Δ .

A serially independent discrete process such as u or v may be regarded as having an effective two-sided bandwidth equal to $\frac{1}{\Delta}$. Consequently the spectral densities are

$$\begin{aligned} G_{v_1} &= G_{v_2} = \overline{v_1^2} \Delta \\ &= \Delta C \end{aligned} \quad 3.42)$$

Thus, to relate to the continuous case, eq. 3.4):

$$C = \frac{2r}{\Delta} \quad 3.43)$$

The integrator gain K as defined by eq. 3.2) for the continuous case is seen to be implicit in equation 3.37). Thus, considering u a constant,

$$x_i = iu$$

or

$$\begin{aligned} x(t) &= \frac{t}{\Delta} u \\ &= \frac{1}{\Delta} \int u dt \end{aligned}$$

Thus by comparison with 3.2) the implicit integrator gain is

$$K = \frac{1}{\Delta}$$

so from 3.3)

$$G_x = \frac{K^2 G_u}{\omega^2} \quad 3.44)$$

$$= \frac{\Delta B}{\Delta^2 \omega^2} \quad 3.45)$$

$$= \frac{q}{\omega^2}$$

or

$$\boxed{B = q \cdot \Delta} \quad 3.46)$$

It will be convenient to define, for future purposes, the basic parameters

$$\boxed{F = \sqrt{\frac{C}{B}} = \frac{1}{\Delta} \sqrt{\frac{2r}{q}}} \quad 3.47)$$

and

$$\boxed{R = \sqrt{BC} = \sqrt{2rq}} \quad 3.48)$$

It will turn out that F plays the role of the filter time constant in sample interval units, while R is related to the variance of the ideal estimate.

4. KALMAN-BUCY FILTER-LINEARIZED PROBLEM

The discrete Kalman-Bucy Filter operates directly in the discrete domain on observation consisting of equations 3.38) and 3.39):

$$z_{1_i} = \cos x_i + v_{1_i} \quad 3.38)$$

$$z_{2_i} = \sin x_i + v_{2_i} \quad 3.39)$$

where $x(t)$, the desired phase information, is governed by the plant model, equation 3.37)

$$x_i = x_{i-1} + u_i \quad 3.37)$$

where v_1, v_2, u_i are serially and mutually independent random variates with

$$\overline{v_1^2} = \overline{v_2^2} = C \quad 3.40)$$

$$\overline{u^2} = B \quad 3.41)$$

Note that the presence of the Sin and Cos functions in 3.38) and 3.39) means that the problem is inherently non-linear. The non-linear filter to be discussed in later sections performs optimally in the presence of this non-linearity. The Kalman-Bucy Filter theory pertains strictly only to the linear problem, i.e., where the observations z are linear functions of the unknown, x . This theory may be brought to bear by approximating the problem by linearization of equations 3.38) and 3.39). This is done by approximating them as first terms in a Taylor's series expansion about a reasonably good estimate. This approximation is good roughly under the same circumstances as the linearized analysis of the phase-locked loop, i.e., in the high signal/noise ratio case where the errors are small. Accordingly, linearizing equations 3.38) and 3.39) around the prior estimate, x_i^*

$$z_{1_i} \approx \cos x_i^* - (x_i - x_i^*) \sin x_i^* + v_{1_i} \quad 4.1)$$

$$z_{2_i} \approx \sin x_i^* + (x_i - x_i^*) \cos x_i^* + v_{2_i} \quad 4.2)$$

in Matrix notation then the linearized problem is

$$Z_i = Z_i^* + H_i \cdot (x_i - x_i^*) + V_i \quad 4.3)$$

$$\text{where } Z_i = \begin{bmatrix} z_{1_i} \\ z_{2_i} \end{bmatrix}$$

$$Z_i^* = \begin{bmatrix} \cos x_i^* \\ \sin x_i^* \end{bmatrix}$$

$$H_i = \begin{bmatrix} -\sin x_i^* \\ \cos x_i^* \end{bmatrix} = \frac{\partial Z_i}{\partial x_i^*}$$

$$V_i = \begin{bmatrix} v_{1_i} \\ v_{2_i} \end{bmatrix}$$

$$\text{and } x_i = x_{i-1} + u_i$$

Denoting the covariance matrix of the random vector V by

$$\Phi = \begin{bmatrix} C & 0 \\ 0 & C \end{bmatrix}$$

The extended Kalman-Bucy one-step predictor of x_{i+1} is given by (Ref. 20, 21)

$$x_{i+1}^* = x_i^* + G_i [Z_i - Z_i^*] \quad 4.4)$$

where the gain:

$$G_i = P_i H_i^T [H_i P_i H_i^T + \Phi]^{-1} \quad 4.5)$$

which simplifies to

$$G_i = \frac{P_i}{P_i + C} H^T \quad 4.6)$$

P_i is the one-step predictor error variance (of the linearized problem) given in general by

$$P_i = (H^T \Phi^{-1} H + P_{i-1}^{-1})^{-1} + B \quad 4.7)$$

which simplifies to

$$P_i = B + \frac{P_{i-1} C}{P_{i-1} + C} \quad 4.8)$$

In the steady state, $P_i = P_{i-1} \equiv \bar{P}$ and we can solve for \bar{P} as the positive root of

$$\bar{P} = B + \frac{\bar{P}C}{\bar{P} + C} \quad 4.9)$$

or

$$\bar{P} = \frac{B}{2} + \sqrt{\frac{B^2}{4} + BC} \quad 4.10)$$

In the present case - since the state transition factor (coefficient of x_{i-1} in 3.8)) is 1, the prediction estimate is identical to the filter estimate, however, their errors are different since

$$x_{i+1/i}^* = x_{i/i}^* \quad 4.11)$$

but

$$x_{i+1} = x_i + u \quad 4.12)$$

so

$$\underbrace{x_{i+1} - x_{i+1/i}^*}_{\text{predictor error}} = \underbrace{x_i - x_{i/i}^*}_{\text{filter error}} + u_i \quad 4.13)$$

or calling S the steady state discrete filter error

$$\bar{P} = \bar{S} + B \quad 4.14)$$

where $B = \text{var}(u)$

Thus

$$\bar{S} = \sqrt{B^2/4 + BC} - \frac{B}{2} \quad 4.15)$$

Note well that \bar{P} and \bar{S} as derived here pertain only to the linear problem and as such only approximate the actual performance of the filter on the real non-linear problem. The true steady state error statistics may be derived by the Fokker-Plank analysis (Ref.6 and Sec.5.1) and are confirmed by our simulations.

Equations 4.10) and 4.16) can be expressed simply in terms of the basic parameters F and R as previously defined by

$$\bar{P} = R \left[\sqrt{1 + \frac{1}{4F^2}} + \frac{1}{2F} \right] \quad 4.16)$$

$$\bar{S} = R \left[\sqrt{1 + \frac{1}{4F^2}} - \frac{1}{2F} \right] \quad 4.17)$$

Notice that for large F , i.e., as we approach the continuous case with a very small sampling interval, the predictor variance and the filter approach one another:

$$\bar{P} \rightarrow \bar{S} \rightarrow R \quad 4.18)$$

and in particular for $F = 10$ the two cases (predictor and filter) are within about 5% of ± 0.2 db of the asymptotic (continuous case) value, R . Notice that $F = 10$ corresponds by equation 5.7) to a sample rate 10 times the time constant of the optimal phase-locked loop.

Also note that in the steady state, as P_i approaches \bar{P} , the gain G_i becomes constant, approaching

$$\bar{G} = \frac{\bar{P}}{\bar{P} + C} H^T \quad 4.19)$$

and the estimator becomes, from 4.4), written out in detail:

$$x_{i+1}^* = x_i^* + \frac{\bar{P}}{\bar{P} + C} \left[A \sin(x_i - x_i^*) - v_1 \sin x_i^* + v_2 \cos x_i^* \right] \quad 4.20)$$

In other words, in the steady state, i.e., after the first few time constants, the K-B filter, with adequate F , approaches the exact point-by-point performance of the phase-locked loop. This point-by-point correspondence was confirmed in the earlier simulation runs, and subsequently, the K-B filter was not run, since its only advantage lies in improved tracking during the initial turn-on transient.

For large R , the gain term here approaches (by 4.18))

$$\frac{\bar{P}}{\bar{P} + C} = \frac{R}{R + C} \quad 4.21)$$

$$= \frac{1}{1 + F} \quad 4.22)$$

So that in the steady state, the K-B filter becomes

$$x_{i+1}^* = x_i^* + \frac{1}{1 + F} e \quad 4.23$$

$$e = \sin(x_i - x_i^*) - v_1 \sin x^* + v_2 \cos x^*$$

As we approach the continuous case by letting $\Delta \rightarrow 0$, F becomes $\gg 1$ and we have in effect

$$x_{i+1}^* = x_i^* + \frac{1}{F} e \quad 4.24)$$

In the limit as $\Delta \rightarrow 0$, 4.23) or 4.24) lead to the corresponding continuous equation

$$\dot{x}^* = \frac{1}{F^*} e \quad 4.25)$$

$$\text{where } F^* = F\Delta$$

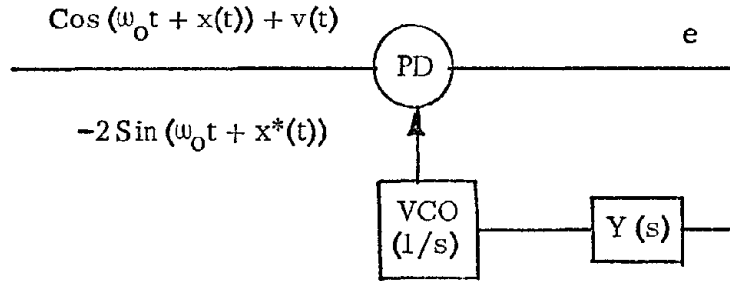
$$= \sqrt{\frac{2r}{q}} \quad 4.26)$$

This is exactly the phase-locked loop equation so that in effect we have shown two things

- 1) The K-B filter for the linearized phase estimation problem reduces to the form of the phase-locked loop in the steady state
- 2) The resulting steady state K-B gain parameters may be taken as the basis for optimization of the phase-locked loop.

5. PHASE-LOCKED LOOP

The generalized phase-locked loop diagram is as shown below



The phase detector equation is:

$$e = \left[-2 \sin(\omega_0 t + x^*(t)) \left[\cos[\omega_0 t + x(t)] + v_1 \cos \omega_0 t - v_2 \sin \omega_0 t \right] \right]_{\text{low pass}} \quad 5.1)$$

$$= \sin[x(t) - x^*(t)] - v_1(t) \sin x^* + v_2 \cos x^* \quad 5.2)$$

$$= -\sin x^* z_1(t) + \cos x^* z_2(t)$$

In the small error case

$$e \approx (x - x^*) - v_1 \sin x^* + v_2 \cos x^* \quad 5.3)$$

and the linearized analysis from the K-B theory of the previous section applies.

From the prototype

$$x^* = \frac{Y(s)}{s} e$$

and as has been shown from the K-B analysis, the optimized loop for the first-order problem at hand satisfies

$$\dot{x}^* = \frac{1}{F^*} e \quad 5.4)$$

so we identify

$$\begin{aligned} Y(s) &= \frac{1}{F^*} \\ &= \sqrt{\frac{q}{2r}} \end{aligned} \quad 5.5)$$

i. e., simply a constant. The corresponding mean-square phase error is then as for the steady-state K-B:

$$\begin{aligned} \overline{(x^* - x)^2} &= R \\ &= \sqrt{2rq} \end{aligned} \quad 5.6)$$

Also the loop time constant may be identified as

$$\tau = \frac{1}{F^*} \quad 5.7)$$

and the loop two-sided noise bandwidth in cps (two-sided) is

$$\begin{aligned} 2B_L &= 1/2\tau \\ &= F^*/2 \end{aligned} \quad 5.8)$$

5.1. Non-Linear Analysis of Phase-Locked Loop

These are the principal results for the linearized first-order phase-locked loop and may be expected to hold quite well provided R in eqtn. 5.6) is less than, say, 0.1. As the noise level increases, however, the linearization inherent in eqtn. 5.3) breaks down. Analysis of the non-linear threshold region of the PLL has been carried out from a number of different points of view (Refs. 7,8,10). Most of these are approximate treatments valid for small nonlinearity, i. e., at the onset of threshold. In the particular case of the first-order loop, however, an exact solution is possible as developed by Viterbi (Ref.6) by the Fokker Plank analysis. Viterbi's analysis is for the case of no noise on the plant, i. e., an essentially static signal (phase) but for a given loop gain or (bandwidth) but can easily be extended to the case including signal dynamics.

The basic describing equations are 3.2), 5.2), and 5.4) which can be written for a fixed gain Y :

$$\dot{x}^* = Y e$$

$$e = \sin(x - x^*) - v_1 \sin x^* + v_2 \cos x^*$$

$$\dot{x} = Ku$$

or denoting $x - x^* = \epsilon = \text{estimate error}$

$$\dot{\epsilon} = -Y \sin(\epsilon) + Ku - Yv_1 \sin x^* + Yv_2 \cos x^* \quad 5.9)$$

Here Ku is the state noise of spectral density q and v_1 and v_2 are independent quadrature components of measurement noise of spectral density $2r$.

Then by the Fokker-Plank equation the differential equation satisfied by the probability density, $p(\epsilon, t)$ of ϵ is

$$\frac{\partial p(\epsilon, t)}{\partial \epsilon} = -\frac{\partial}{\partial \epsilon} (\mu p) + \frac{1}{2} \frac{\partial^2}{\partial \epsilon^2} (\sigma^2 p) \quad 5.10)$$

$$\text{where } \mu = \text{"infinitesimal mean" of } \dot{\epsilon} \\ = -Y \sin \epsilon$$

5.11)

$$\sigma^2 = \text{"infinitesimal variance" of } \dot{\epsilon} \\ = q + Y^2 2r (\sin^2 x^* + \cos^2 x^*) \\ = q + 2rY^2$$

5.12)

In the equilibrium condition $(\frac{\partial p}{\partial t}) = 0$ and for the boundary conditions imposed by the fact that p is a probability density on $-\pi$ to π^\dagger , the solution of 5.10) is

[†] As pointed out by Viterbi, there is no equilibrium variance of error considered on the line $-\infty, \infty$. Only the modulo 2π error has such meaning and it is in this respect that we define ϵ .

$$p(e) = \frac{\exp\left(\frac{\cos e}{R_1}\right)}{2\pi I_0\left(\frac{1}{R_1}\right)} \quad 5.13)$$

$$\text{where } R_1 = \frac{q + 2rY^2}{2Y} \quad 5.14)$$

If there is no state noise ($q = 0$) this reduces to

$$R_1 = rY \quad 5.15)$$

which is just $1/\alpha$ in Viterbi's terms.

If the loop is optimized in terms of Y with state noise on the linearized basis by 5.5) or equivalently, by noting that from 5.13), $\langle e^2 \rangle$ is monotone in R_1 and simply minimizing R_1 , eqn. 5.14), then

$$Y = \sqrt{\frac{q}{2r}}$$

and

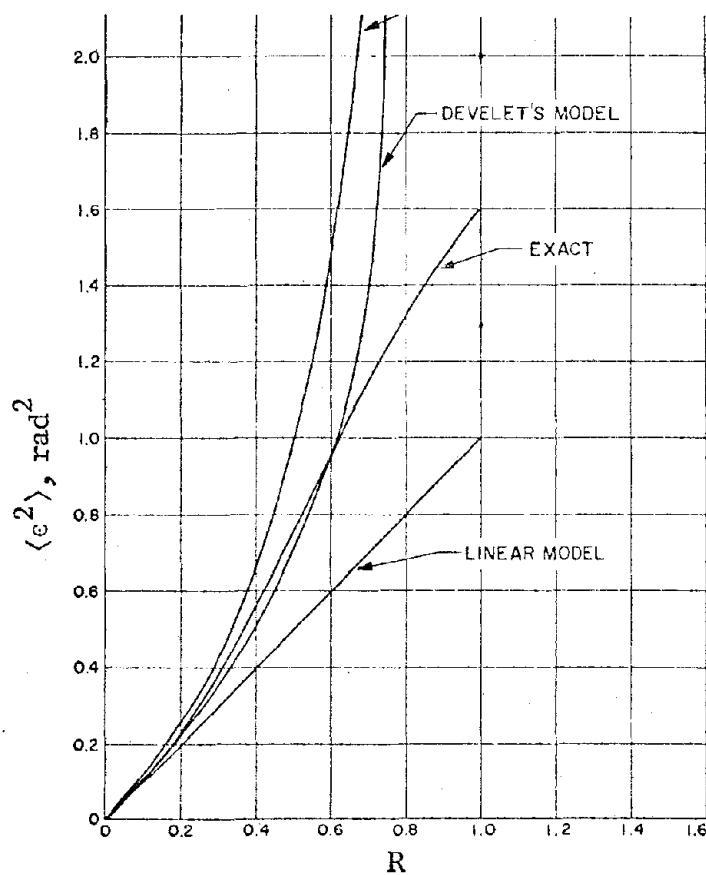
$$\begin{aligned} R_{1\text{opt}} &= \sqrt{2rq} \\ &= R \quad \text{as defined by eq. 3.23).} \end{aligned} \quad 5.16)$$

The variance of this distribution (eq. 5.12)) is plotted in Figure 5-1 (from Viterbi, Ref. 6) and labelled "exact" along with two other approximations (Refs. 7,8) to the non-linear phase-lock error. This will serve as a standard of comparison for the simulation runs later.

It should be noted at this point that in the limit of $R \rightarrow 0$, i.e., zero input signal/noise ratio the phase noise $\langle e^2 \rangle$ approaches a finite limit. This occurs when the distribution in eq. 5.13) approaches uniformity over 0 to 2π and the associated limiting phase noise variance (of error modulo 2π) is

$$\langle e^2 \rangle_{\max} = \frac{\pi^2}{3} \approx 3.29 \text{ rad}^2$$

Also note that at worst the phase-locked loop is 2.2 db worse than the ideal (but unobtainable) linear model. Measured in these terms then, that is, in terms of noise only (ignoring signal suppression effects) it seems clear that 2.2 db is the maximum improvement over the phase-locked loop that one could hope for.



Comparison of variance for first-order-phase-locked-loop
with results of approximate analyses

Figure 5-1

5.2. Discrete Phase-Locked Loop

In the light of the foregoing discussions the discrete phase-locked loop representation may be taken directly from the steady state K-B, eq. 4.23)

$$x_{i+1}^* = x_i^* + \frac{1}{(1+F)} e_i \quad 5.17)$$

$$\begin{aligned} \text{where } e_i &= \sin(x_i - x_i^*) - v_{1i} \sin x^* + v_{2i} \cos x^* \\ &= -\sin x^* z_{1i} + \cos x^* z_{2i} \end{aligned}$$

$$F = \frac{1}{\Delta} \sqrt{\frac{2r}{q}} \quad 5.18)$$

$$= \frac{F^*}{\Delta} \quad 5.19)$$

In general, F may be interpreted as the number of sample points per loop time constant. Preliminary exploratory runs have confirmed that $F = 10$, i.e., 10 points per loop time constant is adequate for roughly 10 per cent accuracy. Specifically it was found that the RMS discrepancy between points run with $F = 10$ and with $F = 30$ for the same continuous noise sample was less than 10 per cent ($R = 0.5$ and $R = 1$).

6. THE NON-LINEAR THEORY

In this section we will describe the results of the general theory necessary to understand our approach to phase estimator design. The details of the theory can be found in Ref.1, while our general technique of sequential determination of the conditional density via Bayes rule is described in Ref.2 and Ref. 4. In particular Ref. 4, which forms Appendix II, treats a very simple problem and consequently may be read to understand our digital computer methods for the realization of sequential update for $J_n(x)$ as well as detailed derivations of the sequential update for J_n , or in statistical parlance, Sequential Bayes Rule. For a general introduction to the aims and methods of filtering the reader might do well to study Ref.5. In order to fully understand the results of the continuous time problem the reader should familiarize himself with the Ito lemma, it is a fundamental tool, which may be replaced by Taylor series arguments only at the risk of long error-prone and devious calculations. We will illustrate this lemma by deriving various results stated in the introduction.

Let $J_n(x)$ denote the conditional density of phase φ_n given the observation $z_{i_{n-1}} \dots z_{i_0}$, then it is easy to establish the following recursion relation

$$J_{n+1}(y) = K \int_{-\infty}^{\infty} e^{\frac{z_{1_n} \cos x + z_{2_n} \sin x}{C}} e^{-\frac{(y-x)^2}{2B}} J_n(x) dx \quad 6.1)$$

$J_0(x)$ = the prior density of x

K chosen so that $\int_{-\infty}^{\infty} J_{n+1}(y) dy = 1.$

For a derivation of eqtn. 6.1), see Ref.1 page 59, or in detail, see Appendix 1. Notice that the model eqtn. 3.1) and 3.2) and the Gaussian assumptions have been used to derive eqtn. 6.2).

For many purposes, it is much easier to derive results in the continuous problem, instead of from the sequential Bayes Rule given by eqtns. 6.1) and 6.2), in Section 3 it has been shown how B and C can be selected to assure that the discrete data rate is equivalent to continuous observations. Of course, the phase detection problem is inherently a continuous problem, however, we consider the analogous discrete problem in order to have accurate digital realization of the filter and also because some facets of the problem are easier in this case. In order to state the continuous analog of eqtn. 6.1) it is necessary to introduce the concept of random differential equations such as

$$dx = f(x) dt + \sigma(x) d\beta \quad 6.4)$$

This may be regarded as a more rigorous and tractable form of the equation

$$\dot{x} = f(x) + \sigma(x) \cdot w(t)$$

where $w(t)$ is a "white noise" process

$$\text{and} \quad \beta(t) = \int_0^t w(x) dx$$

we assume for simplicity x is scalar valued. Physically, eqtn. 6.4) can be interpreted as the change in x in the time interval $(t, t+dt)$ is a mean drift $f(x)dt$ and a diffusion $\sigma(x)d\beta$ with $d\beta$ the corresponding increment of a Brownian motion process, see Ref.1 for details. One of the useful yet disturbing properties for novice of these equations is the Ito Lemma: If $V(y,t)$ is a twice-continuous differentiable function then $V(x_t, t)$ with x_t a solution of eqtn. 6.4) is the solution to the equation

$$dV = \left[\frac{\partial V}{\partial t} + f(x) \frac{\partial V}{\partial x} + \frac{\sigma^2(x)}{2} \frac{\partial^2 V}{\partial x^2} \right] dt + V_x \sigma(x) d\beta \quad 6.5)$$

Formula 6.5) is what one would expect, a direct generalization of the Eulerian derivative except for the term

$$\frac{\sigma^2(x)}{2} \frac{\partial^2 V}{\partial x^2},$$

which arises as the square of the diffusive term, $\sigma(x) d\beta$, is equivalent to a

drift term, $\frac{\sigma^2(x)}{2} dt$. For example, the solution of

$$dy = \beta d\beta$$

is $\frac{\beta^2}{2} - \frac{t}{2}$, not $\frac{\beta^2}{2}$ as the uninitiated might expect. In particular, for the problem which interests us, namely the model eqtns. 2.3) and 2.4), the continuous conditional density $J(t, x)$ of the phase x satisfies

$$dJ(t, x) = \frac{q}{2} \frac{\partial^2 J}{\partial x^2} dt + (\widehat{\cos x} - \widehat{\cos}, \widehat{\sin x} - \widehat{\sin}) \frac{1}{2r} d\tilde{I} J(t, x) \quad 6.6)$$

where $d\tilde{I}$ is vector Innovation, defined by

$$d\tilde{I} = \begin{vmatrix} d\tilde{z}_1 - \widehat{\cos} dt \\ d\tilde{z}_2 - \widehat{\sin} dt \end{vmatrix}$$

The $d\tilde{I}$ process is called the innovation and represents the instantaneous new information⁽¹⁾ carried by $d\tilde{z}_i$ at time t . The spectral density of the

vector additive measurement noise process v is $\begin{vmatrix} 2r & 0 \\ 0 & 2r \end{vmatrix}$, (i.e., it is a

white noise vector process). Equation 6.6) has drift $\frac{q}{2} \frac{\partial^2 J}{\partial x^2} dt$ reflecting mean movement of the phase process inducing a change in J , a model following action and diffuses proportionately to a weighting of the new information. A derivation of eqtn. 6.6) using the vector form of the relation 6.5) can be found in Ref.1, page 50.

From the Ito lemma, eq. 6.6), the conditional expectation \hat{g} of $g(\varphi)$ can be shown to be the solution of the equation

$$d\hat{g} = \frac{q}{2} \frac{\partial^2 \hat{g}}{\partial x^2} dt + (\widehat{g \cos} - \hat{g} \widehat{\cos}, \widehat{g \sin} - \hat{g} \widehat{\sin}) \frac{1}{2r} d\tilde{I} \quad 6.7)$$

1. The information about x carried by $d\tilde{z}_i(t)$ for all $t \leq t_1$ not carried by $d\tilde{z}_i(s)$ for all $s \leq t_2$, $t_2 < t_1$.

Of course eqn. 6.7) follows from 6.6) by multiplying 6.6) by $g(x)$ and integrating both sides of the equation from $-\infty$ to ∞ , with the drift term value a consequence of integration by parts. It follows in particular that for $g = \sin x$ or $\cos x$

$$\begin{aligned} dS &= -\frac{q}{2} S dt + \frac{1}{2r} k_1 \cdot d\tilde{I} \\ dC &= -\frac{q}{2} C dt + \frac{1}{2r} k_2 \cdot d\tilde{I} \end{aligned} \quad 6.8)$$

$$\begin{aligned} \text{where } k_1 &= \begin{vmatrix} \widehat{SC} & \widehat{\widehat{S}\widehat{C}} \\ \widehat{S^2} & \widehat{\widehat{S}^2} \end{vmatrix}^1 \\ k_2 &= \begin{vmatrix} \widehat{C^2} & \widehat{\widehat{C}^2} \\ \widehat{SC} & \widehat{\widehat{S}\widehat{C}} \end{vmatrix}^1 \end{aligned} \quad 6.9)$$

$$\begin{aligned} \text{where } \widehat{S} &= \widehat{\sin x} \\ \widehat{SC} &= \widehat{\sin x \cos x} \\ &\text{etc.} \end{aligned}$$

6.1. Relation to the Phase-Locked Loop

As will be shown later the cyclic estimate, which minimizes the loss function $1 - \cos \epsilon$, is defined by

$$x^* = \tan^{-1} \frac{\widehat{S}}{\widehat{C}} \quad 6.10)$$

and the associated optimal loss is $1 - D$ where $D^2 = \widehat{C}^2 + \widehat{S}^2$. An easy but worthwhile exercise involving the Ito lemma⁽²⁾, as the generalized vector form of 6.5) is known, is to derive the random differential equations satisfied by D and x^* ; they are

$$\begin{aligned} dx^* &= \frac{1}{D^4 2r} \frac{\ell w'}{dt} dt - \frac{w d\tilde{I}}{D^2 2r} \\ dD &= \left(-\frac{q}{2} D + \frac{1}{4r D^3} \|w\|^2 \right) dt + \frac{\ell \cdot d\tilde{I}}{2r D} \end{aligned} \quad 6.11)$$

2. See Ref.1, theorem 2.2, page 21.

$$\begin{aligned}
\text{where } \underline{\ell} &= \hat{C} \underline{k}_2 + \hat{S} \underline{k}_1 \\
\underline{w} &= \hat{S} \underline{k}_2 - \hat{C} \underline{k}_1 \\
\text{with } \hat{C} &\stackrel{\text{def}}{=} \widehat{\cos x} \text{ etc.}
\end{aligned} \tag{6.12}$$

Suppose R is small and D reaches steady-state then it can be shown that to first order in R

$$\begin{aligned}
\underline{\ell} &= 0 \\
\frac{q}{2} D &= \frac{1}{4rD^3} \|\underline{w}\|^2
\end{aligned} \tag{6.13}$$

since both the drift and diffusion must vanish in steady state. From 6.12) \underline{k}_1 and \underline{k}_2 must be parallel and

$$\begin{aligned}
\underline{k}_1 &= a \cos x^* \underline{e} \\
\underline{k}_2 &= -a \sin x^* \underline{e}
\end{aligned} \quad \text{with } \|\underline{e}\| = 1 \tag{6.14}$$

for some as yet unknown a .

But then $\underline{w} = -a D \underline{e}$ and by 6.12) and 6.13)

$$a^2 = (R)^2 D^2 \quad \text{by 6.13)}$$

or $\underline{w} = -R D^2 \underline{e}$

Now \underline{e} may be evaluated as $(\sin x^*, -\cos x^*)$ since, when R is small, the phase is Gaussian with mean x^* and variance R . Hence our assertions in 2.8) are validated. When $B \rightarrow 0$ eqn. 6.1) can be shown to have the explicit solution;

$$J_n(x) = \frac{e^{a_n \cos(x - \Psi_n)}}{2\pi I_0(a_n)} \tag{6.15}$$

whence $x_n^* = \Psi_n$

$$\text{where } a_n e^{i\Psi_n} = \frac{1}{2r} \left[\sum_{j=0}^{n-1} z_{1n} + i \sum_{j=0}^{n-1} z_{2n} \right] \tag{6.16}$$

$$\text{and } z_{10} = a_0 \cos \Psi_0, \quad z_{20} = a_0 \sin \Psi_0$$

$$\text{with } J_0(x) = \frac{e^{a_0 \cos(x - \Psi_0)}}{2\pi I_0(a_0)}$$

I_0 = the zeroth order Bessel function of imaginary argument.

The continuous version of the estimate provided by 6.16) adapted to the case where B is small

$$\begin{aligned} da &= \alpha a dt + \beta dz_1 \\ db &= \alpha b dt + \beta dz_2 \\ x^0 &= \tan^{-1} \frac{b}{a} \end{aligned} \tag{6.17}$$

and if $B = 0$, choose $\alpha = 0$. Again it is interesting to find the stochastic differential equation satisfied by x^0 which is

$$dx^0 = \frac{\beta}{L} (\sin(\varphi - x_0) dt + \cos x_0 dv^2 - \sin x^0 dv^1) \tag{6.18}$$

with $L = (a^2 + b^2)^{1/2}$. We again emphasize that 6.18) is a phase-lock loop but with a non-linear gain $\frac{\beta}{L}$. As we shall see the static phase estimate which we call x^0 exhibits numerically good performance. Notice that 6.17) and 6.18) show that the x^0 estimate no matter what choice of α and β is a phase-lock estimate with a data dependent gain, which can be shown to agree with the general form of the optimal cyclic, when the condition distribution of the signal given the observations is symmetric about x^* $p(x) = p(2x^* - x)$, an assumption which seems valid from our digital runs.

To conclude this section it should be emphasized that a study of the problem where the phase is the output of a second order system can be accomplished easily along the same lines as we propose here.

7. CYCLIC SOLUTIONS TO THE NON-LINEAR PHASE ESTIMATOR

The basic output of the non-linear phase filter is the conditional or a posteriori probability density function of phase, $J_n(x)$ where x denotes the phase and $J_n(x)dx$ is the probability based on all observations up to and including the n^{th} that the phase lies between x and $x+dx$. As originally derived x ranges from $-\infty$ to $+\infty$.

For phase tracking circuits in particular, however, two types of requirement must be distinguished.

- 1) Absolute phase required as in CW cycle counting tracking systems, e.g., MICROLOC, TRANSIT, DOVAP, UDOP, and many others.
- 2) Modular phase required. That is, the integral number of cycles is not important, only the phase modulo 2π , as in frequency or phase modulation discriminators or filters for estimating phase for coherent detection.

For the present, we concentrate on the latter type of problem; this leads to a class of cyclic estimates of the phase.

In general, after having tracked a noisy signal for some period of time the phase density function $J_n(x)$ exhibits a multi-modal nature with modes spaced at intervals of roughly 2π . An example is shown in Figure 7-1 which is the non-linear filter a posteriori probability density after having tracked for 35 time constants of the optimized phase-locked loop and where the signal/noise ratio in the optimized phase-locked loop bandwidth is zero db, i.e., about 4 to 6 db below what would normally be considered phase-locked loop threshold.

The phase density is the complete answer in the sense of Siegert's "Ideal Observer", or Wald's Bayesian theory, i.e., it summarizes all the available information without loss of information but it does not explicitly provide "the phase estimate", and as in all such problems this is somewhat arbitrary and depends on the definition

of a loss function to be minimized. That is, if we associate a loss function $L(\epsilon)$ with a given error of estimate then the expected loss given the a posteriori density, if we estimate x^* , is

$$E(L|x^*) = \int_{-\infty}^{\infty} J(x) L(x - x^*) dx \quad 7.1)$$

and the optimum estimate relative to this loss function is that which minimizes the expected loss, i.e., the solution

$$\begin{aligned} \frac{\partial E(L|x^*)}{\partial x^*} &= 0 \\ 0 &= \int_{-\infty}^{\infty} J(x) L'(x - x^*) dx \end{aligned} \quad 7.2)$$

The common "least-squares estimate" results from assigning a quadratic loss function, i.e.,

$$L(\epsilon) = K\epsilon^2$$

Then

$$L'(\epsilon) = 2K\epsilon \quad 7.3)$$

and the least-squares estimate is the solution of

$$0 = 2K \int_{-\infty}^{\infty} (x - x^*) J(x) dx$$

or since $\int_{-\infty}^{\infty} J(x) dx = 1$

$$x^* = \int_{-\infty}^{\infty} x J(x) dx \quad 7.4)$$

which is to say just the mean or expectation of x .

This is a reasonable sort of estimate for densities which are unimodal but obviously may result in somewhat ridiculous answers for a multimodal, quasi-periodic density such as Figure 7-1. For example, in this case the least-squares or mean value estimate may tend to fall midway between the two major modes where the probability density is actually very low. By attempting to compromise in this sense we would actually come up with a very poor estimate, one for which the error, modulo 2π is much larger than the width of the individual modes.

Clearly what is needed is a cyclic loss function, i.e., one for which

$$L(\epsilon) = L(\epsilon + n2\pi) \quad 7.5)$$

for all n . If the loss function is cyclic in this sense, then the total expected loss becomes

$$\begin{aligned} E(L | x^*) &= \int_{-\infty}^{\infty} J(x) L(x - x^*) dx \\ &= \sum_{n=-\infty}^{\infty} \int_{-\pi}^{\pi} J(x + n2\pi) L(x) dx \\ &= \int_{-\pi}^{\pi} \tilde{J}(x) L(x) dx \end{aligned} \quad 7.6)$$

where by definition

$$\tilde{J}(x) \equiv \sum_{n=-\infty}^{\infty} J(x + n2\pi) \quad 7.7)$$

In effect we have thus taken the density J defined on the infinite line and by wrapping it around the unit circle and adding the contribution from each wrap come up with a cyclic density function \tilde{J} completely defined by its values in any one principal 2π interval and from which the expected loss for any cyclic loss function can be computed. Note that for normalization

$$\int_{-\pi}^{\pi} \tilde{J}(x) dx = 1 \quad 7.8)$$

since $J(x)$ is a density function.

Now we come to the question of choice of a loss function. Consider the cyclic density as representing a mass density distribution around a unit circle as shown in Figure 7-2. How would we rationally estimate "the phase" x^* . One way that is attractive from several points of view is stick a pin through the center of the circle and see what point hangs down under the attraction of downward gravity, calling this the "center of mass on the circle" or the phase estimate. Mathematically this is determined by setting the resultant turning

moment to zero or

$$0 = \int_{-\pi}^{\pi} \tilde{J}(x) \sin(x - x^*) dx \quad 7.9)$$

Note that this results from choosing a cyclic loss function

$$\begin{aligned} L(e) &= 2(1 - \cos e) \\ &= 4 \sin^2 \frac{e}{2} \end{aligned} \quad 7.10)$$

as shown in Figure 7-3 for then

$$L'(e) = 2 \sin e \quad 7.11)$$

leading to equation 7.9) for the minimum loss estimate. This is an attractive loss function from several points of view, namely

- 1) In the vicinity of $e = 0$ it is quadratic, i.e., $L(e) \rightarrow e^2$
- 2) It is symmetric and cyclic.

In order to solve equation 7.9) we can expand the Sin term

$$0 = \int_{-\pi}^{\pi} \tilde{J}(x) (\sin x \cos x^* - \cos x \sin x^*) dx \quad 7.12)$$

or defining

$$\hat{C} = \int_{-\pi}^{\pi} \tilde{J}(x) \cos x dx \quad 7.13)$$

$$\hat{S} = \int_{-\pi}^{\pi} \tilde{J}(x) \sin x dx \quad 7.14)$$

the conditional expected values of $\cos(x)$ and $\sin(x)$ respectively, the solution for x^* follows from

$$\begin{aligned} 0 &= \hat{S} \cos x^* - \hat{C} \sin x^* \\ x^* &= \tan^{-1} \frac{\hat{S}}{\hat{C}} \end{aligned} \quad 7.15)$$

It is of interest to consider the expected loss associated with this estimate, which is the natural generalization from the variance in the case of the least-squares estimate.

Thus

$$E(L|x^*) = \int_{-\pi}^{\pi} \tilde{J}(x) 2(1 - \cos(x - x^*)) dx \quad 7.16)$$

$$= 2 - 2 \int_{-\pi}^{\pi} \tilde{J}(x) (\cos x \cos x^* + \sin x \sin x^*) dx$$

$$= 2 - 2(\hat{C} \cos x^* + \hat{S} \sin x^*)$$

$$= 2 - 2 \left(\frac{\hat{C}^2}{\sqrt{\hat{C}^2 + \hat{S}^2}} + \frac{\hat{S}^2}{\sqrt{\hat{C}^2 + \hat{S}^2}} \right)$$

$$= 2(1 - \sqrt{\hat{C}^2 + \hat{S}^2}) \quad 7.17)$$

It is clear that $\hat{C}^2 + \hat{S}^2 < 1$ with equality only if all the density in \tilde{J} is concentrated at one point.

7.1. Recursion Relation for the Cyclic Density

One of the attractive features of the cyclic density is that it affords potential significant simplification of the recursive computation of the density function which comprises the bulk of the computational problem. In fact, we can derive a recursive algorithm for computing \tilde{J} directly without ever computing J . This proceeds as follows. The recursion for J is

$$J_{n+1}(x) = K \int_{-\infty}^{\infty} Q_s(y-x) Q_m(Z_n - H(y)) J_n(y) dy \quad 7.18)$$

where $Q_s(t)$ is the probability density function of state change t

$Q_m(t)$ is the probability density function of measurement noise, t

Z_n is the n^{th} observation = vector (z_{1_n}, z_{2_n})

$H(y)$ is the value of the sensor for phase y ,

e.g., $\sin y$ or $\cos y$

K is a normalization constant.

For Gaussian state noise and measurement noise, Q_s and Q_m are Gaussian functions.

Now let us form \tilde{J}_{n+1} from J_{n+1}

$$\tilde{J}_{n+1}(x) = \sum_{m=-\infty}^{\infty} J_{n+1}(x+m2\pi) \quad 7.19)$$

$$= \sum_{m=-\infty}^{\infty} \int_{-\infty}^{\infty} Q_s(y-xm2\pi) Q_m(z_n-H(y)) J_n(y) dy \quad 7.20)$$

Let $u = y - m2\pi$

$$\tilde{J}_{n+1}(x) = K \sum_{m=-\infty}^{\infty} \int_{-\infty}^{\infty} Q_s(u-x) Q_m(z_n-H(u+m2\pi)) J_n(y) du \quad 7.21)$$

But since the observation function $H(y)$ is already itself a cyclic function ($\sin y, \cos y$) of its argument, the $m2\pi$ has no effect in the argument of H , consequently

$$\tilde{J}_{n+1}(x) = K \int_{-\infty}^{\infty} Q_s(u-x) Q_m(z_n-H(u)) \tilde{J}_n(u) du \quad 7.22)$$

$$\text{where } \tilde{J}_n(u) = \sum_{m=-\infty}^{\infty} J_n(u+m2\pi) \quad 7.23)$$

Finally, since Q_m and \tilde{J} are both cyclic the integration range can be reduced to the principal interval by defining in similar way

$$\tilde{Q}_s(t) = \sum_{p=-\infty}^{\infty} Q_s(t+p2\pi) \quad 7.24)$$

then

$$\boxed{\tilde{J}_{n+1}(x) = K \int_{-\pi}^{\pi} \tilde{Q}_s(y-x) Q_m(z_n-H(y)) \tilde{J}_n(y) dy} \quad -\pi < x < \pi \quad 7.25)$$

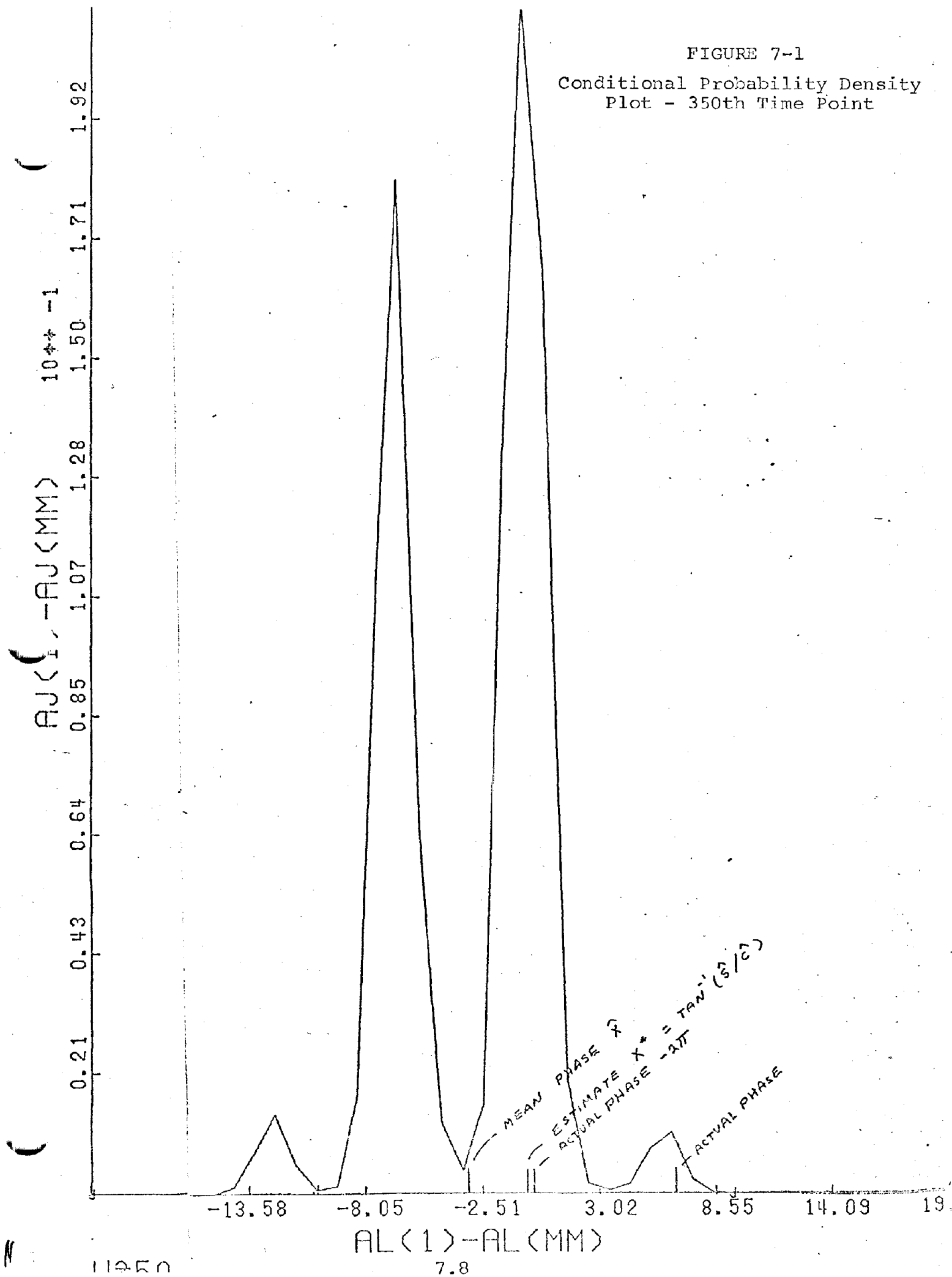
That is, \tilde{J}_{n+1} follows from a recursion of identical form to that for J_{n+1} . In this case the normalizing constant K may be found from the condition

$$\int_{-\pi}^{\pi} J_{n+1}(x) dx = 1 \quad 7.26)$$

What we have accomplished here is that \tilde{J} need only be computed on the range $-\pi$ to π rather than the much larger range representing the total diffusion of probability density on the infinite line. This may represent a substantial reduction of computations.

The program, D13, was originally written to compute density on the line $-\infty < x < \infty$ but subsequently rewritten as D14 to compute density as above on the circle $-\pi < x < \pi$ in order to achieve greater accuracy (finer grid meshing) for large R . Both programs are described in Appendix III.

FIGURE 7-1
Conditional Probability Density
Plot - 350th Time Point



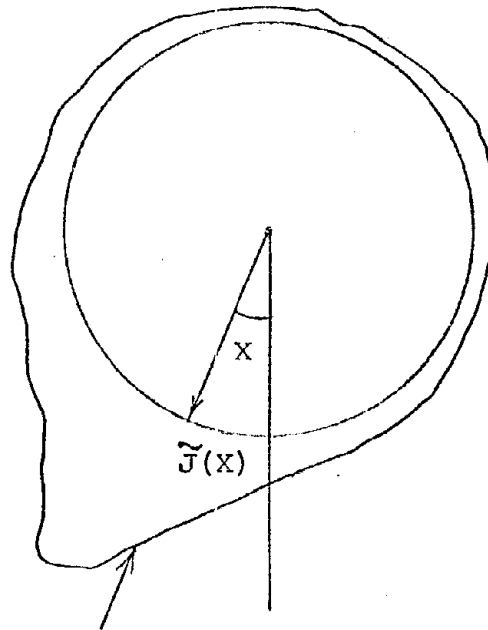


FIGURE 7-2
CYCLIC DENSITY ON THE UNIT CIRCLE

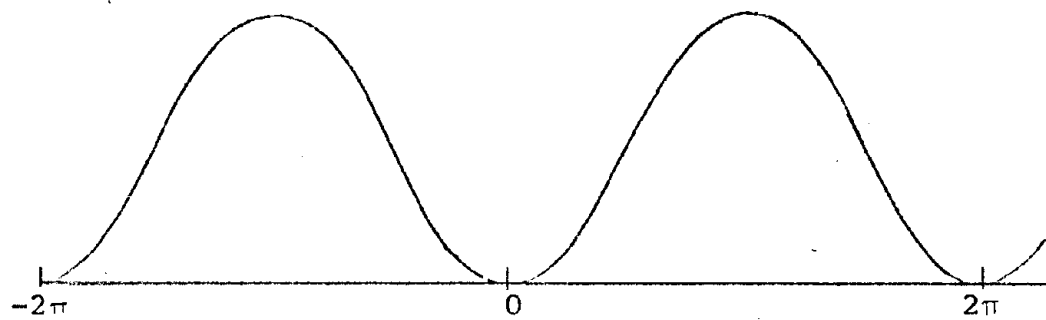


FIGURE 7-3
CYCLIC LOSS FUNCTION $L(\epsilon) = 2(1 - \cos \epsilon)$

8. FOURIER SERIES EXPANSION OF THE CYCLIC DENSITY

The periodicity of $\tilde{J}(x)$ suggests the possibility of representation in Fourier series. The Fourier coefficients themselves in place of the $\tilde{J}(x)$ function afford attractive possibilities for simpler computation if convergence can be established and a direct recursion relation between the Fourier series is established.

Define F_k as the complex Fourier series coefficient of order k in the expansion of $\tilde{J}(x)$

$$F_k = \int_{-\pi}^{\pi} \tilde{J}(x) e^{ikx} dx \quad 8.1)$$

Then

$$\tilde{J}(y) = \frac{1}{2\pi} \sum_{p=-\infty}^{\infty} F_p e^{-ipy} \quad 8.2)$$

Now $\tilde{J}(x)$ has been shown to follow the recursion

$$\tilde{J}_{n+1}(x) = K \int_{-\pi}^{\pi} \tilde{Q}_s(y-x) Q_m(Z_n - H(y)) \tilde{J}_n(y) dy \quad 8.3)$$

Using similar expansions for \tilde{Q}_s and Q_m define

$$S_t = \int_{-\pi}^{\pi} \tilde{Q}_s(x) e^{itx} dx \quad 8.4)$$

$$\begin{aligned} &= \frac{1}{\sqrt{2\pi B}} \int_{-\infty}^{\infty} e^{-\frac{x^2}{2B} + itx} dx \\ &= e^{-\frac{Bt^2}{2}} \end{aligned} \quad 8.5)$$

so

$$\tilde{Q}_s(y-x) = \frac{1}{2\pi} \sum_{t=-\infty}^{\infty} S_t e^{-it(y-x)}$$

$$\boxed{\tilde{Q}_s(y-x) = \frac{1}{2\pi} \sum_{t=-\infty}^{\infty} e^{-\frac{Bt^2}{2}} e^{-it(y-x)}} \quad 8.6)$$

A similar expansion for Q_m is available by writing

$$\begin{aligned} Q_m(Z-H(y)) &= \frac{1}{\sqrt{2\pi C}} e^{-\frac{(z_1 - \cos y)^2 + (z_2 - \sin y)^2}{2C}} \\ &= K_1 e^{\frac{z_1 \cos y + z_2 \sin y}{C}} \end{aligned} \quad 8.7)$$

$$\text{where } K_1 = \frac{1}{\sqrt{2\pi C}} e^{-\frac{z_1^2 + z_2^2 + 1}{2C}} \quad 8.8)$$

or defining

$$\begin{aligned} z_1 + iz_2 &= ve^{i\Psi} \\ z_1 &= v \cos \Psi \\ z_2 &= v \sin \Psi \end{aligned}$$

so

$$Q_m(Z-H(y)) = K_1 e^{\frac{v}{C} \cos(\Psi-y)}$$

$$\boxed{Q_m(Z-H(y)) = K_1 \sum_{r=-\infty}^{\infty} I_r\left(\frac{v}{C}\right) e^{ir(\Psi-y)}} \quad 8.9)$$

The latter following from, e.g., Ref. 19, #9.6.34.

Then using 8.1), 8.2), 8.6), and 8.9) in 8.3) gives

$$F_{k_{n+1}} = \frac{KK_1}{(2\pi)^2} \int_{-\pi}^{\pi} \int_{-\pi}^{\pi} \sum_{p=-\infty}^{\infty} \sum_{t=-\infty}^{\infty} \sum_{r=-\infty}^{\infty} e^{-\frac{Bt^2}{2}} e^{-it(y-x)} I_r\left(\frac{v}{C}\right) e^{ir(\Psi-y)} F_{p_n} e^{-ipy} e^{ikx} dy dx$$

(footnote 1)

The x integral gives $2\pi \delta(t+k)$ so

$$F_{k_{n+1}} = \frac{KK_1}{2\pi} \int_{-\pi}^{\pi} \sum_{p=-\infty}^{\infty} \sum_{r=-\infty}^{\infty} F_{p_n} e^{-\frac{Bk^2}{2}} e^{i(ky+r\Psi-rypy)} I_r\left(\frac{v}{C}\right) dy$$

Then the y integral gives $2\pi \delta(-r-p+k)$ so

$$F_{k_{n+1}} = KK_1 \sum_{p=-\infty}^{\infty} F_{p_n} e^{-\frac{Bk^2}{2}} e^{i(k-p)\Psi} I_{k-p}\left(\frac{v}{C}\right)$$

$$F_{k_{n+1}} = (KK_1) e^{-\frac{Bk^2}{2}} \sum_{p=-\infty}^{\infty} F_{p_n} e^{i(k-p)\Psi} I_{k-p}\left(\frac{v}{C}\right) \quad 8.10)$$

The normalization constants may be evaluated by simply noting that the zero order coefficient is just the total probability integral

$$F_{0_n} = \int_{-\pi}^{\pi} \tilde{f}_n(x) dx$$

$$= 1$$

or

$$1 = (KK_1) \sum_{p=-\infty}^{\infty} F_{p_n} e^{-ip\Psi} I_p\left(\frac{v}{C}\right) \quad 8.11$$

Note that the cyclic phase estimate defined previously

$$x^* = \tan^{-1}(\hat{S}/\hat{C})$$

1. F_{k_n} denotes (F_{k_n}) , i.e., the n^{th} discrete time point of the k^{th} order Fourier coefficient.

is given simply in terms of these complex Fourier coefficients since

$$\begin{aligned} F_1 &= \int_{-\pi}^{\pi} \tilde{J}(x) e^{ix} dx \\ &= \hat{C} + i\hat{S} \end{aligned}$$

by their definitions, so

$$x^* = \arg(F_1) \quad 8.12)$$

Also note that 8.10) can be simplified if desired by using the symmetry relations, the first arising from the fact that $J(x)$ is a real function

$$\begin{aligned} F_p &= F_p^* & (* = \text{complex conjugate}) \\ I_v(x) &= I_{-v}(x) \end{aligned}$$

so

$$\begin{aligned} F_{k_{n+1}} &= (K_3) e^{-\frac{Bk^2}{2}} e^{ik\psi} \left[I_k\left(\frac{v}{C}\right) + 2\Re \sum_{p=1}^{\infty} F_{p_n} e^{-ip\psi} I_{k-p}\left(\frac{v}{C}\right) \right] \\ \text{where } K_3 &= \left[I_0\left(\frac{v}{C}\right) + 2\Re \sum_{p=1}^{\infty} F_{p_n} e^{-ip\psi} I_p\left(\frac{v}{C}\right) \right]^{-1} \end{aligned} \quad 8.13)$$

8.1 Difference Equation Form

Equation 8.10) provides a closed solution to the problem of a discrete update for the Fourier series.

In this form it is not immediately clear how this approaches the continuous case as $\Delta \rightarrow 0$. What we need is the difference equation corresponding to eq. 8.13) in this limiting case. This can, in principal, and has, in fact, been worked out by a careful Taylor's series expansion.

A much more direct route, however, lies in the simple application of eq. 6.7) which states that, for the problem at hand and given any functional $g(x)$, the conditional expectation of \hat{g} satisfies the differential equation given in eq. 6.5)

$$d\hat{g} = \frac{q}{2} \frac{\partial^2 \hat{g}}{\partial x^2} dt + \frac{1}{2r} \begin{vmatrix} \widehat{g \cos x} - \hat{g} \widehat{\cos x} & d\tilde{I}_1 \\ \widehat{g \sin x} - \hat{g} \widehat{\sin x} & d\tilde{I}_2 \end{vmatrix}^T \quad 8.14)$$

$$\begin{aligned} \text{where } d\tilde{I}_1 &= d\tilde{Z}_1 - \widehat{\cos x} dt \\ d\tilde{I}_2 &= d\tilde{Z}_2 - \widehat{\sin x} dt \end{aligned}$$

Notice that since this is linear in \hat{g} it applies for complex as well as real g . and if we define the complex innovation $\tilde{I} = \tilde{I}_1 + i\tilde{I}_2$ this can be written

$$d\hat{g} = \frac{q}{2} \frac{\partial^2 \hat{g}}{\partial x^2} dt + \frac{1}{2r} \Re \left\{ \left[\widehat{g e^{-ix}} - \hat{g} \widehat{e^{-ix}} \right] d\tilde{I} \right\}$$

for real g or

$$d\hat{g} = \frac{q}{2} \frac{\partial^2 \hat{g}}{\partial x^2} dt + \frac{1}{4r} \left\{ \left[\widehat{g e^{-ix}} - \hat{g} \widehat{e^{-ix}} \right] d\tilde{I} + \left[\widehat{g e^{ix}} - \hat{g} \widehat{e^{ix}} \right] d\tilde{I}^* \right\} \quad 8.15$$

$$\text{where } \tilde{I} = (z_1 + iz_2) - F_1$$

Applied to the case at hand, let

$$g_k = e^{ikx}$$

so that

$$\begin{aligned} g_k &= e^{ikx} \\ &= F_k \quad (\text{per defining eq. 8.1}). \end{aligned}$$

Then

$$dF_k = -\frac{qk^2}{2} F_k dt + \frac{1}{4r} \left\{ (F_{k-1} - F_k F_1^*) d\tilde{I} + (F_{k+1} - F_k F_1) d\tilde{I}^* \right\} \quad 8.16)$$

In particular the first order coefficient is given by

$$dF_1 = -\frac{qk^2}{2} F_1 dt + \frac{1}{4r} \left\{ (1 - F_1 F_1^*) dI + (F_2 - F_1^2) dI^* \right\} \quad 8.17)$$

This will be found to lead to an easy circuit mechanization of the optimal non-linear filter.

Separating 8.16) into its real and imaginary parts denoting

$$F_k = C_k + iS_k$$

$$dC_k = \frac{qk^2}{2} C_k dt + \frac{1}{4r} \left\{ (C_{k-1} + C_{k+1} - 2C_k C_1) d\tilde{I}_1 + (-S_{k-1} + S_{k+1} - 2C_k S_1) d\tilde{I}_2 \right\} \quad 8.18)$$

$$dS_k = \frac{qk^2}{2} S_k dt + \frac{1}{4r} \left\{ (S_{k-1} + S_{k+1} - 2S_k S_1) d\tilde{I}_1 + (C_{k-1} - C_{k+1} - 2S_k C_1) d\tilde{I}_2 \right\} \quad 8.19)$$

$$\begin{aligned} \text{where} \quad C_k &= \widehat{\cos kx} \\ S_k &= \widehat{\sin kx} \end{aligned}$$

By the appropriate trig identities this can easily be shown identical to the form in eqs. 6.8) and 6.9).

These differential equations for the Fourier Coefficients are attractive from the point of view of medianization in a simple real-time tracking circuit as will be shown later. The crucial question, however, is can a reasonable number of terms of the form F_k , eq. 8.16), yield adequate accuracy and we have not had time to answer this question in the present study.

9. COMPUTING DETAILS

9.1. Determining M and F

As the reader may see from the Basic Language Program of Appendix 2 and the later portions of this section the conditional density is computed by representing it as a set of $(2M + 1)$ point masses. A natural question arises as to the choice of M in relation to the statistical parameters $F = \sqrt{\frac{C}{B}}$ and $R = \sqrt{BC}$. In Section 2, we have indicated that F should be fixed at about 10 or more in order for the discrete simulation of the phase-lock loop to have a sufficiently fast data rate in order that its performance very closely approximate that of the phase-lock loop. Later in this section we will indicate further experiments which justify this choice of F . Returning now to the problem of selecting M for fixed F , it is clear that too small an M will produce inaccurate determination of the conditional distribution and hence effect the quality of the optimal estimate. We determined M experimentally by running our simulation of the non-linear filter with larger and larger M on the same random sequence and selecting that M_0 so that the optimal estimates⁽¹⁾ produced by our program with M_0 agreed to four places with those produced when $M = 2M_0$. Using this procedure it was found that $M = 56$ sufficed for $R < 1$, while $M = 112$ was necessary for $R = 1$. These M 's were determined for the program which realized the density on the line, however, it is clear that these M suffice also for the intrinsically more accurate program realizing the density on the circle.

Now, in Section 3, F was determined by noting that the extended Kalman-Bucy is the phase-lock loop and requiring the pseudo-steady-state performance (i.e., the steady-state solution of the riccati equation, not the true error performance, since the model is not linear) of the discrete loop simulated by

1. The estimates are more sensitive to M than other parameters of the conditional density, for example, its second-order moment.

the digital computer to be close to the pseudo-steady-state performance of the continuous time phase-lock loop. Because of this formal argument, a further check seemed to be necessary. This check was provided by considering two phase-lock loops

$$\begin{aligned} \text{A} \quad \hat{\varphi}_{n+1}^1 &= \hat{\varphi}_n^1 + \frac{1}{1+F} \left[\sin(\varphi_n - \hat{\varphi}_n^1) + v_n^2 \cos \hat{\varphi}_n^1 - v_n^1 \sin \hat{\varphi}_n^1 \right] \\ n &= 1, 2, 3, \dots \end{aligned} \quad 9.1)$$

and

$$\begin{aligned} \text{B} \quad \hat{\varphi}_{n+3}^3 &= \hat{\varphi}_n^3 + \frac{1}{1+F} \left[\sin(\varphi_n - \hat{\varphi}_n^3) + \ddot{v}_n^2 \cos \hat{\varphi}_n^3 - \ddot{v}_n^1 \sin \hat{\varphi}_n^1 \right] \\ n &= 3, 6, 9, \dots \end{aligned} \quad 9.2)$$

$$\text{with} \quad \ddot{v}_n^i = \frac{v_n^i + v_{n-1}^i + v_{n-2}^i}{3}$$

Loop A receives data every Δ seconds while loop B receives data every 3Δ seconds and they are both approximations to the continuous loop (see Section 3),

$$d\hat{\varphi} = \sqrt{\frac{q}{2r}} (\sin(\varphi - \hat{\varphi}) dt + dv^2 \cos \hat{\varphi} - dv^1 \sin \hat{\varphi}) \quad 9.3)$$

Of course, A performs closer to the performance of eq. 5.4) than B and as $\Delta \rightarrow 0$ both A and B approach the error performance of 5.4). Our second and more accurate determination of the appropriate F then consists in comparison of $\hat{\varphi}_{3n}^2$ with $\hat{\varphi}_{3n}^1$. This was done and the choice of F as about 10 sufficed to produce agreement between $\hat{\varphi}^1$ and $\hat{\varphi}^2$ estimates which insures the accurate simulation by a discrete system of the phase-lock loop.

9.2. Monte Carlo Analysis

In order to compare the error performance of one non-linear filter with another it becomes necessary to evaluate the performance statistically by a Monte Carlo analysis. We decided to run both the non-linear and phase-lock loops for 500 time steps; 40 different times to find the mean-square errors of the various estimators, phase-lock loop, static-phase filter, and the optimal cyclic estimate at R increases towards 1, the expected time to slip decreases, and our simulation was, in fact, checked again these mean-slip times, see Ref.6, of the phase-lock loop.

On each run of length N time steps the error variance was calculated as

$$S^2 = \frac{1}{N} \sum_{i=1}^N (\epsilon_i)^2.$$

The distribution of S^2 is then χ^2 with a reduced number of degrees of freedom dependent on the sampling rate parameter F . It can be shown that the effective number of degrees of freedom is

$$N_{\text{eff}} = \frac{N}{1 + \frac{2F^2}{1+2F}}$$

$$\rightarrow \frac{N}{F} \quad \text{for large } F.$$

Then the sample variance is that of χ^2 with N_{eff} degrees of freedom or standard deviation

$$\sigma_{S^2} = \sqrt{\frac{2}{N_{\text{eff}}}}$$

Thus with $N = 500$, $F = 10$, $N_{\text{eff}} = 47.5$

$$\frac{\sigma_{S^2}}{S^2} = .205$$

Averaging over 40 such independent runs, for a pooled estimate gives a further $\sqrt{40}$ reduction for

$$\frac{\sigma_{\bar{S}^2}}{\bar{S}^2} = .0324$$

That is, the overall error variance estimates are expected to have sampling errors of about 3%.

The results summarized in Section 10 for the phase-lock loop agree very well with those predicted by Viterbi in Ref. 6 except at $R = 1$. This exceptional case can be explained by our rule for slipping. The reader can examine our program with a detailed description in the next section.

10. SIMULATION RESULTS

10.1 Details of a Typical Run

Figure 10-1a,b,c, shows a plot of the phase-lock loop error and of the cyclic non-linear estimate, $x^* = \text{atan}(S/C)$ for a typical 500 point run. This was for the case $R = 1$ (signal/noise ratio parameter) or about 6 db below what is normally considered phase-lock threshold and $F = 10$ (sample points per optimal phase-lock time constant). Overall statistics computed for this run were

$$\begin{aligned}\overline{(M(e_p))^2} &= \text{mean-square modulo } 2\pi \text{ phase-lock error} \\ &= 1.22 \text{ rad}^2\end{aligned}$$

$$\begin{aligned}\overline{(M(e_c))^2} &= \text{mean-square modulo } 2\pi \text{ cyclic non-linear error} \\ &= 1.62 \text{ rad}^2\end{aligned}$$

which is typical of the relative performance of the two estimators. It is to be pointed out that we have here evaluated the performance in terms of mean-square error criterion while the non-linear loop was actually optimized on the $L(e) = 2(1 - \cos e)$ criterion. Some comparisons of the two computed criteria indicated that there was no significant difference between the errors and even less difference in the relative performance of the phase-lock and non-linear estimate as between the two error criteria.

Several interesting points emerge from a close inspection of the error plots of Figure 10-1. In the beginning for about the first 70 Points or 7 time constants the phase-lock and non-linear estimates agree very closely. At about this time the non-linear loop skips a cycle and at about point 90 has restabilized about a point one cycle lower. The phase-lock loop is also skipping a cycle at about this time (in the opposite direction) but takes considerably longer to restabilize. This has been seen to be a typical point of difference between the two loops, namely, that when the non-linear estimator skips a cycle it tends to restabilize more rapidly. This is a natural consequence of the adaptive feature inherent in the non-linear estimator; it has the capability of recognizing when it is in

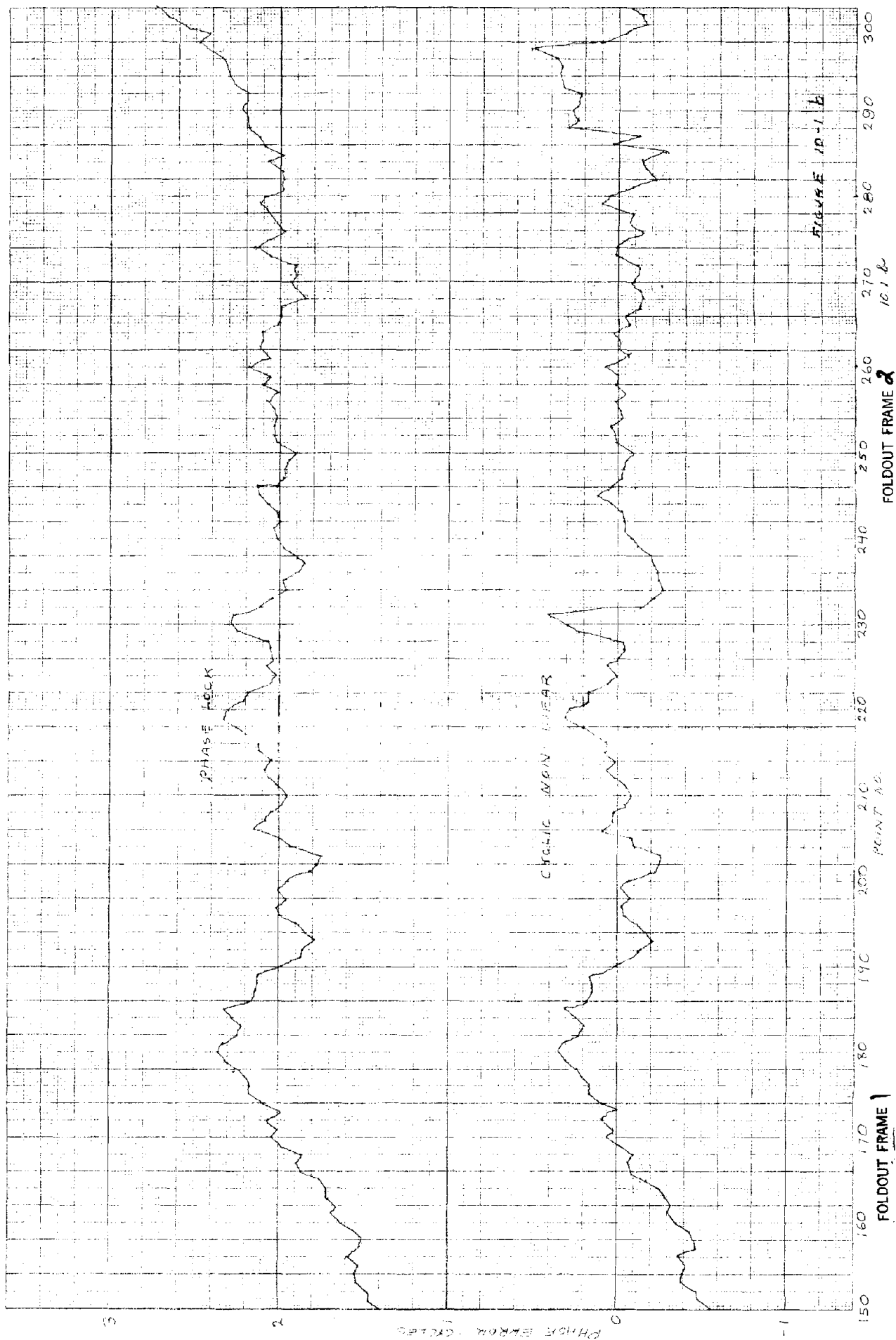
60 60
 40 40
 20 20

27743 NON-LINEAR

FILED 10-1-0

FOLDOUT FRAME 2

FOLDDOUT FRAME



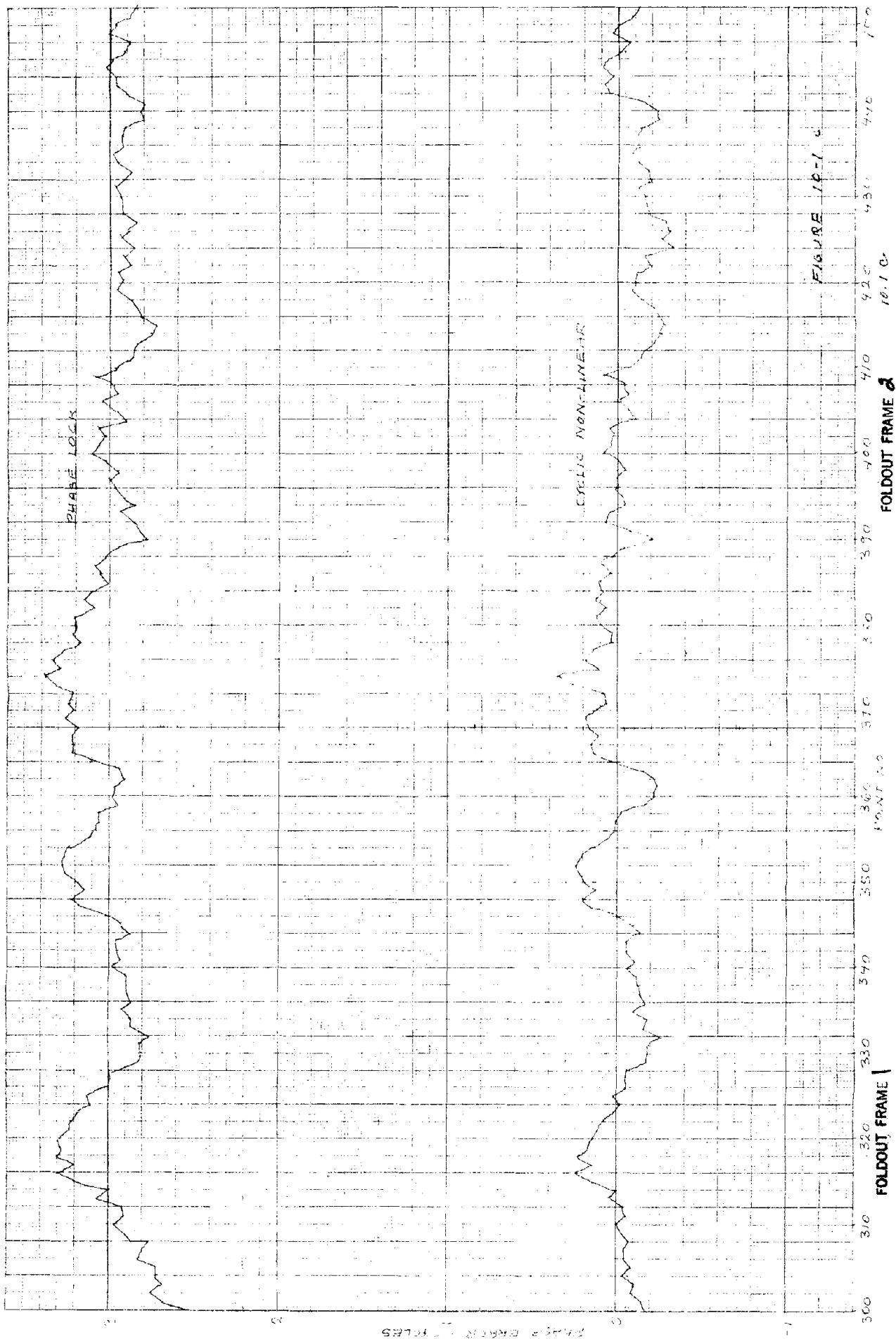


FIGURE 10-1

FOLDOUT FRAME 2

an ambiguous situation and at such times tends to quickly discard old information and be more rapidly receptive to the new. Recognizing that cycle slips are going to be inevitable for any phase estimator at sufficiently low signal/noise ratio, it is desirable that the transient occur as rapidly as possible in order to minimize the low frequency content of the resulting step. The high frequency components will be largely rejected by any subsequent data filter.

After about point 150 the two estimates again assume a very nearly parallel trajectory, separated by two cycles. The fact that the non-linear estimate then settles around the zero cycle error line can only be regarded as fortuitous. Over the entire length of record (45 time constants) the phase-lock suffers three slips and the non-linear two. Although the statistics at this point are inadequate to prove the point this also appears to be typical relative behaviour.

As a point of reference it may be noted that for $R = 1$, Viterbi (Ref.6) predicts mean-time between slips for the phase-lock loop theoretically as 7 time constants while Tausworth (Ref.23) finds experimentally, 16 time constants, compared to 15 here.

In order to provide some further insight into the behaviour of the non-linear estimator around slip times, Figures 10-2 - 10-9 show the transitions in the shape of the computed a posteriori or conditional probability density $J(x)$ around the time of first slip from point 70 to point 105. At 70, the density is a well-behaved unimodal, approximately Gaussian shape. Beginning at point 80 a secondary mode begins to appear at one cycle below the true value. By 95 the lower mode has captured most of the mass and the estimate shifts to this lower value. Eventually, at point 200, Figure 10-10, the mass finally recoalesces into a single predominant mode. However, as a worst case for this run, Figure 10-11 (point 350) shows a case where there are 4 discernable modes.

It should be pointed out that the means of resolving cycle ambiguities is by no means optimized in the present implementation. What is done in the present program is simply to enforce maximum phase continuity by choosing the additive integral cycles for each estimate so as to ensure that the difference from the

Figure 10-2

Conditional
Probability Density
Plot - 70th Time Point

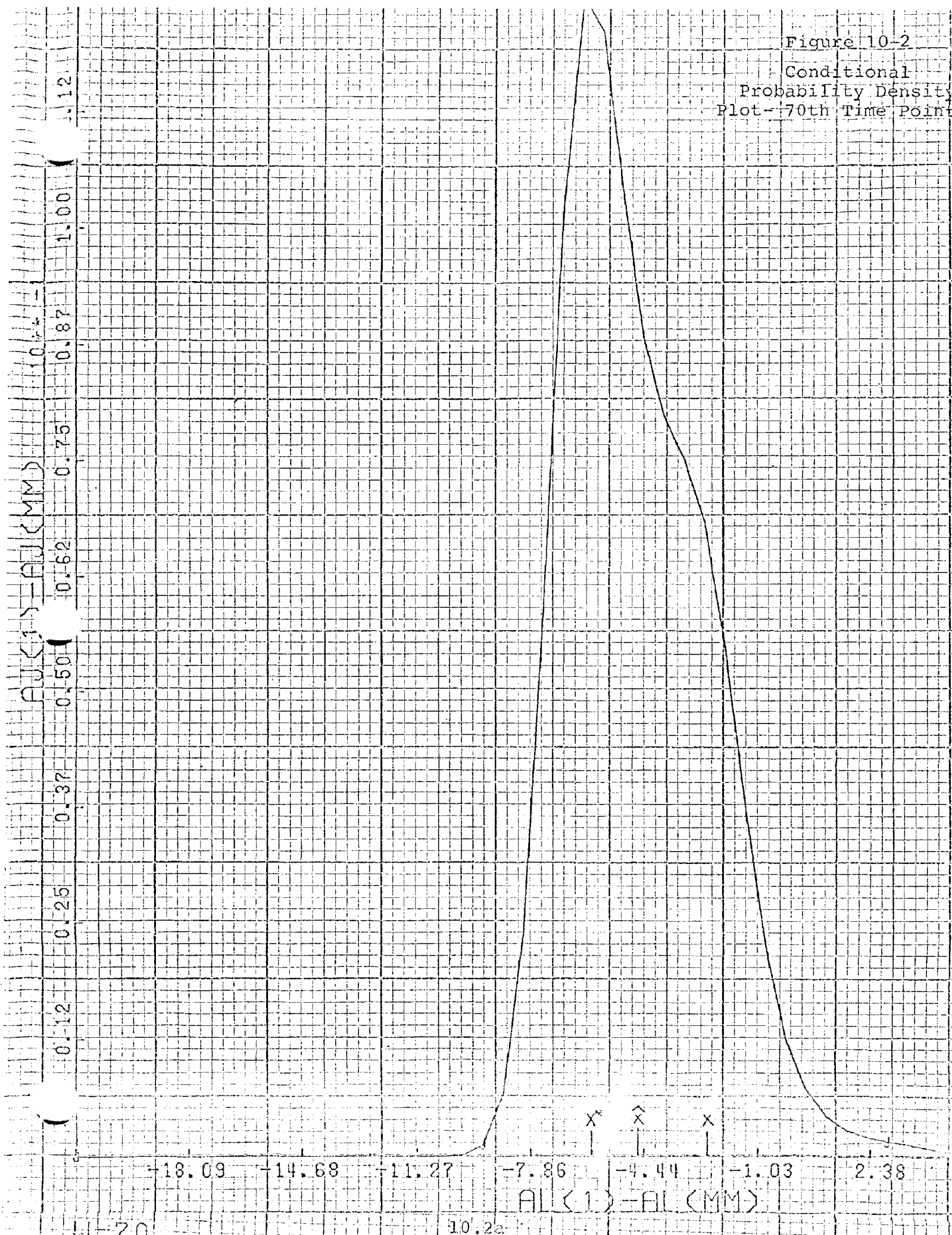


Figure 10-3

Conditional
Probability Density
Plot- 75th Time Point

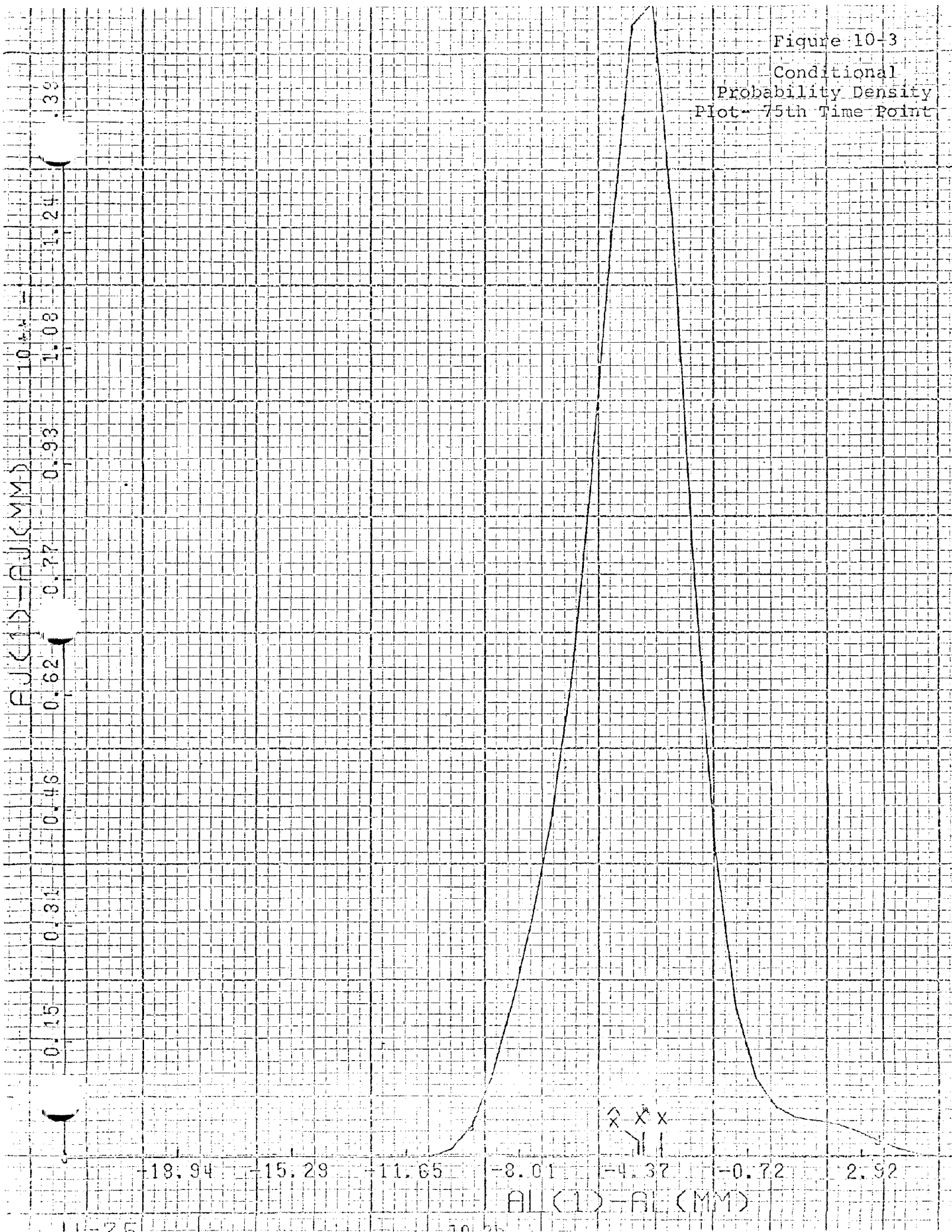
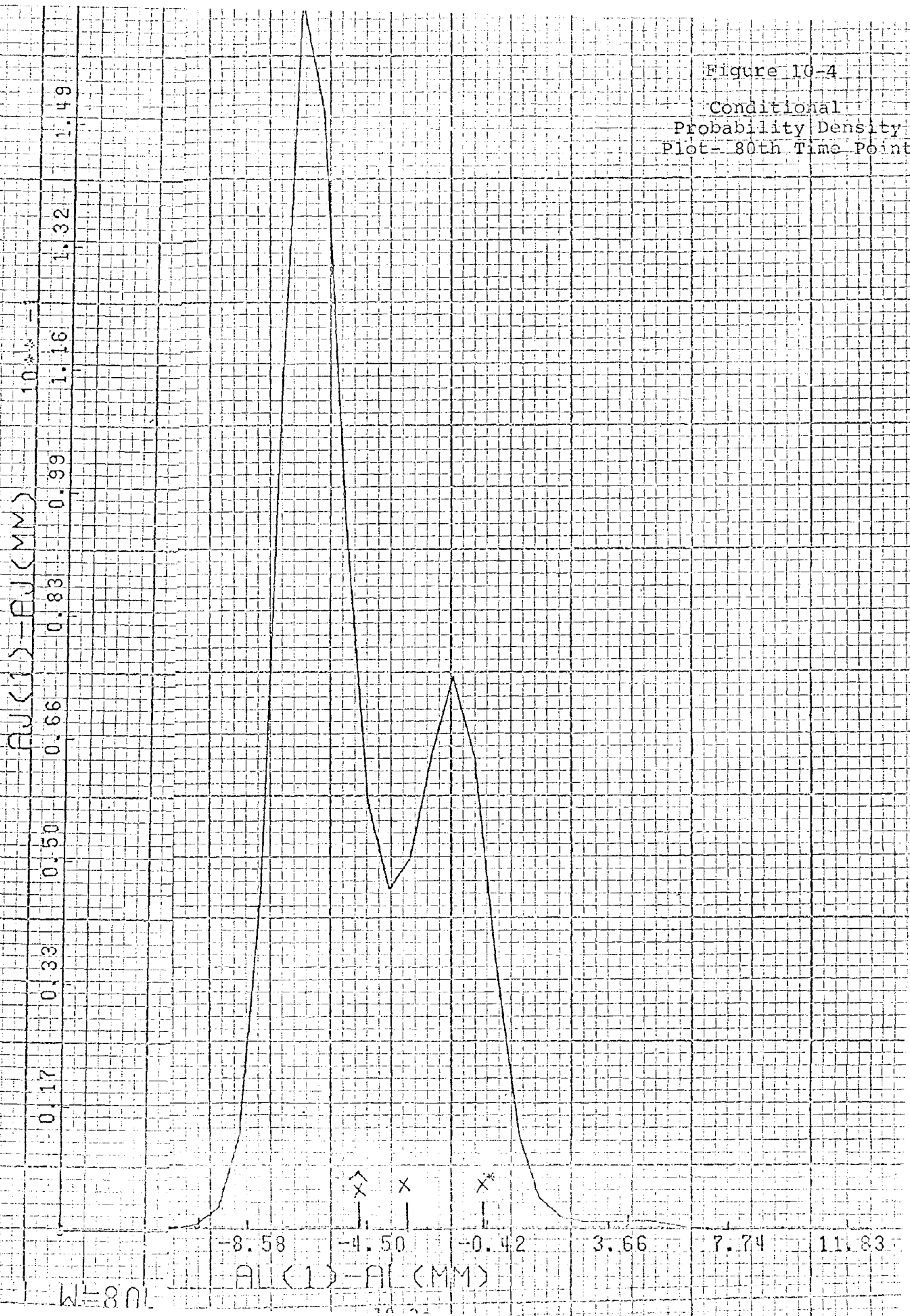


Figure 10-4
Conditional
Probability Density
Plot- 80th Time Point



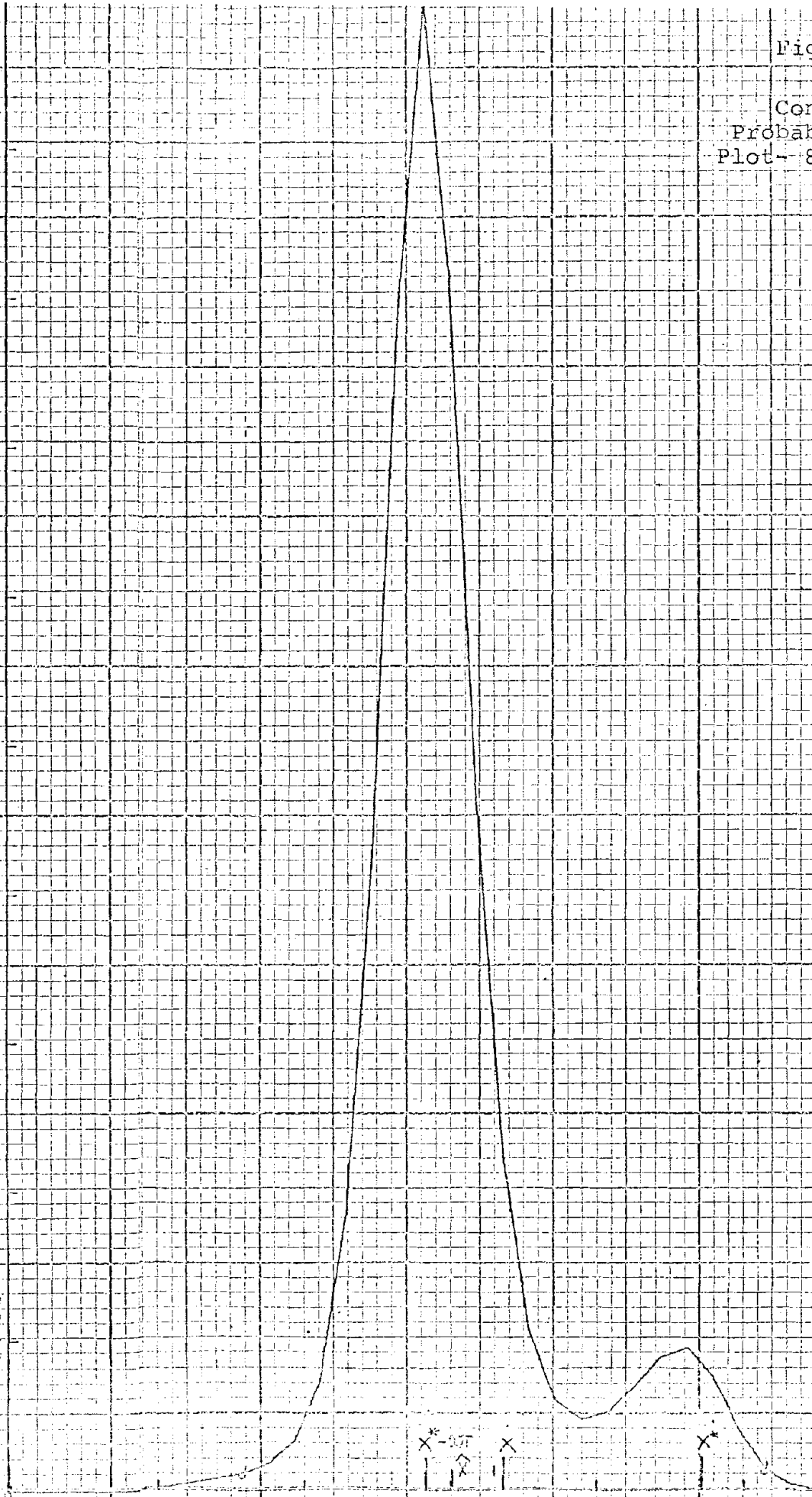
W=80

Figure 10-5

Conditional
Probability Density
Plot- 85th Time Point

$P_{JK}(1) - P_{JK}(MM)$

1.90
1.69
1.48
1.27
1.06
0.84
0.63
0.42
0.21



$P_{JK}(1) - P_{JK}(MM)$

10.26

Figure 10-6

Conditional
Probability Density
Plot - 90th Time Point

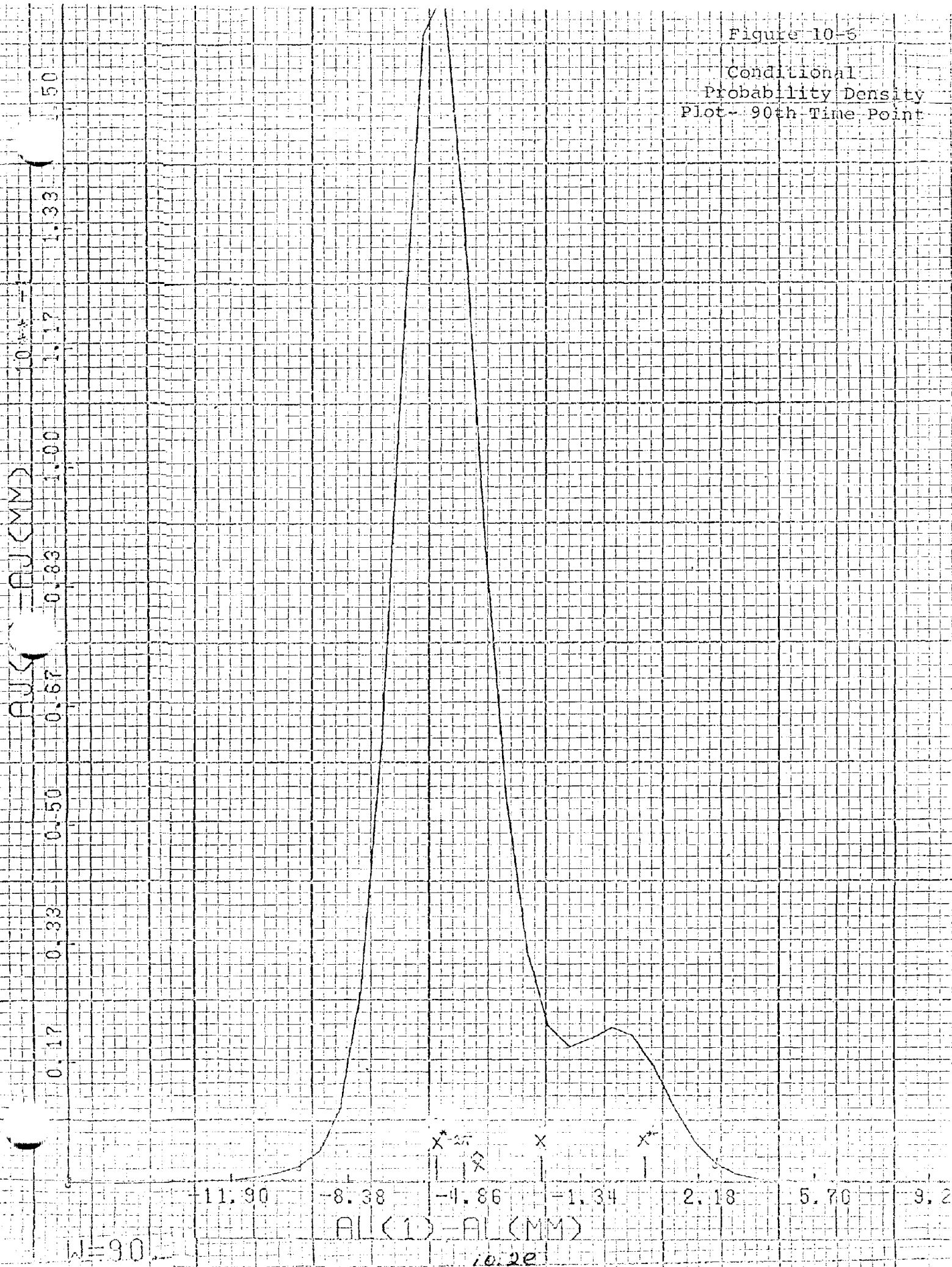


Figure 10-7

Conditional
Probability Density
Plot - 95th Time Point

$PJ(1) - PJ(MM)$

10^{**4}

0.21 0.42 0.64 0.85 1.06 1.27 1.48 1.70 1.91

$X^{*-4\pi}$ \hat{X} $X^{*-2\pi}$ X^*
-9.50 -4.93 -0.35 4.22 8.79 13.25
 $PJ(1) - PJ(MM)$

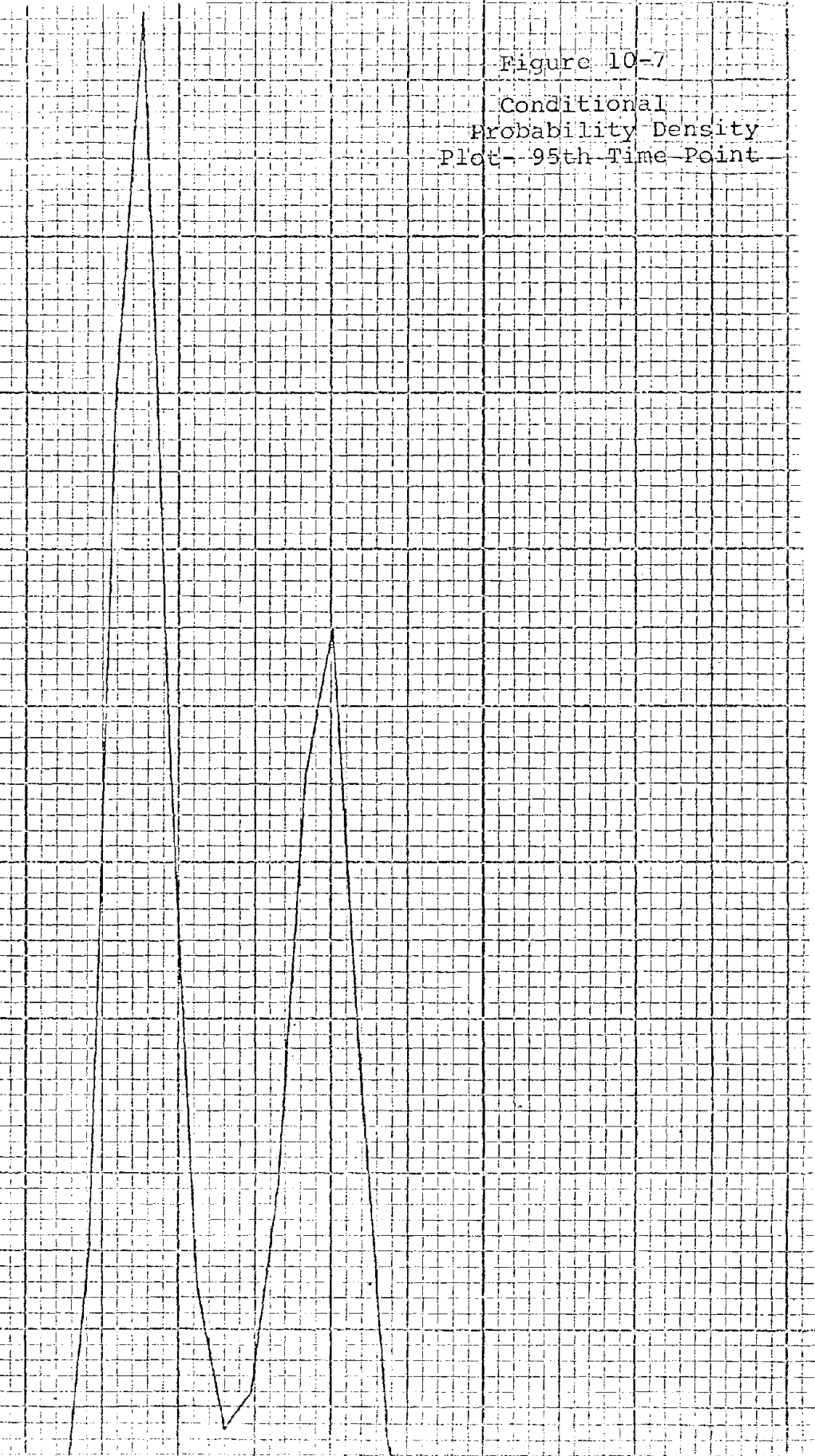


Figure 10-8
Conditional
Probability Density
Plot- 100th Time Point

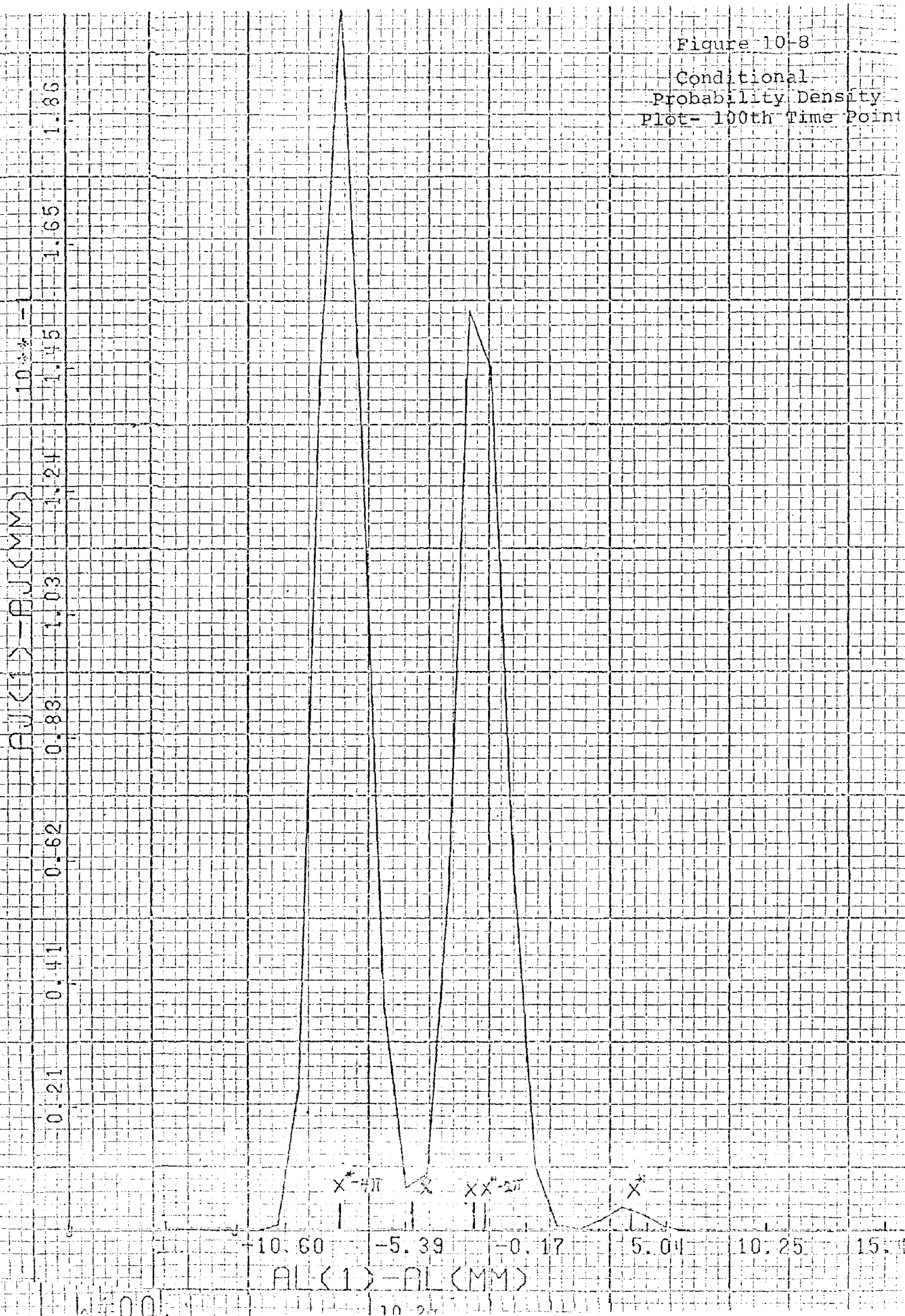


Figure 10-9

Conditional
Probability Density
Plot - 105th Time Point

$PJ(1) - PJ(MM)$

10^{x^*}

0.19 0.38 0.56 0.75 0.94 1.13 1.31 1.50 1.69

-10.71 -5.40 -0.10 5.21 10.51 15.

$AJ(1) - AJ(MM)$

W105

10.25

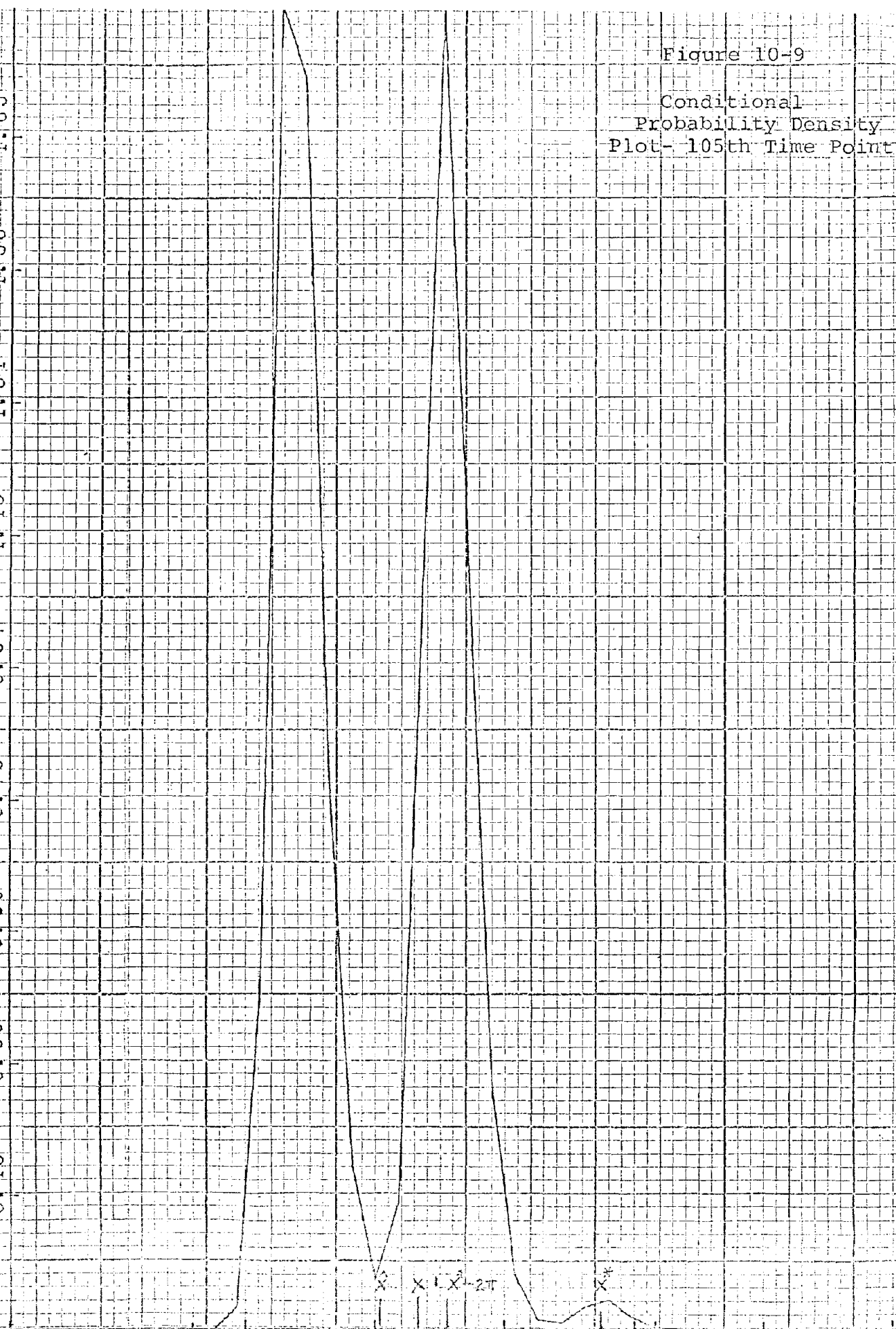
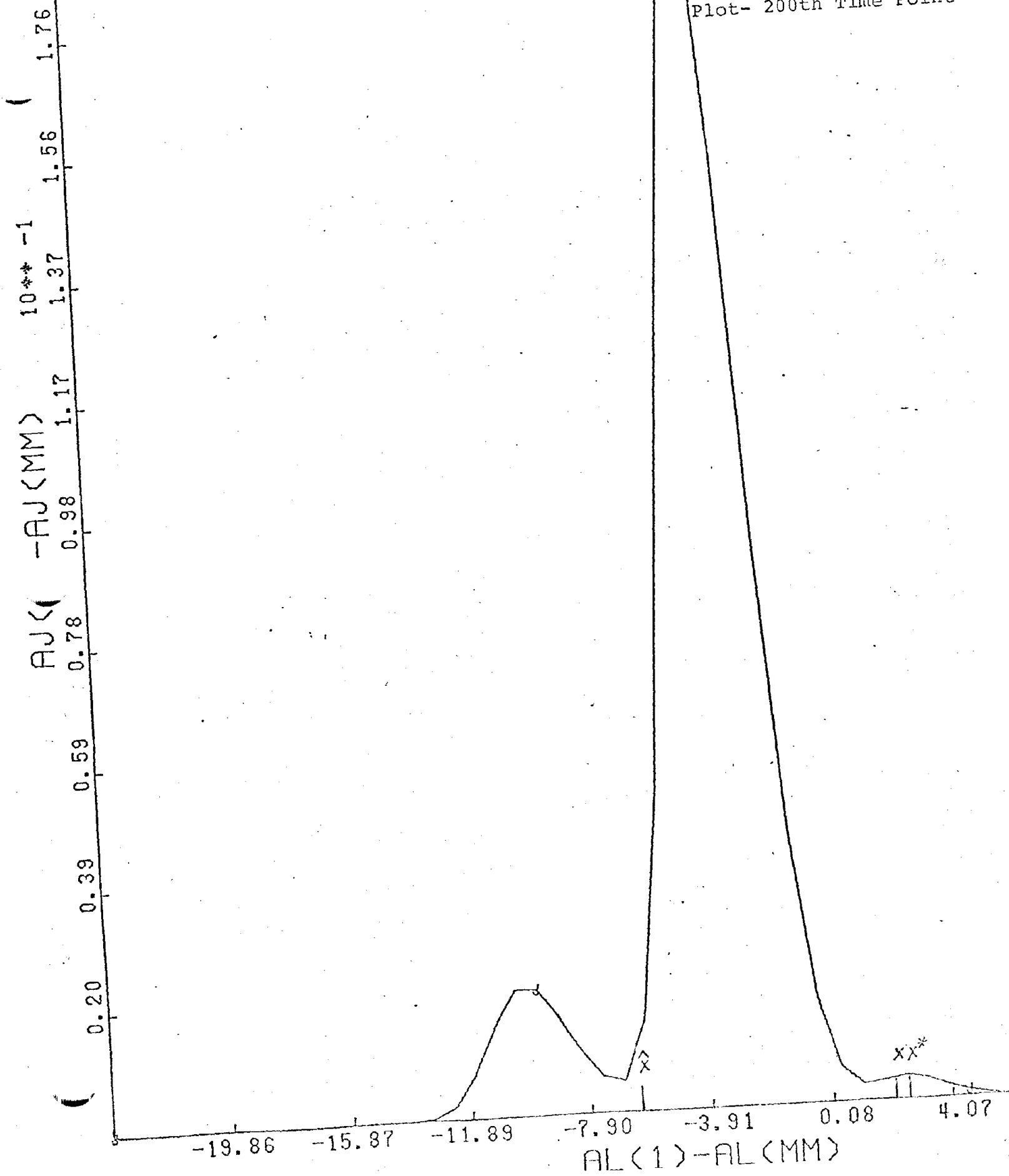


Figure 10-10
Conditional
Probability Density
Plot- 200th Time Point

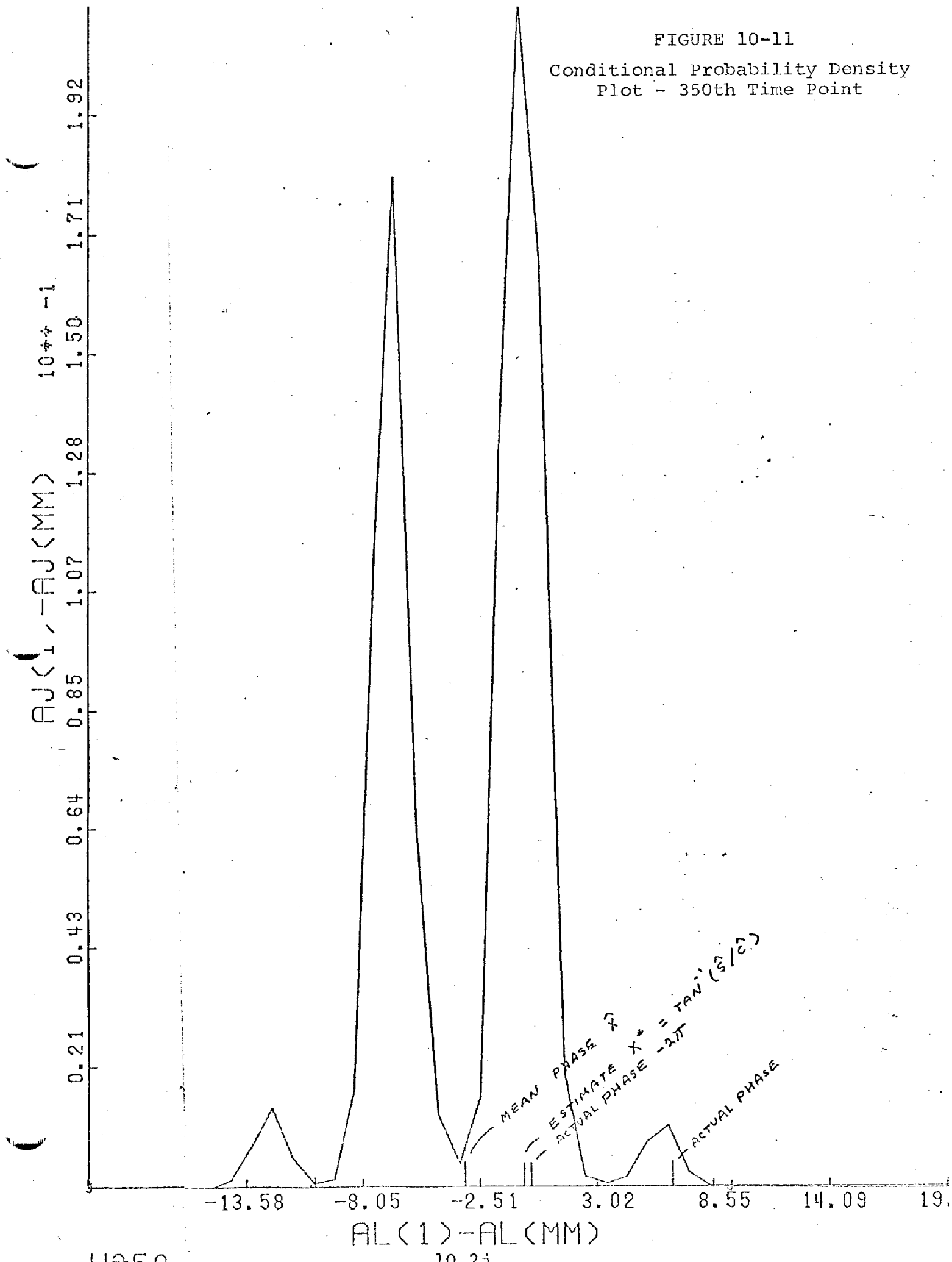


10.21

W200

FIGURE 10-11

Conditional Probability Density
Plot - 350th Time Point



last previous estimate is less than $1/2$ cycle. This was motivated partly by the consideration that our emphasis was on cyclic loss functions $(1 - \cos e)$ for which full cycle errors are irrelevant and partly by the consideration of working toward estimates which only computed the cyclic density function (on the circle) in which case the multimodal density information such as Figures 10-2 - 10-11 is not available to the estimator. The question of optimal usage of the multimodal density information to resolve cyclic ambiguities is as yet open.

10.2 Monte Carlo Results

The principal simulation results consist of a series of 40 runs each of length 500 points, all at $F = 10$ (points per PLL time constant) and at $R = 1.0, .75, .5$, and $.25$ (linear PLL noise/signal ratio). The results of these individual runs are given in Tables 10.1 - 10.4 along with the cumulative statistics. The cumulative results are plotted in Figure 10-12 along with Viterbi's exact theoretical result for the first-order PLL. The theoretical sampling error in these runs is $\pm .14$ db (see Section 9.2) except for the case $R = 1$ for which only 20 runs were available and the sampling error is $\pm .18$ db. The PLL results are reasonably close to Viterbi's result but with an apparently significant bias of about -0.2 db which is just the expected effect due to the use of finite $F = 10$, see eqn. 4.17). The cyclic non-linear estimate appears consistently some 0.6 to 0.7 db better than the phase-locked loop. In view of the fact that we can probably regard the linear model as an ideal lower bound throughout this range of R , this improvement is considered significant; it reflects only about half as much "excess" error (relative to the linear ideal) as the phase-locked loop.

M=56
R=1.0
F=10.

RUN	MEAN-SQUARE MODULO 2π ERROR	
	CYCLIC	PHASE LOCKED
1	1.75 rad ²	2.64 rad ²
2	1.14	.95
3	1.02	1.47
4	.93	1.16
5	.84	.93
6	1.75	1.24
7	2.01	2.37
8	.92	1.02
9	1.57	2.53
10	.78	1.17
11	.99	1.02
12	1.29	1.12
13	1.92	1.59
14	.96	1.20
15	.81	.93
16	2.14	3.19
17	1.46	1.25
18	1.11	1.36
19	1.21	1.26
20	3.20	3.87

RESULTS OF INDIVIDUAL RUNS

TABLE 10-1

M=56
R=.75
F=10.

RUN	MEAN-SQUARE MODULO 2π ERROR	
	CYCLIC	PHASE LOCKED
1	1.46 rad ²	1.35 rad ²
2	1.09	1.10
3	1.19	1.27
4	.77	.93
5	.62	.84
6	1.22	1.09
7	1.80	2.27
8	1.03	1.28
9	1.81	2.30
10	.83	1.07
11	1.01	1.21
12	.86	.90
13	.89	.83
14	.84	.97
15	.51	.63
16	1.43	1.74
17	1.00	.82
18	.67	.79
19	.94	1.01
20	3.58	3.58
21	.97	1.09
22	1.48	1.91
23	.64	.72
24	.81	.87
25	.90	1.34
26	1.02	.89
27	1.70	2.02
28	.70	.73
29	.86	1.03
30	1.79	2.02
31	1.05	1.15
32	1.30	1.48
33	1.06	1.63
34	1.04	1.46
35	1.16	1.77
36	.95	.68
37	1.68	1.70
38	.55	1.32
39	.90	.95
40	.70	1.03

TABLE 10-2
RESULTS OF INDIVIDUAL RUNS

M=56
R=.50
F=10.

RUN	MEAN-SQUARE MODULO 2π ERROR	
	CYCLIC	PHASE LOCKED
1	.99 rad ²	.77 rad ²
2	.76	.57
3	1.09	1.02
4	.55	.59
5	.40	.43
6	.84	.92
7	.77	1.72
8	.49	.56
9	.59	.59
10	.51	.60
11	.41	.64
12	.52	.53
13	.44	.41
14	.56	.85
15	.30	.47
16	1.09	1.25
17	.47	.51
18	.45	.53
19	.52	.52
20	.78	.75
21	.59	.76
22	.70	.70
23	.37	.39
24	.60	.65
25	.45	.56
26	.76	.82
27	.93	.98
28	.45	.45
29	.55	.63
30	.93	.97
31	.67	.73
32	.87	.98
33	.56	.64
34	.49	.31
35	.68	.81
36	.52	.51
37	.94	1.31
38	.46	.51

RESULTS OF INDIVIDUAL RUNS

TABLE 10-3

M=56
R=.25
F=10.

RUN	MEAN-SQUARE MODULO 2π ERROR	
	CYCLIC	PHASE LOCKED
1	.40 rad ²	.50 rad ²
2	.25	.24
3	.41	.44
4	.23	.24
5	.20	.20
6	.29	.34
7	.32	.30
8	.27	.27
9	.27	.26
10	.21	.23
11	.21	.24
12	.26	.25
13	.19	.18
14	.24	.26
15	.16	.18
16	.39	.42
17	.18	.20
18	.25	.25
19	.26	.28
20	.27	.26
21	.27	.30
22	.29	.29
23	.18	.18
24	.34	.35
25	.25	.27
26	.22	.22
27	.37	.42
28	.22	.22
29	.27	.29
30	.36	.37
31	.36	.38
32	.28	.29
33	.25	.28
34	.22	.23
35	.34	.38
36	.16	.15
37	.44	.50
38	.22	.23
39	.32	.33
40	.22	.23

TABLE 10-4

RESULTS OF INDIVIDUAL RUNS

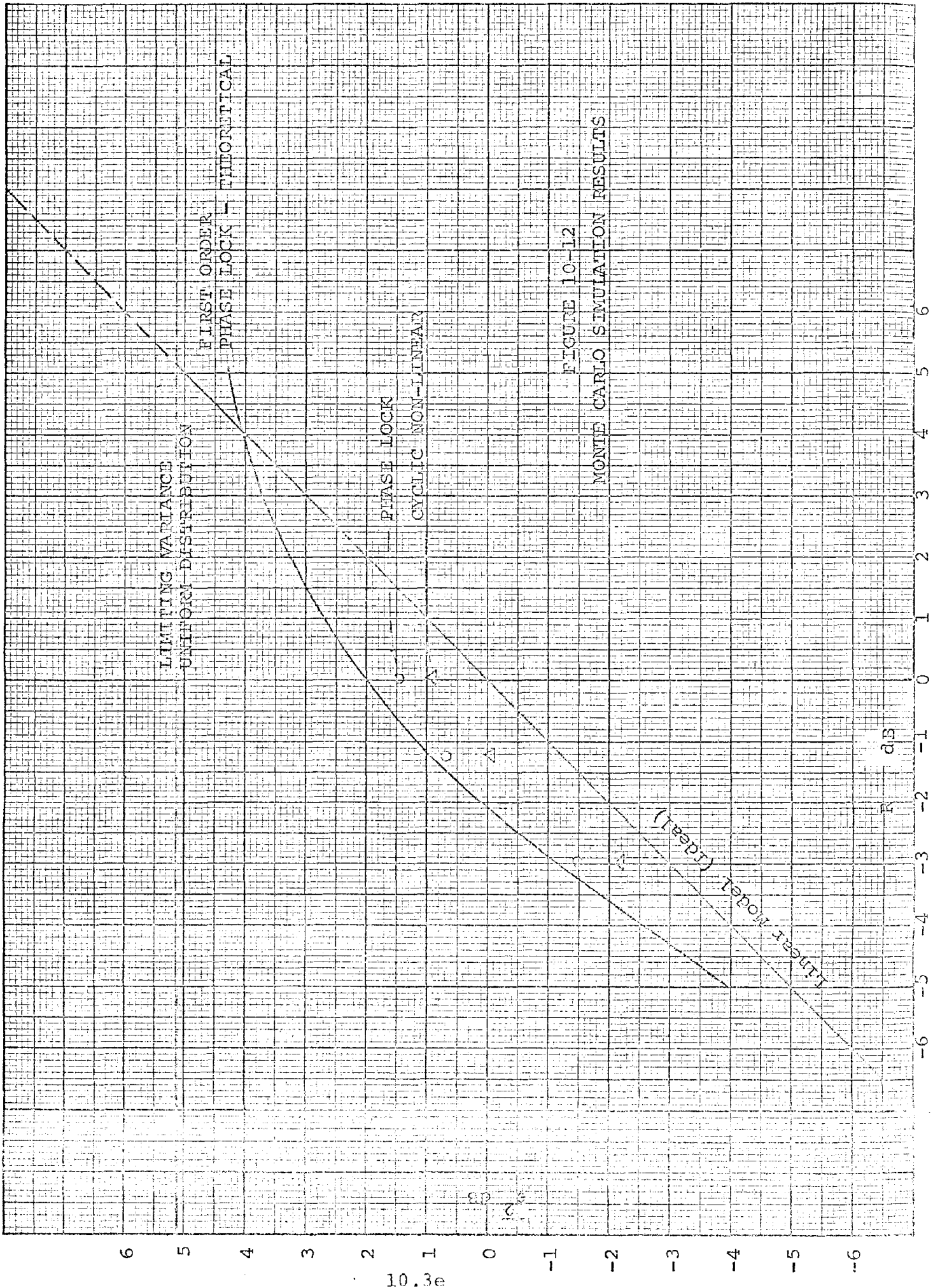


FIGURE 10-12
 MONTE CARLO SIMULATION RESULTS

10.3. Significance of the Phase Noise Results

In view of the small db difference between the two it appears necessary to give some consideration at this point to the overall significance of these results. What we have computed here is just the phase estimate error or noise, i.e., just one-half of the total signal/noise question. Since the maximum possible phase noise is that of a uniform distribution of $\pi^2/3 = +5.1$ db (rad) and the phase-lock loop performs reasonably close to the linear ideal the maximum conceivable improvement in phase noise is limited.

What about signal? In the retrospective light of these results it is clear that here is where the major difference between various phase estimators must show up and indeed there is room for very considerable differences in this respect. It has to be recognized that signal output is also a function of signal/noise input. This is the phenomenon of signal suppression.

How do we measure the "signal" component of signal/noise output. Since this is most certainly a non-linear function of the phase signal (i.e., phase modulation) input it must be defined on an incremental basis, also it is clearly a function of frequency. For fixed signal and noise statistics then we can define the "spot signal suppression factor" (analogously to the spot noise figure) following conventional usage as the ratio of the coherent component of phase signal out (radians) at frequency f to the corresponding phase signal input for a small increment of phase modulation at f . This can be measured as shown in Figure 10-13. Here a small increment, δ , of phase modulating signal is introduced at frequency f_1 . The corresponding coherent component of the output phase estimate is detected coherently with respect to the input, averaged, and normalized to yield the ratio, S , of the increment of coherent output to input. This signal suppression factor S is in general less than unity (see Middleton, Ref. 24, Ch. 19) and only approaches unity at high input signal/noise ratios (small R).

Note that this is quite a general definition of signal suppression, applicable to any sort of stochastic black box phase estimator.

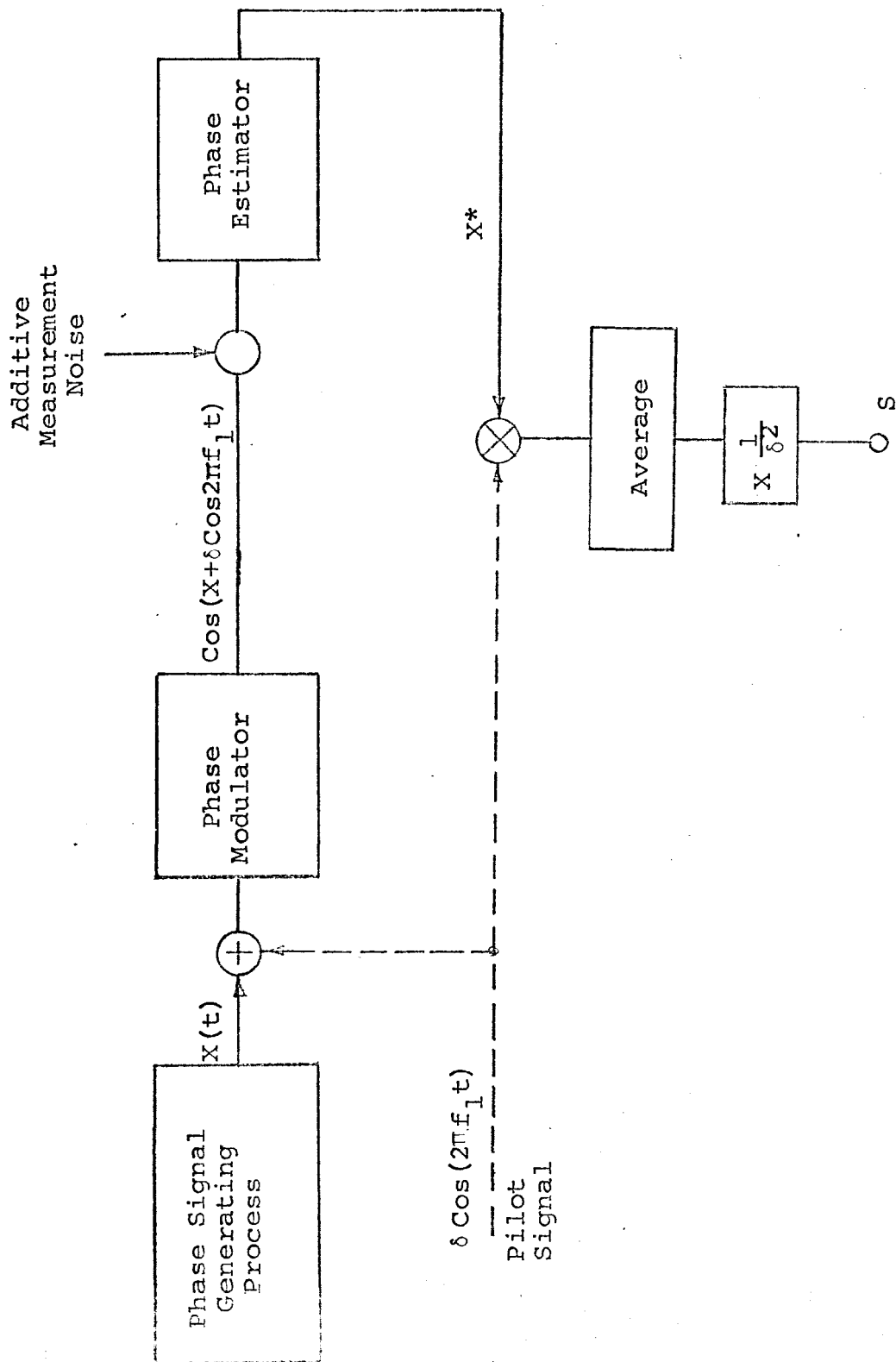


FIGURE 10-13
SIGNAL SUPPRESSION MEASUREMENT

It is suggested, though the concept has yet to be fully explored, that an equivalent measure of the spot signal suppression factor is afforded in the general case of experiments such as we have run by computing the input spectral density

$$G_{xx}(f)$$

and the input-output cross spectral density

$$G_{xx^*}(f)$$

and forming the ratio such as

$$S(f) = \frac{|G_{xx^*}(f)|}{G_{xx}(f)}$$

Unfortunately due to computing difficulties in the last two months of the contract there has been no opportunity to test this concept.

It also appears probable that this factor can be related to the information rate of the systems viewed as channels and in turn to theoretical closed forms for the output signal/noise ratio for the general non-linear filter.

11. IMPLEMENTATION

Consider the increment equation for the harmonic equations developed in eq. 8.16). This is in effect a set of differential equations to be satisfied by the F 's.

$$\frac{dF_k}{dt} = -\frac{qk^2}{2} F_k + \frac{1}{2r} \left[(F_{k+1} - F_1 F_k)(z^* - F_1^*) + (F_{k-1} - F_1^* F_k)(z - C_1) \right] \quad 11.1)$$

Consider that we have available the various F_k as complex modulation functions on carrier frequencies $e^{ik\omega t}$ and the measurement in the form $ze^{i\omega t}$. Then notice that by multiplying both sides of eq. 11.1) by $e^{i\omega t}$ where ω is a carrier frequency high with respect to $\frac{qk^2}{2}$, we can transform eq. 11.1) into

$$\begin{aligned} \frac{dF_k}{dt} e^{ik\omega t} = & -\frac{qk^2}{2} F_k e^{ik\omega t} + \frac{1}{2r} \left[(F_{k+1} e^{i(k+1)\omega t} - F_1 e^{i\omega t} F_k e^{ik\omega t})(z^* e^{-i\omega t} - F_1^* e^{-i\omega t}) \right. \\ & \left. + (F_{k-1} e^{i(k-1)\omega t} - F_1^* e^{ik\omega t} F_k e^{9k\omega t})(z e^{i\omega t} - F_1 e^{i\omega t}) \right] \end{aligned} \quad 11.2)$$

In overall form this corresponds to the solution for a first-order (single pole pair) bandpass filter at center frequency ω , having bandwidth $\frac{qk^2}{2}$.

Straightforward implementation of this relation appears as in Figure 11-1. Only the k^{th} branch is shown completely for ease of presentation. Tracing through the various signals it can be confirmed that this circuit does indeed implement eqn. 11.2).

The current value of F_k is assumed stored in the first or computing Band-Pass Filter on a carrier frequency of $k\omega$. This is mixed with $F_1 e^{i\omega t}$ in a double side-band (suppressed carrier) modulator. The resulting lower and upper side-bands are, respectively, the terms

$$F_1^* F_k e^{i(k-1)\omega t}$$

$$F_1 F_k e^{i(k+1)\omega t}$$

⊖ Denotes a linear subtractor

⊗ Denotes a mixer

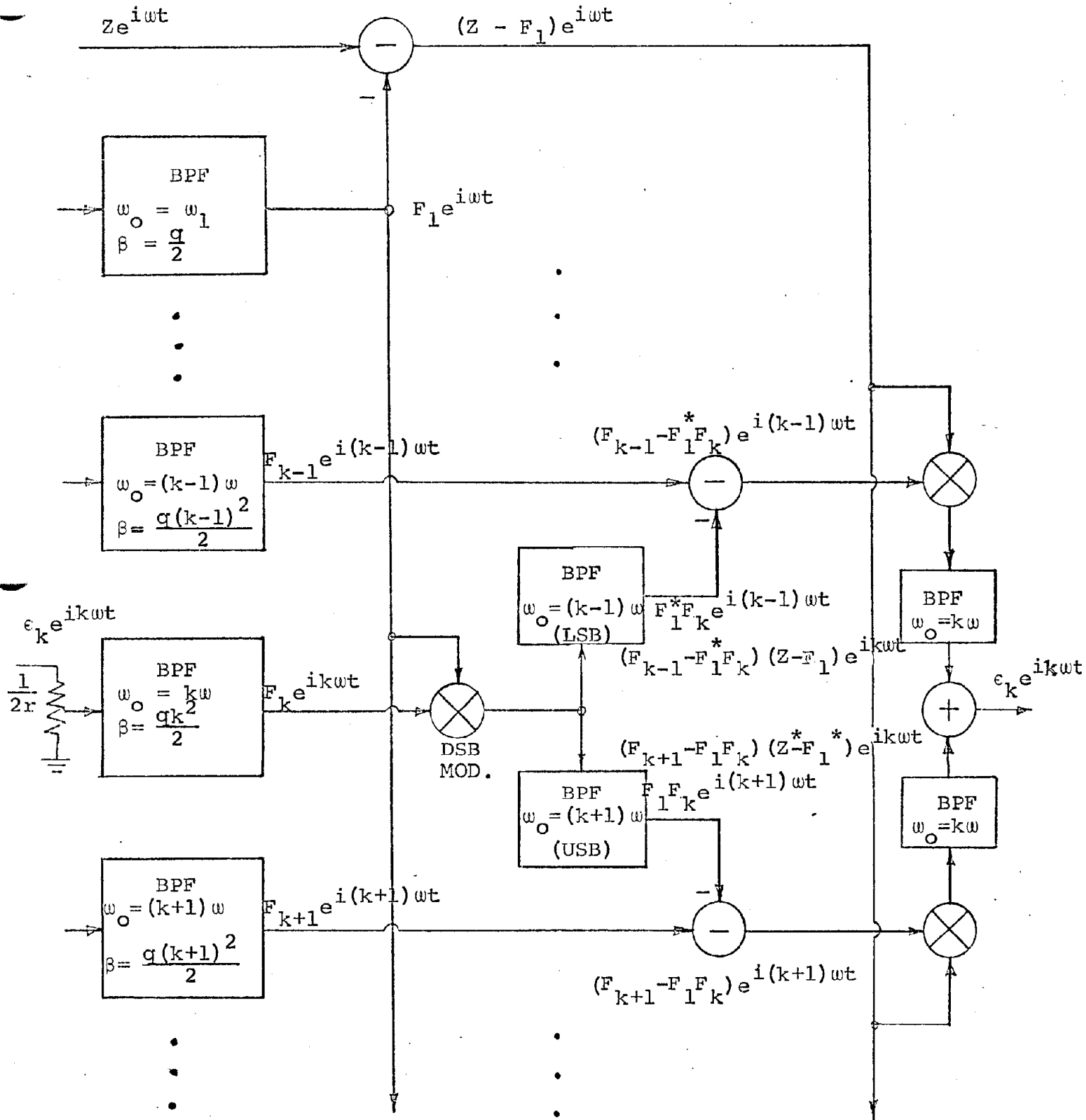


FIGURE 11-1
IMPLEMENTATION #1

These are subtracted (linearly) from the F_{k-1} and F_{k+1} terms to give the terms

$$(F_{k-1} - F_1^* F_k) e^{i(k-1)\omega t}$$

$$(F_{k+1} - F_1 F_k) e^{i(k+1)\omega t}$$

Finally these are mixed with $(z_1 - C_1) e^{i\omega t}$ choosing in both cases the $k\omega$ sidebands which are then added to give

$$\epsilon_k e^{ik\omega t} \equiv \left[(F_{k-1} - F_1^* F_k)(z - F_1) + (F_{k+1} - F_1 F_k)(z^* - F_1^*) \right] e^{ik\omega t}$$

The fraction $\frac{1}{2r}$ of this is the driving term which feeds back to the computing bandpass filter.

This mechanization can be considerably simplified by combining linear operations. The final two filters are clearly redundant of the first or "computing filter". Also the first two filters and the double second multipliers can be seen to be redundant so that the k^{th} branch reduces to the form shown on Figures 11-2a and 11-2b. It is to be emphasized that the multipliers or mixers denoted \otimes in these diagrams must all be linear with respect to each of their inputs, and the carrier must be reasonably well suppressed in the first multiplier. These requirements can all be met with balanced square-law-type multipliers.

The more or less complete implementation including $F_0 (=1)$, F_1 , F_2 , and F_3 stages are shown in Figure 11-3. The output is directly F_1 .

Note that this mechanization may be considered as a series of harmonic phase-locked loops, each aiding its adjacent neighbors in a particular way as shown.

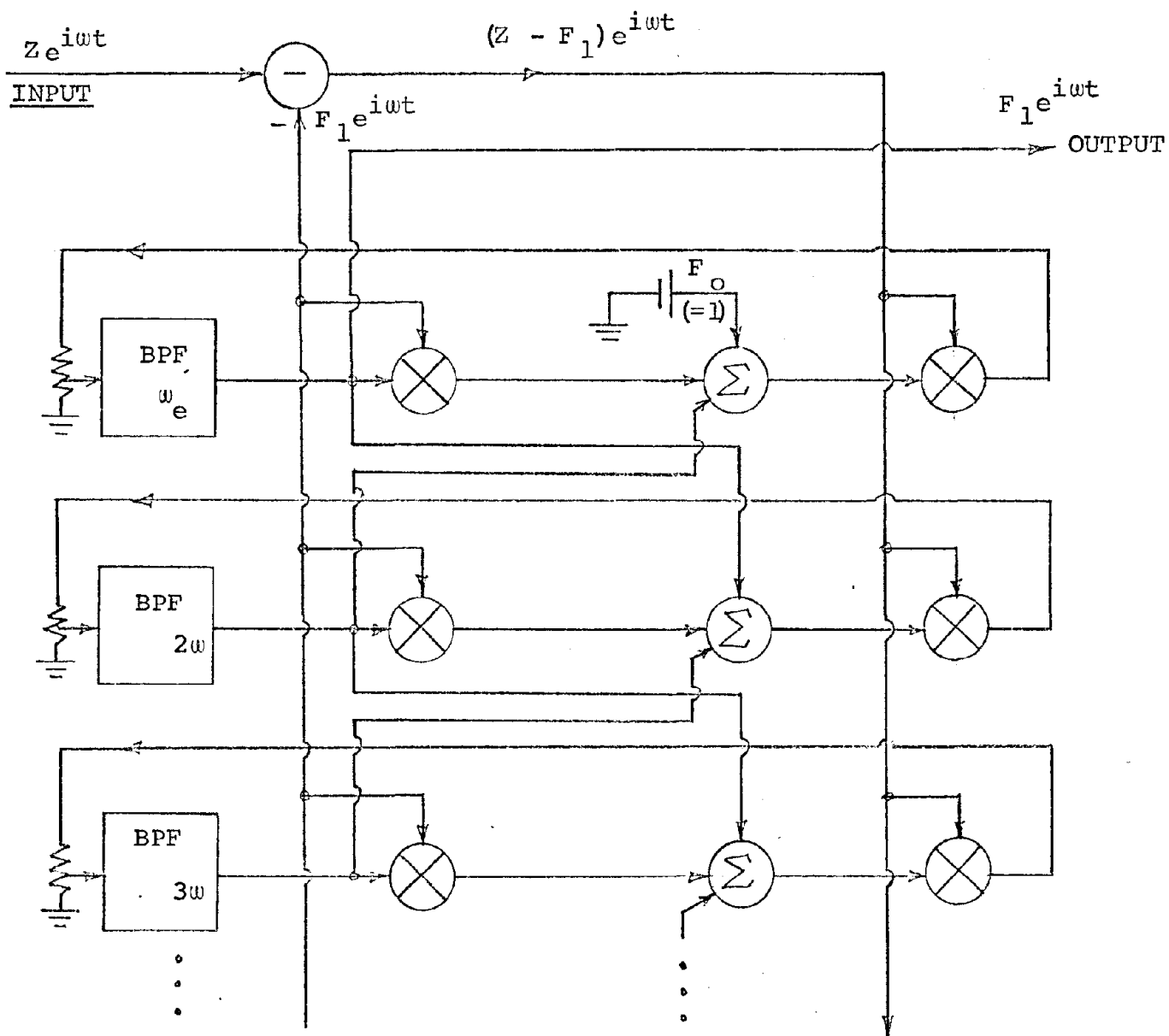


FIGURE 11-3
IMPLEMENTATION

12. CONCLUSIONS

1. The Bayes sequential non-linear phase estimator has been shown by simulation to provide an improved phase estimator relative to the Phase-Locked Loop.
2. The improvement has only been measured in terms of noise output and in these terms the improvement is about 0.6 to 0.7 db relative to maximum conceivable improvement of 2.2 db. Expressed in another way, excess noise relative to the ideal is about 1/3 less in db than that of the phase-locked loop.
3. A means for measuring the signal suppression factor in hardware experiments or simulation has been devised but there has not been time in the present contract to explore this avenue. This is unfortunate because it is clear that only in this respect could a significant difference between various phase estimators, i.e., more than about 2 db possibly exist (see discussion, Section 10.3).
4. The optimization herein was on the basis of a cyclic loss function $2(1 - \cos \epsilon)$. The means for resolving cyclic ambiguities was somewhat arbitrarily chosen as minimizing the change between successive phase estimates in terms of the cyclic ambiguity. The question of optimum resolution of the cyclic ambiguity for problems such as doppler tracking where the proper resolution is important, is as yet open.
5. Several different potential realizations of the optimal non-linear filter have been developed. Of these the most attractive for real hardware mechanization is that based on the Fourier series representation of the cyclic density function (see Section 11). This may be envisioned as a series of harmonic phase-locked loops, aiding each other in a particular way as shown.

6. Within the limitations of the study the overall results are considered highly encouraging. However, these limitations are significant and more work along these lines is strongly recommended. In particular, questions to be answered include

- Include in the simulation means for determination of signal suppression and comparison with phase-locked loop in this respect.
- Proceed to study of the second-order problem and comparison with second-order PLL
- Digital simulation of the two forms (update and increments) of the Fourier coefficients of the conditional density function and comparison with present form.
- Derive optimal resolution of cyclic ambiguity for doppler tracking problem.
- Conditional on the above simulation results, proceed to hardware implementation and test of the differential Fourier form of the optimal non-linear filter.

APPENDIX 1

SEQUENTIAL BAYES ESTIMATION

This appendix is written to serve as a very basic introduction to Bayes sequential estimation or optimal non-linear filtering as used herein. For this purpose consider a scalar observation and state and first-order dynamics.

Assume that the state dynamics, i.e., the model for the information process are known to be of the first-order form

$$x_{i+1} = x_i + u_i \quad \text{A1.1)}$$

where u_i is a zero mean, serially uncorrelated random deviate having probability density $G(u)$.

The observations are G taken to be some non-linear function of the state plus additive measurement noise

$$z_{i+1} = h(x_{i+1}) + v_{i+1} \quad \text{A1.2)}$$

where v_i is zero mean, serially uncorrelated, independent of u_i and has probability density $N(v)$

Let us start an induction process by assuming that we know the conditional probability density $p_{i/i-1}(x)$ of x given all the measurements up through the $(i-1)^{\text{th}}$. That is

$$\begin{aligned} p(x_i | z_{i-1}, z_{i-2}, \dots, z_1) dx &= \text{Prob}(x_i < x < x_i + dx) \text{ given } z_{i-1}, z_{i-2}, \dots, z_1 \\ &= \text{"one-step predictor density"}. \end{aligned}$$

Then given the observation z_1 straightforward successive applications of the rules of conditional probability (Bayes rule) lead to

$$\begin{aligned}
p(x_i | z_i, \dots) &= \frac{p(x_i, z_i, \dots)}{p(z_i, \dots)} \\
&= \frac{p(z_i | x_i, z_{i-1}, \dots) p(x_i, z_{i-1}, \dots)}{p(z_i, \dots)} \\
&= p(z_i | x_i, z_{i-1}, \dots) p(x_i | z_{i-1}, \dots) \left[\frac{p(z_{i-1}, \dots)}{p(z_i, \dots)} \right] \\
&= \frac{p(z_i | x_i, z_{i-1}, \dots) p(x_i | z_{i-1}, \dots)}{p(z_i | z_{i-1}, \dots)}
\end{aligned}$$

Now consider the three terms on the right-hand side

- 1) $p(z_i | x_i, z_{i-1}, \dots)$. Since z_i as given by A1.2) is only a function of x_i v_i , and since v_i is independent of v_{i-1}, v_{i-2}, \dots we have

$$\begin{aligned}
p(z_i | x_i, z_{i-1}, \dots) &= p(z_i | x_i) \\
&= N(z_i - f(x_i))
\end{aligned}$$

- 2) $p(x_i | z_{i-1}, z_{i-2}, \dots)$. This is available as the a priori density with which we started

- 3) $p(z_i | z_{i-1}, z_{i-2}, \dots)$. Since this is not a function of x it may be regarded simply as a normalization constant, K , required to bring the total probability back to unity.

Thus

$$\boxed{p(x_i | z_i, z_{i-1}, \dots) = K N(z_i - f(x_i)) p(x_i | z_{i-1}, z_{i-2}, \dots)}$$

= "filter density"

Thus the one-step predictor density is updated to the "filter density" by simply multiplying by the N density function of argument $z_i - f(x_i)$.

To complete the iteration cycle we must then update the filter density to the prediction density at the next step. To do this note that

$$\begin{aligned}
p(x_{i+1} | z_i, z_{i-1}, \dots) &= \int p(x_{i+1}, x_i | z_i, z_{i-1}, \dots) dx_i \\
&= \int p(x_{i+1} | x_i, z_i, z_{i-1}, \dots) p(x_i | z_i, \dots) dx_i
\end{aligned}$$

but by equation A1.1, x_{i+1} depends only on x_i and v_i which is independent; the first term in the integral is thus just the density function G of argument $x_{i+1} - x_i$ or

$$p(x_{i+1} | z_i, z_{i-1}, \dots) = \int G(x_{i+1} - x_i) \cdot p(x_i | z_i, z_{i-1}, \dots) dx_i$$

This completes the iteration and we are ready to start another cycle in the same way.

If G and N are Gaussian density functions with zero mean and variances respectively B and C then, and defining for simplicity

$$\begin{aligned} p_{i/i}(x) &= p(x | z_i, z_{i-1}, \dots) \\ &= \text{conditional density of } x \text{ based on all measurements} \\ &\quad \text{through the } i^{\text{th}} \end{aligned}$$

$$\begin{aligned} p_{i/i-1}(x) &= p(x | z_{i-1}, \dots) \\ &= \text{conditional density of } x \text{ based on all measurements} \\ &\quad \text{through the } i-1^{\text{th}}. \end{aligned}$$

Then the iteration is

$$\text{given } p_{i/i-1}(x)$$

$$\begin{aligned} p_{i/i}(x) &= K_1 \exp \left[- \frac{(z_i - f(x))^2}{2C} \right] p_{i/i-1}(x) \\ p_{i+1/i}(x) &= K_2 \int \exp \left[- \frac{(x-y)^2}{2B} \right] p_{i/i}(y) dy \end{aligned}$$

These are the principal equations used for the non-linear filter in this report. The extension to vector observations is relatively simple and in the Gaussian case results simply in the substitution of the appropriate quadratic form in the observational residuals in the argument of the N density function.

Bayes Theorem and Digital Realizations for Non-Linear Filters¹

R. S. Bucy²

1.0 Introduction

Even though the theory of optimal non-linear filtering is theoretically fairly well understood today (see [1] for a description of the theory and relevant references), the attendant problem of synthesis of non-linear filters is almost untouched. Since one of the unsettling features of the non-linear theory is an almost total non-existence of examples, it is clear that the synthesis problem is not only practically relevant, but also theoretically relevant for the problem of asymptotic behavior. The forthcoming thesis of Lo (see [3]) will provide some closed form resolutions for non-linear filters, however.

In this paper, we will describe our results on the synthesis of a one-dimension discrete time, non-linear filters. In the discrete case, it has been pointed out by many investigators in control ([2], [3] and [4]), non-linear filtering basically consists of a sequential application of Bayes' rule. Of course, this idea is well known in the statistical literature (see in particular [6]). We have chosen the discrete time case in order to avoid the well-known dilemma arising in the simulation of a diffusion process and the relevant stochastic integrals. The mechanics of the realization we describe are not limited to the one-dimensional situation, but for reasons of simplicity of description in the section dealing with the time-sharing basic program and numerical results, we will confine ourselves to this one-dimensional case.

¹This research was supported in part by the United States Air Force Office of Aerospace Research, Applied Mathematics Division, under Grants No. AF-AFOSR 1244-67A and AF-AFOSR 1244-67B. Manuscript submitted June 1969.

²University of Southern California, Los Angeles, California and Electrac Inc., Anaheim, California.

The paper will be divided into three parts; the first being a description of the signal and noise processes and the sensor, the second a review of the sequential formulae for the conditional distributions of the signal given the observations derived via Bayes' rule, a description of our synthesis method and a Basic Program as well as a comparison of our results to the performance of a linearized filter.

2.0 Modeling

In general, bold-face, lower-case latin letters denote vectors, while lower-case, latin letters denote scalars. The signal process $\{x_n\}_{n=1, \dots, m \dots}$ is a discrete time index set of n -vector valued random variables and satisfies

$$\begin{aligned} x_n &= \phi(x_{n-1}) + \sigma(x_{n-1}) u_{n-1} \\ x_0 &= c \end{aligned} \quad (1.0)$$

with ϕ a function from R^n to R^n and σ a function from R^n to $n \times r$ matrices, with $\sigma' \sigma$ invertible.

The stochastic process $\{u_n\}_{n=1, \dots, m \dots}$ is a set of independent and identically distributed r -vector valued random variables with density $g(u)$. While c is an n -vector valued random variable independent of the u_n processes and having density $l(c)$. Now the observation process $\{z_n\}_{n=1, \dots, m \dots}$ is an s -vector valued process related to the signal process as

$$z_n = h(x_n) + v_n \quad (1.1)$$

with h a function from R^n to R^s and $\{v_n\}$ a set of independent and identically distributed s -vector valued variables, each having density $n(v)$ and independent of c and the u_n .

The filtering problem then consists of the determination of

$$J_{n|t}(y) dy = P(x_n \in dy | z_t, \dots, z_0) \quad (1.2)$$

where P is the conditional distribution of the n the signal given the first t observations. We remark for future use that x_n is a stationary Markov process and define its transition density as

$$p(r, x, y) dy = P(x_{r+j} \in dy | x_j = x) \quad (1.3)$$

3.0 Sequential Relations

Our purpose in this section will be to derive sequential relations satisfied by the various $J_{n|t}(y)$. Our first result is:

Theorem 1: $J_{n|n}(y)$ is uniquely determined by the difference equation

$$J_{n|n}(y) = \frac{1}{K(n)} n(z_n - h(y)) \int \int g(\sigma(x)) (y - \phi(x)) J_{n-1|n-1}(x) \quad (2.1)$$

with

$$J_{0|0}(y) = \frac{1}{K^*} n(z_0 - h(y)) l(y) \quad (2.2)$$

where

$$K^* = p(z_0) \quad K(n) = p(z_n | z_{n-1}, \dots, z_0)$$

and

$$P(z_0 \in dl) = p(l) dl$$

$$P(z_n \in dk | z_{n-1}, \dots, z_0) = p(k | z_{n-1}, \dots, z_0) dk.$$

Proof. Using the relevant densities, we find

$$\begin{aligned} J_{0|0}(y) dy &= P(x_0 \in dy | z_0) = \frac{p(z_0 | y_0) p(y_0) dy}{p(z_0)} \\ &= \frac{1}{p(z_0)} n(z_0 - h(y)) l(y) dy \end{aligned}$$

using Bayes' rule.

Now

$$\begin{aligned} J_{n|n}(y) dy &= P(x_n \in dy | z_n, \dots, z_0) = \frac{P(x_n \in dy, z_n, \dots, z_0)}{p(z_n, \dots, z_0)} \\ &= \frac{1}{K(n)} P(x_n \in dy, z_n | z_{n-1}, \dots, z_0) \\ &= \frac{1}{K(n)} \int \int P(x_n \in dy, z_n, x_{n-1} | z_{n-1}, \dots, z_0) dx_{n-1} \\ &= \left(\frac{1}{K(n)} n(z_n - h(y)) \int \int g(\sigma(x)) (y - \phi(x)) J_{n-1|n-1}(x) dx \right) dy \end{aligned}$$

using Bayes' rule and the fact that v_n, u_{n-1} and z_{n-1}, \dots, z_0 are independent.

Corollary for $r > 0$

$$J_{n+r|n}(y) = \int \cdot n \cdot \int p(r, x, y) J_{n|n}(x) dx \quad (2.3)$$

$$J_{n+1|n}(y) = \frac{1}{K(n)} \int \cdot n \cdot \int g\left(\left(\sigma(x)\right)\left(y - \phi(x)\right)\right) n \left(z_n - h(x)\right) J_{n|n-1}(x) dx \quad (2.4)$$

$$J_{n-r|n}(y) =$$

$$\frac{1}{C(n, r)} J_{n-r|n-r}(y) \left[\int \cdot r \cdot \int L_{n,r}(y_n, \dots, y_{n-r+1}, y) dy_n, \dots, dy_{n-r+1} \right] \quad (2.5)$$

$$L_{n,r}(y_n, \dots, y_{n-r}) = \prod_{j=n-r+1}^n n(z_j - h(y_j)) g(\sigma^+(y_{j-1})(y_j - \phi(y_{j-1})))$$

$$C(n, r) = p(z_n, \dots, z_{n-r+1} | z_{n-r}, \dots, z_0).$$

Proof. Now

$$\begin{aligned} J_{n+r|n}(y) &= \iiint p(x_{n+r}, x_n | z_n, \dots, z_0) dx_n \\ &= \int \cdot n \cdot \int p(x_{n+r} | x_n, z_n, \dots, z_0) p(x_n | z_n, \dots, z_0) dx_n \\ &= \int \cdot n \cdot \int p(r, x, y) J_{n|n}(x) dx \end{aligned}$$

by the Markov property. Noting that $p(1; x, y) = g(\sigma^1(x)(y - \phi(x)))$ using Eqs. (2.1) and (2.3), (2.4) is then a consequence.

In order to establish Eq. (2.5), note that

$$\begin{aligned} J_{n-r|n}(y) &= p(x_{n-r} = y | z_n, \dots, z_0) = \frac{1}{C(n, r)} \frac{p(x_{n-r} = y, z_n, \dots, z_0)}{p(z_n, \dots, z_0)} \\ &= \frac{1}{C(n, r)} \int \cdot n \cdot \int \frac{p(x_{n-r} = y, z_n, \dots, z_0, z_n, x_n = y_n, \dots, x_{n-r+1} = y_{n-r+1}) dy_n, \dots, dy_{n-1}}{p(z_n, \dots, z_0)} \\ &= \frac{1}{C(n, r)} \int \cdot r \cdot \int J_{n-r|n-r}(y) p(z_i, x_i = y \cdot n - r + 1 \leq i \leq n | x_{n-r} = y_{n-r}) dy_n, \dots, dy_{n-1} \\ &= \frac{J_{n-r|n-r}(y)}{C(n, r)} \int \cdot r \cdot \int L_{n, r} dy_n, \dots, dy_{n-r+1} \end{aligned}$$

4.0 Synthesis and Realization

In this section, we will assume $\{x_n\}$ and $\{z_n\}$ are *scalar valued*, further we will define $J_{n+1}(y) \equiv J_{n+1|n}(y)$. The first question that arises is how can the function $J_n(y)$ be conveniently stored by the digital computer. For the purposes of this section, a probability density will be represented sufficiently accurately by a pair (J, f) where J is a $2M + 1$ vector and f is a map from the set $\{1, 2, \dots, 2M + 1\}$ to the reals. The components of J can be considered as non-negative masses, while $f(i)$ is the point in R^1 which carries the i th mass, the value of this mass being the i th coordinate of J .

For illustrative purposes, we will specialize to a particular problem, the obvious modifications for any other particular problem being left to the reader, given by

$$\begin{aligned} x_n &= ax_{n-1} + u_{n-1} \\ x_0 &= c \\ z_n &= (x_n)^3 + v_n \end{aligned} \quad (3.1)$$

specializing Eqs. (1.0) and (1.1). The solution of the filtering problem then hinges on determination of the set of functions $\{J_n(y)\}_{n=1} \dots$ or replacing these probability densities by mass distributions $\{J_n, f_n(\cdot)\}$ for purposes of synthesis; we find

$$J_{n+1}(i) \sim \sum_{j=1}^{2M+1} g(f_{n+1}(i) - af_n(j)) n(z_n - f_n^3(j)) J_n(j) \quad (3.2)$$

$$J_0(i) \sim l(f_0(i))$$

in view of Eq. (2.4) where of course \sim denotes proportionality and

$$\sum_{i=1}^{2M+1} J_n(i) = 1$$

for all n . It remains only to determine $f_n(i)$, the gridding to determine the filter, and we found the following an effective choice:

$$f_{n+1}(i) = \mu_n - 8\sigma_n + \frac{8\sigma_n}{M}(i-1) \quad n \geq 0$$

$$f_0(i) = f_1(i)$$
(3.3)

where

$$\mu_n = \sum_{i=1}^{2M+1} f_n(i) J_n(i)$$

$$\sigma_n^2 = \sum_{i=1}^{2M+1} (f_n(i) - \mu_n)^2 J_n(i)$$
(3.4)

The philosophy is to center the n th grid at the previous estimate with a mesh proportional to the standard deviation and the $16\sigma_n$ width of the grid was found to be necessary in order that true signal did not escape the moving grid, for when the true signal does not lie within the grid, the iteration scheme becomes very inaccurate.

To see the power of the above scheme, when the linear filter is solved this way with $M = 7$, the sequence μ_n, σ_n^2 agree with the solutions of the linear filter equations to 6 or more places.

Now Fig. 1 depicts the flow chart of the synthesis of the optimal filter and Fig. 2 the actual basic program for this synthesis when l, g and γ are Gaussian with means 0 and variances A, B, C respectively. In Figs. 3, 4, 5 actual non-linear filter outputs are given.

5.0 Linearized Filters

Again consider the model (3.1)

$$x_n = ax_{n-1} + u_{n-1}$$

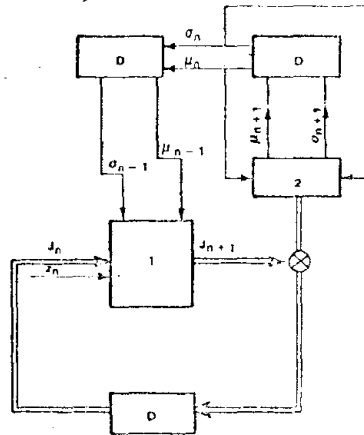


FIG. 1

```

10 PRINT "INPUT A SET OF VALUES A,B,C,N,M,G,D"
15 INPUT A,B,C,N,M,G,D
20 LET T9=2*M+1
21 DIM J(T9),L(T9),H(T9)
35 T=Y1=0
36 S1=A^(0.5)
37 P1=A
38 X1=0
40 FOR I=1 TO T9
45 L=(C/M)^(I=1)-8
50 J(I)=(1/(2*PI*A)^(0.5))*EXP(-0.5*L^2)
60 T=T+J(I)
65 NEXT I
70 FOR I=1 TO T9
80 J(I)=J(I)/T
90 NEXT I
95 K=1
100 X=SQR(A)*SQR(-2*LOG(RND(-1)))*COS(2*PI*RND(-1))
109 W=1
110 V=SQR(C)*SQR(-2*LOG(RND(-1)))*COS(2*PI*RND(-1))
120 U=SQR(B)*SQR(-2*LOG(RND(-1)))*SIN(2*PI*RND(-1))
124 Z=X^2+V
130 X=G*X+U
133 Y0=Y1
139 S0=S1
140 Y1=S1=0
142 FOR I=1 TO T9
143 L(I)=Y0-3*SO+8*SO/M*(I-1)
150 Y1=Y1+J(I)*L(I)
152 S1=S1+L(I)^2*(1)
156 NEXT I
157 S1=S1-Y1^2
158 K=Y2=S2=0

```

```

159 S1=SQR(S1)
160 FOR I=1 TO T9
162 H=0
165 L(I)=Y1-8*S1+3*S1/M*(I-1)
170 FOR F=1 TO T9
175 Q=Y0-8*(SO)+(3*(SO)/M)*(F-1)
177 R=EXP(-L(I)-G*Q)^2/(2*B)
190 Q=EXP(-(Z-Q^2)/2/(2*C))
185 H=H+Q*R*(J(F)
190 NEXT F
191 H(I)=H
200 K=K+H(I)
201 S2=S2+L(I)^2*H(I)
202 Y2=Y2+L(I)*H(I)
210 NEXT I
211 Y2=Y2/K
212 S2=SQR(S2/K-Y2^2)
220 FOR I=1 TO T9
225 H(I)=H(I)/K
230 NEXT I
231 FOR I=1 TO T9
232 J(I)=H(I)
233 NEXT I
235 GO TO 300
241 PRINT "X","Y2","S2","Z"
242 PRINT X,TAB(16);Y2,TAB(31);S2^2,TAB(46);Z
251 W=W+1
260 IF W<N THEN 110
300 X2=G*X1+G*P1/(P1+C)*(Z-X1)
310 P2=C*G^2*P1/(P1+C)+B
320 X1=X2
321 P1=P2
330 GO TO 241

```

FIG. 2

<RUN
 INPUT A SET OF VALUES A,B,C,N,M,G,D
 ?-1,1,1,100,28,0,5,3

X	Y2	S2	Z
-0.626713664	-7.21096771E-03	1.082460276	-0.061269082
X	Y2	S2	Z
0.174233842	0.281603879	1.098365541	1.729668579
X	Y2	S2	Z
3.107302746	0.101557808	1.084383581	0.450681052
X	Y2	S2	Z
1.0397463	1.488286808	1.000002777	29.83663919
X	Y2	S2	Z
0.424397218	0.248842188	1.062254019	0.21460984
X	Y2	S2	Z
-0.53420807	0.050586494	1.082736927	0.0920627
X	Y2	S2	Z
-1.51678737	-0.028555029	1.08446859	-0.300751202
X	Y2	S2	Z
-0.375670138	-0.728327511	1.011782685	-3.782497717
X	Y2	S2	Z
-0.860187797	-0.215462635	1.078218119	-0.752476644
X	Y2	S2	Z
-0.953289574	-0.177153465	1.089599856	-1.034709837
X	Y2	S2	Z
-1.252639799	-0.671950375	1.02158232	-3.291268051
X	Y2	S2	Z
-3.579140751	-0.574517959	1.039936074	-2.557312928
X	Y2	S2	Z
-0.793037782	-1.779880267	0.999999999	-46.94926414
X	Y2	S2	Z
-0.355264521	-0.316930636	1.055037501	-0.48116593
X	Y2	S2	Z
-0.137670378	0.048319706	1.083314383	0.796062291
X	Y2	S2	Z
0.994986456	0.134199658	1.090361175	0.948025548
X	Y2	S2	Z
-0.874632224	0.279280452	1.094231554	1.613952893
X	Y2	S2	Z
-0.994831115	-0.25511048	1.106106724	-1.82029243
X	Y2	S2	Z
0.243522124	-0.057927168	1.083492355	-0.152925109
X	Y2	S2	Z
0.493904941	0.176798593	1.096072635	1.293479301
X	Y2	S2	Z
-0.133336886	0.714298931	1.013096844	3.625369919
X	Y2	S2	Z
-1.163363547	0.188221642	1.077896102	0.584422792
X	Y2	S2	Z
-1.212483872	-0.594665673	1.050132145	-2.974561468
X	Y2	S2	Z
-1.522165016	-0.5423488	1.049136471	-2.435385056
X	Y2	S2	Z
-0.75219402	-0.563766509	1.046580992	-2.534544307

m = 1.14

m = 1.07

FIG. 3

```

>RUN
INPUT A SET OF VALUES A,B,C,N,M,G,D
? 1,1,10,100,28,0.5,3

```

X	Y2	S2	Z
-0.626713664	-7.66634109E-03	1.143442054	-0.199489387
X	Y2	S2	Z
0.174233842	0.362627213	1.199835733	6.00194633
X	Y2	S2	Z
3.107302746	0.158907622	1.154129465	1.443467115
X	Y2	S2	Z
1.0397463	1.534442006	1.005647891	29.47900856
X	Y2	S2	Z
0.424397218	0.320534672	1.098283136	-1.751832833
X	Y2	S2	Z
-0.53420807	0.092699349	1.146040824	0.125844491
X	Y2	S2	Z
-1.51678737	-1.03765016E-03	1.15116427	-0.621416614
X	Y2	S2	Z
-0.375670138	-0.228243036	1.18164216	-4.41585062
X	Y2	S2	Z
-0.860187797	-0.163992444	1.159645294	-2.2640132
X	Y2	S2	Z
-0.953289574	-0.12768512	1.156771378	-1.895808942
X	Y2	S2	Z
-1.252639799	-0.718656156	1.151797643	-8.534695485
X	Y2	S2	Z
-3.579140751	-0.400765397	1.151018841	-3.836922289
X	Y2	S2	Z
-0.793037782	-1.835628393	1.005485025	-49.32686496
X	Y2	S2	Z
-0.355264521	-0.461137472	1.08737794	-0.443147448
X (DII	Y2	S2	Z
-0.137670378	-0.019237882	1.151243087	2.614324278
X	Y2	S2	Z
0.994986456	0.131987889	1.165645072	3.00356201
X	Y2	S2	Z
-0.874632224	0.175381465	1.165404846	2.973848763
X	Y2	S2	Z
-0.994831115	-0.167527736	1.181521438	-4.309538766
X	Y2	S2	Z
0.243522124	0.028262743	1.155877354	1.645329324
X	Y2	S2	Z
0.493904941	0.211808955	1.177252095	4.05911395
X	Y2	S2	Z
-0.133336886	1.000441847	1.045880587	11.203905
X	Y2	S2	Z
-1.163363547	0.351535002	1.127273231	1.853232947
X	Y2	S2	Z
-1.212483872	-0.23467883	1.208706668	-6.001854186
X	Y2	S2	Z
-1.522165016	-0.26273182DH	1.174029079	-3.847118269
X	Y2	S2	Z
-0.75219402	-0.085167227	1.15103151	-0.388935127
--			
>RUN			

FIG. 4

INPUT A SET OF VALUES A,B,C,N,M,G,D
 ? 1, 1, 100, 25, 28, 0.5, 3

X	Y2	S2	Z
-0.626713664	-5.71231531E-03	1.207084502	-0.636580369
X	Y2	S2	Z
0.174233842	0.302522308	1.326693338	19.51207482
X	Y2	S2	Z
3.107302746	0.169843509	1.252808299	4.553206893
X	Y2	S2	Z
1.0397463	0.808079262	1.386524369	28.34808124
X	Y2	S2	Z
0.424397218	0.187388014	1.239243125	-7.970270567
X	Y2	S2	Z
-0.53420807	0.076921313	1.2363536	0.232671896
X	Y2	S2	Z
-1.51678737	0.01134297	1.237083048	-1.635449684
X	Y2	S2	Z
-0.375670138	-0.07070696	1.245463477	-6.418688354
X	Y2	S2	Z
-0.860187797	-0.111720796	1.249881121	-7.047608086
X	Y2	S2	Z
-0.953289574	-0.096918009	1.244129366	-4.618843405
X	Y2	S2	Z
-1.252639799	-0.585853101	1.39368123	-25.11586892
X	Y2	S2	Z
-3.579140751	-0.335943853	1.267020386	-7.883402385
X	Y2	S2	Z
-0.793037782	-1.813194725	1.018603823	-56.84549891
X	Y2	S2	Z
-0.355264521	-0.650741007	1.138083593	-0.322922453
X	Y2	S2	Z
-0.137670378	-0.165896435	1.209426125	8.364173538
X	Y2	S2	Z
0.994986456	0.043993423	1.247771711	9.503739045
X	Y2	S2	Z
-0.874632224	0.103471057	1.250737015	7.274217094
X	Y2	S2	Z
-0.994831115	-0.115170595	1.267160983	-12.18122684
X	Y2	S2	Z
0.243522124	0.045290224	1.248425042	7.331909147
X	Y2	S2	Z
0.493904941	0.189155163	1.277583089	12.80481862
X	Y2	S2	Z
-0.133336886	1.242588905	1.240402613	35.16934135
X	Y2	S2	Z
-1.163363547	0.548213554	1.210012625	5.865562956
X	Y2	S2	Z
-1.212483872	0.030684143	1.253369976	-15.57499432
X	Y2	S2	Z
-1.522165016	-0.08633278	1.254152365	-8.311410573
X	Y2	S2	Z
-1.522165016	-0.08633278	1.254152365	-8.311410573
X	Y2	S2	Z
-1.522165016	-0.08633278	1.2541-	

FIG. 5

$$\begin{aligned}x_0 &= c \\z_n &= x_n^3 + v_n.\end{aligned}\tag{4.1}$$

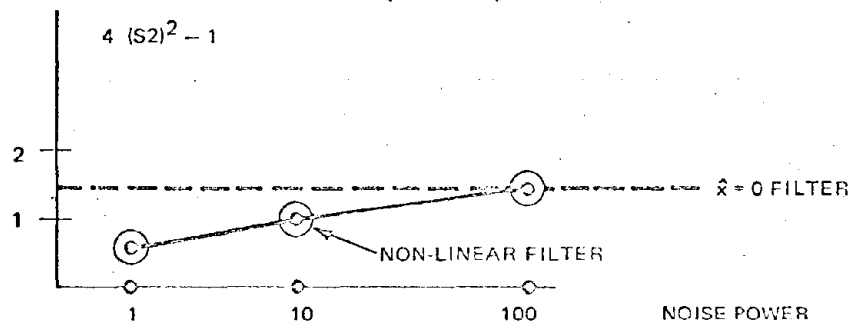
Defining H_n as $3\hat{x}_n^2$ it follows that a linearized filter for Eqs. (4.1) is given by

$$\begin{aligned}\hat{x}_n &= a\hat{x}_{n-1} + K_{n-1}(z_{n-1} - \hat{x}_{n-1}^3) \\ \hat{x}_0 &= 1 \\ K_n &= aP_n H_n (H_n^2 P_n + C)^{-1} \\ P_{n+1} &= a^2 P_n C (H_n^2 P_n + C)^{-1} + B.\end{aligned}\tag{4.2}$$

Noting that $\hat{x}_n = 0$ is a stable equilibrium for the estimate, we take $\hat{x}_0 = 1$ and simulate the behavior of Eqs. (4.2) on the *same* observation sequence as the non-linear filter runs (see Figs. 6, 7, and 8 which should be compared with Figs. 3, 4, and 5 respectively). Notice that the non-linear filter is markedly better and in particular the linearized estimate when once small stays small, so that its long-term behavior is quite poor. Figure 9 is the time-sharing program for the synthesis of the linearized filter.

6.0 Remarks On the Data

Now Figs. 3 through 5 give the conditional error standard deviations of the one-step predictor. Hence, the filtering error is $((S2)^2 - 1)4$



We point out that somewhere between a signal-to-noise level of .1 to .01 the data has very little information useful for filtering. Notice from Figs. 6 through 8, the linearized filter differs little from the filter

$$\hat{x}(t) \equiv 0.$$

It may be of interest to the reader to discuss some preliminary results concerning the implementation of higher order examples. In joint work with Dr. Roger Geesey and Dr. Kenneth Senne, we have found that in the two dimensional case, computing time

```
>RUN
INPUT A SET OF VALUES A,B,C,N,G,D
? 1, 1, 1, 25, 0.5, 3
```

X	X2	P2	
-0.626713664	0.340809638	1.025	
X	X2	P2	
0.174233842	0.43881852	1.22788809	
X	X2	P2	
3.107302746	0.313897009	1.217746038	
X	X2	P2	
1.0397463	5.005466843	1.27515915	
X	X2	P2	
0.424397218	1.670032142	1.000044244	
X	X2	P2	
-0.53420807	0.566021129	1.003520779	
X	X2	P2	
-1.51678737	0.162361853	1.130189266	
X	X2	P2	
-0.375670138	0.086862446	1.280564136	
X	X2	P2	
-0.860187797	0.054320184	1.319931126	
X	X2	P2	
-0.953289574	-0.033203353	1.329948656	
X	X2	P2	
-1.252639799	-0.023840069	1.332482327	
X	X2	P2	
-3.579140751	-0.014825045	1.333119291	
X	X2	P2	
-0.793037782	-0.028046398	1.33327963	
X	X2	P2	
-0.355264521	-0.014780099	1.333317433	
X	X2	P2	1.333329167
-0.137670378	-7.04225066E-03		
X	X2	P2	1.333332282
0.994936456	-3.42709413E-03		
X	X2	P2	1.33333307
-0.874632224	-1.67563542E-03		
X	X2	P	1.333333267
-0.994831115	3.48039586E-04		
X	X2 0	P2	1.333333317
0.243522124	-4.24239747E-04		
X	X2	P2	1.333333329
0.493904941	-2.11654274E-04		
X	X2	P2	1.333333332
-0.133336886	-1.05502322E-04		
X			

FIG. 6

>RUN
 INPUT A SET OF VALUES A,B,C,N,G,D
 ? 1,1,10,25,0.5,3

X	X2	P2	
-0.626713664	0.405303469	1.131578947	
X	X2	P2	
0.174233842	0.36372004	1.275328163	
X	X2	P2	
3.107302746	0.216477319	1.312553514	
X	X2	P2	
1.0397463	0.379427161	1.327289313	
X	X2	P2	
0.424397218	0.139187005	1.323805439	
X	X2	P2	
-0.53420807	0.0700670W1	1.330803438	
X	X2	P2	
-1.51678737	0.034424199	1.332691256	
X	X2	P2	
-0.375670138	0.016166016	1.333172253	
X	X2	P2	
-0.860187797	0.00796464	1.333293036	
X	X2	P2	
-0.953289574	3.95826858E-03		1.333323257
X	X2	P2	
-1.252639799	1.95239036E-03		1.333330814
X	X2	P2	
-3.579140751	9.73270055E-04		1.333332704
X	X2	P2	
-0.793037782	4.77290007E-04		1.333333176
X	X2	P2	
-0.355264521	2.38624813E-04		1.333333294
X	X2	P2	
-0.137670378	1.1934218E-04		1.333333323
X	X2	P2	
0.994986456	5.96796455E-05		1.333333331
X	X2	P2	
-0.874632224	2.98419411E-05		1.333333333
X	X2	P2	
-0.994831115	1.4920203E-05		1.333333333
X	X2	P2	
0.243522124	7.46017474E-06		1.333333333
X	X2	P2	
0.493904941	3.73013255E-06		1.333333333
X	X2	P2	
-0.133336886	1.86509746E-06		1.333333333
X	X2	P2	
-1.163363547	9.32550027E-07		1.333333333
X	X2	P2	
-1.212483872	4.66273965E-07		1.333333333
X	X2	P2	
-1.522165016	2.33136815E-07		1.333333333

FIG. 7

INPUT A SET OF VALUES A,B,C,N,G,D
 ? 1,1,100,25,0.5,3

X	X2	P2	
-0.626713664	0.477478252	1.229357798	
X	X2	P2	
0.174233842	0.319846447	1.30558208	
X	X2	P2	
3.107302746	0.168968668	1.325994632	
X	X2	P2	
1.0397463	0.100577922	1.331466414	
X	X2	P2	
0.424397218	0.048678501	1.332862522	
X	X2	P2	
-0.53420807	0.024350268	1.333215406	
X	X2	P2	
-1.51678737	0.012155741	1.333303837	
X	X2	P2	
-0.375670138	6.05890224E-03		1.333325958
X	X2	P2	
-0.860187797	3.02427675E-03		1.33333149
X	X2	P2	
-0.953289574	1.51129348E-03		1.333332872
X	X2	P2	
-1.252639799	7.54499441E-04		1.333333218
X	X2	P2	
-3.579140751	3.77159965E-04		1.333333305
X	X2	P2	
-0.793037782	1.88418258E-04		1.333333326
X	X2	P2	
-0.355264521	9.42089005E-05		1.333333332
X	X2	P2	
-0.137670378	4.71059345E-05		1.333333333
X	X2	P2	
0.994986456	2.3553389E-05		1.333333333
X	X2	P2	
-0.874632224	1.17767752E-05		1.333333333
X	X2	P2	
-0.994831115	5.88835381E-06		1.333333333
X	X2	P2	
0.243522124	2.94418199E-06		1.333333333
X	X2	P2	
0.493904941	1.47209322E-06		1.333333333
X	X2	P2	
-0.133336886	7.36048132E-07		1.333333333

FIG. 8

```

10  PRINT "INPUT A SET OF VALUES A,B,C,N,G,D"
15  INPUT A,B,C,N,G,D
37  P1=A
38  X1=0
100 X=SQR(A)*SQR(-2*LOG(RND(-1)))*COS(2*PI*RND(-1))
109 W=1
110 V=SQR(C)*SQR(-2*LOG(RND(-1)))*COS(2*PI*RND(-1))
120 U=SQR(B)*SQR(-2*LOG(RND(-1)))*SIN(2*PI*RND(-1))
124 Z=X1D+V
130 X=G*X+U
235 GO TO 300
245 PRINT "X", "X2", "P2"
247 PRINT X, X2, P2
251 W=W+1
260 IF W < N THEN 110
300 M=3*X1*X1
302 X2=G*X1+P1*G*M/(P1*M+G)*C*(Z-M/3*X1)
310 P2=G*G*P1*C/(M*P1+G)*C*B
320 X1=X2
321 P1=P2
330 GO TO 245

```

FIG. 9

varies as M^4 if the analog of the convolution equation (3.2) is performed over the entire grid. However, by summing the convolution over on the interior of a moving ellipse of points, with center and axis determined by a suboptimal filter, we have found significant time reductions without loss of accuracy. For real time synthesis of higher order examples it seems that parallel processing is the only effective technique, although Gauss-Hermite integration is being considered.

Acknowledgements

My graduate students, James Lo, Alex Liang, and David Rappaport were quite helpful in writing and debugging the various programs. Discussions with Dr. Jack Mallinckrodt were quite helpful. Thanks are also due to AFOSR for providing a time-share remote terminal without which none of the results presented here could have been obtained.

REFERENCES

- [1] BUCY, R. S. and JOSEPH, P. D., *Filtering for Stochastic Processes with Applications to Guidance*, Interscience, New York, 1968.
- [2] KIPINJACK, V., Private Communication, 1960.
- [3] LO, J. T., "Finite Dimensional Sensor Orbits and Nonlinear Filtering," PhD Thesis, Aerospace Engineering, University of Southern California, 1969.
- [4] HO, Y. C. and LEE, R. K., "A Bayesian Approach to Problems in Stochastic Estimation and Control," *I.E.E.E. Transaction on Auto. Control*, 186.
- [5] SWERLING, P., "Topics in Signal Estimation," Rand Corp. Report P-3007, Oct. 1964.
- [6] WALD, A., *Statistical Decision Functions*, Wiley, New York, 1950.

APPENDIX 3
MONTE CARLO SIMULATION PROGRAMS

Two Monte Carlo simulation programs, D13 and D14, were run for statistical data. Program D13 simulates the conditional mean non-linear estimator and the cyclic non-linear estimator on the line, while D14 simulates the cyclic phase non-linear estimator on the circle. Program D13 together with the corresponding flow chart, are shown in the following, where:

PP 6.28318530

R7 Parameter R, variance of the ideal estimate (Wiener)

AI Floating Point Number of I

F9 Parameter F, filtering time constant in sample interval units

X Signal Phase

Y2 Conditional Mean Non-Linear Estimate

Z8 Phase Lock Estimate

X2 Cyclic Phase Non-Linear Estimate

SA Cos Component of the Cyclic Phase Estimate

CA Sin Component of the Cyclic Phase Estimate

E(I) Measurement Density Function

R(I) Random Variates, uniformly distributed from 0 to 1.

AJ(I) Probability Density Function

QQ(I) Old Grid Point Value

V1 Independent Random Normal Variate V_1

V2 Independent Random Normal Variate V_2

U	Independent Random Normal Variate U
Z1	Observation Z_1
Z2	Observation Z_2
YE2	Phase Error, conditional mean non-linear estimate ϵ_s , cycles
XE2	Phase Error, cyclic phase non-linear estimate ϵ_c , cycles
ZE8	Phase Error, phase lock estimate, ϵ_p , cycles
B	Variance of U
C	Variance of V1 or V2
G	Integrator Gain K
G1	Mean of the Cyclic Estimate Error, $\bar{\epsilon}_c$
G2	Mean of the Phase-Lock Error, $\bar{\epsilon}_p$
G3	Mean of the Non-Linear Estimate Error, $\bar{\epsilon}_m$
W	Discrete Time Index
AK	Normalization Factor
MM	Number of Grid Points from $-\pi$ to π , $MM=2*M+1$
N	Number of Sampling Points per Trial
NRUN	Number of Trials per Experiment
SM1	Modulo 2π Error, Conditional Mean Non-Linear Estimate, $M(\epsilon_m)$
SM2	Modulo 2π Error, Cyclic Phase Non-Linear Estimate, $M(\epsilon_c)$
SM3	Modulo 2π Error, Phase Lock Estimate, $M(\epsilon_p)$
XXA1	Mean Square Error, Conditional Mean Non-Linear Estimate, $\overline{(\epsilon_m)^2}$
XXA2	Mean Square Error, Cyclic Phase Non-Linear Estimate, $\overline{(\epsilon_c)^2}$

- XXA3 Mean Square Error, Phase Lock Estimate, $\overline{(\epsilon_p)^2}$
- XXM1 Mean Square Modulo 2π Error, Conditional Mean Non-Linear Estimate, $\overline{(M(\epsilon_m))^2}$
- XXM2 Mean Square Modulo 2π Error, Cyclic Phase Non-Linear Estimate, $\overline{(M(\epsilon_c))^2}$
- XXM3 Mean Square Modulo 2π Error, Phase Lock Estimate, $\overline{(M(\epsilon_p))^2}$

Input data are read in and printed out when program starts. Initial conditions for each run, which includes the initial values for estimates, cumulative statistics, probability density and density grid are set at this point.

Gaussian random variates are generated using Vector algorithm:

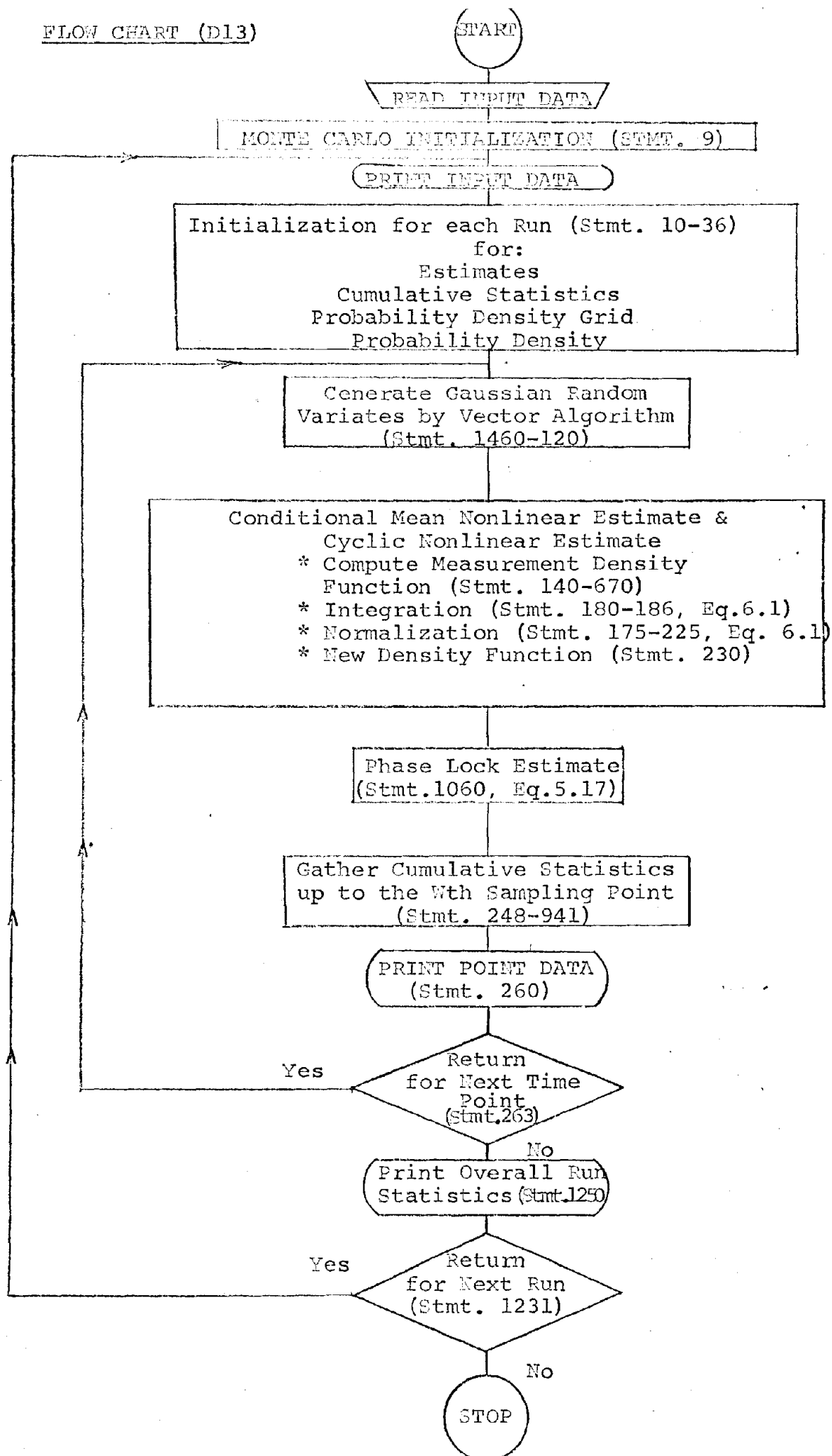
$$X_1 = (-2 \ln U_1)^{\frac{1}{2}} \cos 2\pi U_2$$

$$X_2 = (-2 \ln U_1)^{\frac{1}{2}} \sin 2\pi U_2$$

Where U_1 and U_2 are independent random variables having a rectangular density function on the interval (0, 1). Therefore, $-2 \ln U$, consequently, $r^2 = X_1^2 + X_2^2$, has a Chi-squared distribution with two degrees of freedom, which implies that X_1 , X_2 are independent normal random variates with zero mean and unit variance (Ref. 19, p. 953). In D13, uniformly distributed variables are generated using IBM system 360 subroutine RANDU.

Conditional mean non-linear, cyclic phase non-linear and phase-lock estimates are computed and data are printed out for each discrete time point. The stmt. and Eq. numbers appearing in the flow chart are the statement and equation numbers used in the program and the text.

FLOW CHART (D13)



PROGRAM D13

```

      DIMENSION AJ(500),AL(500),H(500),QO(500),E(500),AML(500),PN(8)
      PP=6.2831853
      7 READ(5,8) AM,R7,F9,N,NRUN
      8 FORMAT(3F10.0,2I5)
      9 NNN=0
      ARUN=NRUN
      IX=314159
      10 NS=0
      11 A=P7
      P1=A
      X1=0
      ZS=0
      C=R7*F9
      B=R7/F9
      TA=0.
      G1=0
      G2=0
      G3=0
      GM3=0.
      A17=199.
      AN=N
      M=AM
      G=1.
      P9=0
      TM8=0
      TM9=0
      T3=0
      T9=0
      WRITE(6,60) M
      60 FORMAT(3H M=,I4)
      WRITE(6,62) R7
      62 FORMAT(4H R7=,F6.3)
      WRITE(6,64) F9
      64 FORMAT(4H F9=,F7.2)
      WRITE(6,66) B
      66 FORMAT(3H B=,F7.3)
      WRITE(6,68) C
      68 FORMAT(3H C=,F7.3)
      WRITE(6,2)
      2 FORMAT(10)1H X NLE CYCLICE PLE NLEM CYEM PLEM
      1 NLMSE CYMSE PLMSE NLMSEM CYMSEM PLMSEM W1)
      17 S6=0
      S8=0
      SWS=0.
      S9=0
      T=C
      Y1=0
      S1=SQRT(A)
      30 MM=2*M+1
      35 DO 45 I=1,MM
      A1=I
      A17=(1./A1)*TAT=1.F9.
      40 AJ(I)=(1./SQRT(PP*A))*EXP(-.5*AL1*AL1)
      45 T=T+AJ(I)
      70 DO 75 I=1,MM

```

Set up initial probability density.

75 AJ(I)=AJ(I)/T

91 W=1.

RANDOM VARIATE GENERATION

1460 DO 1470 I=1,3

1470 IY=IX*.65533

IF(IY) 15,16,16

15 IY=IY+2147483647+1

16 YFL=IY

YFL=YFL*.4656613E-9

IX=IY

1480 RN(I)=YFL

1500 IF(W=2.) 100,110,110

100 X=SQRT(A)*SQRT(-2.*ALOG(RN(1)))*COS(PP*RN(2))

110 V1=SQRT(C)*SQRT(-2.*ALOG(RN(3)))*COS(PP*RN(4))

V2=SQRT(C)*SQRT(-2.*ALOG(RN(5)))*COS(PP*RN(6))

120 U=SQRT(3)*SQRT(-2.*ALOG(RN(7)))*SIN(PP*RN(8))

130 X=G*X+U

Z1=COS(X)+V1

Z2=SIN(X)+V2

140 Y0=Y1

NON-LINEAR DENSITY COMPUTATION

S0=S1

Y1=0

S1=0

Q5=Y0-8.*S0

Q6=8.*S0/AM

145 DO 670 I=1,MM

AI=I

QQ(I)=Q5+Q6*(AI-1.)

150 Y1=Y1+AJ(I)*QQ(I)

155 S1=S1+QQ(I)*AJ(I)*QQ(I)

JQ=QQ(I)/PP

AQ=JQ

636 E(I)=PP*(QQ(I)/PP-AQ)

637 E(I)=((Z1-COS(E(I)))**2+(Z2-SIN(E(I)))**2)/(2.*C)

639 IF(E(I)-50.) 667,667,663

667 E(I)=EXP(-E(I))

Measurement Density Function

GO TO 670

669 E(I)=0

670 CONTINUE

160 S1=SQRT(S1-Y1*Y1)

Q5=Y1-8.*S1

Q6=8.*S1/AM

DO 164 I=1,MM

163 AI=I

164 AL(I)=Q5+Q6*(AI-1.)

165 AK=0

Y2=0

S2=0

675 F4=AI*SQRT(B)/Q6

AI=AM/4.

IF(F4-AT) 677,677,175

677 F4=AM/4.

175 DO 215 I=1,MM

Integration

AM=0

AI=1

```

J1=AI-F4
IF(J1-1) 723,723,724
723 J1=1
724 J2=AI+F4
725 IF(J2-MM) 180,726,726
726 J2=MM
180 DO 186 I=J1,J2
    QQQ=(AL(I)-G*QQ(I1))*2/(2.*B)
    IF(QQQ-50.) 183,183,187
187 R=0
    GO TO 186
183 R=EXP(-QQQ)
185 AH=AH+E(I1)*R*AJ(I1)
186 CONTINUE
210 H(I)=AH
    AK=AK+H(I)
    S2=S2+AL(I)*AL(I)*H(I)
215 Y2=Y2+AL(I)*H(I)
220 Y2=Y2/AK
    S2=S2/AK-(Y2**2)
225 DO 230 I=1,MM
    H(I)=H(I)/AK
230 AJ(I)=H(I)
231 TL=TA
    SA=0
    CA=0
    DO 232 I=1,MM
    SA=SA+AJ(I)*COS(AL(I))
232 CA=CA+AJ(I)*SIN(AL(I))
233 TA=ATAN2(CA,SA)
500 TB=TA-TL
    IF(TB-3.1415927) 505,505,510
510 TA=TA-6.2831853
    GO TO 500
525 IF(TB+3.1415927) 515,525,525
515 TA=TA+6.2831853
    GO TO 500
525 CONTINUE
530 X2=TA
236 W1=0
    Y01=Y0-3.1415927
    Y02=Y0+3.1415927
    DO 238 I=1,MM
    IF(AL(I).LT.Y01.OR.AL(I).GT.Y02) GO TO 238
238 W1=W1+AJ(I)
238 CONTINUE
1060 U3=SIN(X-Z3)-V1*SIN(Z2)+V2*COS(Z3)
    Z3=Z3+U3/(1.+F9)
245 S6=S6+1.
250 IF(S6-4.) 259,257,257
257 S8=S8+((X-Y2)**2)
    T3=T3+((X-X2)**2)
    T3=T3+((X-Z3)**2)

```

Renormalization

New Conditional Phase Density

CYCLIC NON-LINEAR ESTIMATE

PHASE LOCK

GATHER CUMULATIVE STATISTICS


```

      S9=S9+1.
      G1=G1+X-X2
      G2=G2+X-Z8
      G3=G3+X-Y2
259  SM1=X-Y2
      SM2=X-X2
      SM3=X-Z3
910  IF(SM1+3.1415927) 905,903,903
905  SM1=SM1+PP
      GO TO 910
903  IF(SM1-3.1415927) 920,920,909
909  SM1=SM1-PP
      GO TO 903
920  IF(SM2+3.1415927) 915,913,913
915  SM2=SM2+PP
      GO TO 920
913  IF(SM2-3.1415927) 930,930,919
919  SM2=SM2-PP
      GO TO 913
930  IF(SM3+3.1415927) 925,923,923
925  SM3=SM3+PP
      GO TO 930
923  IF(SM3-3.1415927) 940,940,929
929  SM3=SM3-PP
      GO TO 923
940  IF(S9-1.) 262,941,941
941  SM8=SM8+SM1**2
      TM8=TM8+SM2**2
      TM9=TM9+SM3**2
      XXA1=S9/S9
      XXA2=T8/S9
      XXA3=T9/S9
      XXM1=SM8/S9
      XXM2=TM8/S9
      XXM3=TM9/S9
      YE2=(X-Y2)/PP
      XE2=(X-X2)/PP
      ZE2=(X-Z3)/PP
260  WRITE(6,261) W,X,YE2,XE2,ZE2,SM1,SM2,SM3,XXA1,XXA2,XXA3,XXM1,XXM2,
      1XXM3,W1
261  FORMAT(F5.0,1X,13F7.2,1X,E12.5)
262  YE=ABS(X-Y2)
2009 W=W+1.
263  IF(W-AN) 1460,1460,265
265  S8=S8/S9
      T8=T8/S9
      T9=T9/S9
      G1=G1/S9
      G2=G2/S9
      G3=G3/S9
      SM8=SM8/S9
      TM8=TM8/S9
      TM9=TM9/S9
      WRITE(6,1300)
1300 FORMAT(10H 1 J(1))
1400 DO 1400 I=1,WM

```

PRINT POINT DATA

Return for next time point

~~1203 WRITE (6,1310) I,AJ(I)~~

~~1210 FORMAT (14,2X,E12.5)~~

~~113) WRITE (6,1200)~~

Print Overall Statistics

~~1200 FORMAT(53H N.L. CYCLIC P.L.)~~

~~1250 WRITE(6,1210) SB,T2,TS,SMB,TMB,TMS~~

~~1210) FORMAT(10H MEAN SQ ERR ,E12.5,2X,E12.5,2X,E12.5,2X,E12.5,2X,E12.5,2X,E12.5/)~~

~~1220 WRITE(6,1230) G3,G1,G2~~

~~1230) FORMAT(10H MEANS ,E12.5,1X,E12.5,2X,E12.5/)~~

~~1231 NNN=NNN+1~~

~~IF (NNN-NRUN) 10,1240,1240~~

~~1240 STOP~~

Return for next run.

~~END~~

REFERENCES

1. Bucy, R.S., and Joseph, P.D., "Filtering for Stochastic Processes with Applications to Guidance", Interscience, New York, 1968.
2. Bucy, R.S., and Senne, K.E., "Digital Realization of Non-Linear Filters", submitted Automatica. Also Seiler Lab. Report SRL 70-0010, Air Force Systems Command, U.S. Air Force, July 1970.
3. Lo, J.T., Finite Dimensional Sensor Orbits and Non-Linear Filtering, Thesis, Dept. of Aerospace Engineering, U.S.C., 1969.
4. Bucy, R.S., "Bayes Theorem and Digital Realizations of Non-Linear Filters," J.A.A.S., XVII,2,1970, 80-94.
5. Bucy, R.S., "Linear and Non-Linear Filtering", Proc.I.E.E.E., 58, 6, pp.854-864, 1970.
6. Viterbi, A.J., "Phase-Locked Loop Dynamics in the Presence of Noise by Fokker-Planck Techniques", NASA TR #32-427, 1963. Also Proc. IEEE, V.51, p.1737, Dec. 1963.
7. Van Trees, H.L., "Functional Techniques for the Analysis of the Non-Linear Behavior of Phase-Locked Loops," Proc.IEEE, Vol.52, pp.894-911, August 1964.
8. Develet, J.A., Jr., "An Analytic Approximation of Phase-Lock Receiver Threshold," Trans.IEEE, SET-9, pp.9-11, March 1963.
9. Develet, J.A., Jr., "A Threshold Criterion for Phase-Lock Demodulator," Proc.IEEE, Vol.51, pp.349-356, February 1963. Correction in Proc. IEEE, p.580, April 1963.
10. Cahn, C.R., "Piecewise Linear Analysis of Phase-Lock Loops," Trans. IRE, PGSET, SET-8, p.8, March 1962.
11. Spilker, J.J., Jr., "Threshold Comparison of Phase-Lock, Frequency-Lock and Maximum-Likelihood Types of FM Discriminators," presented at the IRE Wescon Conf., San Francisco, Calif. August 22-25, 1961.
12. Charles, F.J., and Lindsey, W.C., "Some Analytical and Experimental Phase-Locked Loop Results for Low Signal-to-Noise Ratios", Proc.IEEE, V.54, No.9, p.1152, September 1966.
13. Robinson, L.M., "Tanlock, A Phase-Locked Loop of Extended Tracking Capability", Proc.1962 Conf. Mil.Elect., February 7-9, 1962.
14. Fillippi, C.A., "Advanced Threshold Reduction Techniques Study", Adcom, Inc., NASA CR-682, January 1967.
15. Balodis, M., "Laboratory Comparison of Tanlock and Phase-Lock Receivers," Proc.1964 NTC, p.5-4, June 1964.
16. Enloe, L.H., "Decreasing the Threshold in FM by Frequency Feedback," Proc.IRE, V.50, p.18, January 1962.
17. Luby, D.D., "Demodulation of Angle-Modulated Telemetry Signals, Vol.I: Advanced Modulation Techniques", Philco Report No.ESD-TR-66-408, AD 639 787, August 1966.

References, cont'd.

18. Gupta, Bayless, and Hummels, "Threshold Investigation of Phase-Locked Discriminators", IEEE Trans.AES, V.AES 4,p.855, November 1968.
19. Abramowitz and Stegun, "Handbook of Mathematical Functions", National Bureau of Standards, AMS 55, U.S.Gov't Printing Office, June 1964.
20. Kalman, R.E., "A New Approach to Linear Filtering and Prediction Problems", Jour. of Basic Engineering, ASME, p.35, March 1960.
21. Kalman, R.E., and Bucy, R.S., "New Results in Linear Filtering and Prediction Theory," Jour. of Basic.Eng., ASME, p.95, March 1961.
22. McKean, H.P., "Stochastic Integrals", Academic Press, 1969.
23. Tausworth, R., "Cycle Slipping in Phase-Locked Loops", JPL Tech. Rpt. No.32-1127, Also, IEEE Trans. on Comm.Tech., V.COM-15, No.3, p.417, June 1967.
24. Middleton, David, "Statistical Communication Theory", McGraw-Hill, 1960.